Predicting the thermal performance of bio-based cold chain packaging systems

Abid Hassan

Thesis submitted to the faculty of the Virginia Polytechnic Institute and State University in partial fulfillment of the requirements for the degree of

Master of Science

In

Forest Products

Eduardo Molina, Committee Chair

Laszlo Horvath

Jennifer Russell

William Pelletier

December 4th ,2025

Blacksburg, VA

Keywords: cold chain, packaging, insulation, thermal performance, phase change material

Predicting the thermal performance of bio-based cold chain packaging system

Abid Hassan

Abstract (Academic)

Cold chain logistics play a critical role in ensuring the safe transport of temperature-sensitive products such as pharmaceuticals, biologics, and perishable foods. Maintaining stable internal temperatures within insulated shipping containers (ISCs) requires an in-depth understanding of how materials, design, and environmental factors influence heat transfer. This research combines experimental and computational approaches to improve the thermal efficiency and environmental sustainability of passive cold chain packaging systems.

The first phase of the study (Chapter 1) focuses on predicting the thermal performance of bio-based ISCs through finite element modeling (FEM). Material characterization was conducted using Differential Scanning Calorimetry (DSC) and Heat Flow Meter techniques to obtain the thermal properties of corrugated fiberboard, honeycomb paperboard, and phase change materials (PCMs). The FEM framework was validated through experimental data, showing strong correlation with measured results and a mean prediction deviation of less than 8% when maintaining temperatures below the critical 8 °C threshold. These findings confirm that FEM can serve as an accurate and efficient alternative to conventional performance testing while supporting the integration of renewable insulation materials in package design.

The second phase (Chapter 2) examines how environmental humidity influences the thermal behavior of ISCs. Laboratory experiments were performed across relative humidity levels from 30 % to 80 % to evaluate temperature evolution and hold-time performance. The results revealed that higher humidity significantly accelerated the warming rate, particularly in fiber-based insulation systems, due to moisture absorption that increased effective thermal conductivity. In contrast, polymer-based materials such as expanded polystyrene (EPS) and polyurethane (PU) remained relatively stable. Energy-balance modeling supported these observations, confirming humidity as a major external driver of heat transfer in porous materials. Beyond performance, the study underscores the environmental benefits of fiber-based materials, which are renewable and recyclable, while emphasizing the need for design strategies that balance thermal reliability and sustainability under real-world humidity conditions.

Predicting the thermal performance of bio-based cold chain packaging system

Abid Hassan

Abstract (General Audience)

Cold chain packaging helps keep medicines, vaccines, and food products safe by maintaining low temperatures during shipping. However, designing boxes that stay cold long enough while also being environmentally friendly is a major challenge. This research explores how different materials and environmental conditions affect the performance of insulated boxes used in cold-chain transport.

In the first part of the study, computer modeling and laboratory tests were used to predict how well various paper-based insulation materials keep products cold. The models closely matched real experimental results, showing that computer simulations can accurately estimate temperature performance without the need for long and expensive tests. These findings also support using bio-based materials such as corrugated fiberboard and honeycomb paperboard as sustainable alternatives to conventional foams.

The second part of the study looked at how humidity in the air changes how these boxes perform. Tests showed that when humidity is high, paper-based materials absorb moisture and lose some of their insulating power, causing the inside temperature to rise faster. Plastic foams such as EPS and polyurethane were less affected. Although fiber-based packaging is more sensitive to humidity, it offers major environmental advantages because it comes from renewable sources and can be recycled. Together, these results show that future cold chain packaging can be both efficient and eco-friendly if designed with careful attention to how materials behave under real shipping conditions, including humidity.

Table of Contents

1 Introduction 9
1.1 Objectives 13
2 Literature review 14
2.1 Passive cold chain system 14
2.2 Phase Change Material (PCM) 15
2.3 Insulation in Passive cold chain system 21
2.4 Modelling of Passive cold chain system 23
2.5 Standards 26
3 References 28
4 Chapter 1: Predicting the thermal performance of bio-based cold chain packaging systems through finite element modelling for passively cooled containers 34
4.1 Introduction 34
4.2 Methodology 37
4.2.1 Experimental simulation 38
4.2.2 Material Property Analysis 40
4.2.3 Finite Element Model (FEM) 42
4.3 Results and Discussion 44
4.4 Conclusion 50
4.5 References 52
5 Chapter 2: Effect of relative humidity on the performance of passive thermal cold chain packaging systems 54
5.1 Introduction 54
5.2 Methodology 57
5.2.1 Materials and Packout Construction 57
5.2.2 Preconditioning and Experimental Simulation 60
5.3 Results and Discussion 62
5.4 Conclusion 69
5.5 References 70
6 Chapter 3: Environmental Analysis of Passive Cold-Chain Packaging Systems Using a Performance-Based Functional Unit 73
6.1 Introduction 73
6.2 Methodology 74
6.2.1 Goal and Scope Definition 74

6.2.2 System Boundary 74
6.2.4 Impact Assessment Methods 75
6.2.5 Functional Unit: Environmental Impact per Hour of Thermal Protection 76
6.3 Results and Discussion 76
6.3 Conclusion 80
6.4 References 81
7 Summary 82
8 Conclusion 83
Appendix 84
Appendix A. 84
Appendix B. 89

List of Figures

Figure 1: Comparison of sensible and latent energy storage systems during the melting process. 16
Figure 2: Different types of PCM 17
Figure 3: Comparison of sensible and latent energy storage systems during the melting process. 35
Figure 4: Cross-sectional view for the modelled insulated shipping container with the probe location (right) and a top-view picture of the partially assembled unit. 39
Figure 5: Temperature profiles followed for the shipping container evaluation 40
Figure 6: Thermal resistivity of the materials 40
Figure 7: Representative example of a Differential Scanning Calorimetry enthalpy characterization testing result for the phase change material. 41
Figure 8: Cross-sectional view and temperature gradient of transient thermal solution 44
Figure 9: Internal temperature versus time of the shipping container with BC double wall corrugated board insulation at constant 25 ° C. 46
Figure 10: Internal temperature versus time of the shipping container with Honeycomb board insulation at constant 25 ° C. 47
Figure 11: Internal temperature versus time of the shipping container with BC double wall corrugated board 47
Figure 12: Internal temperature versus time of the shipping container with Honeycomb board insulation at uncontrolled temperature 48
Figure 13: Internal temperature versus time of the shipping container with BC double wall corrugated insulation at ISTA 7E Heat Profile 48
Figure 14: Internal temperature versus time of the shipping container with Honeycomb board insulation at ISTA 7E Heat Profile 49
Figure 15: Schematic and representative picture of configuration 1 and 2 small shippers. 59
Figure 16: Thermal performance of configuration 1, Subcategory: Small 65
Figure 17: Thermal performance of configuration 4 66
Figure 18: Scatter plot with regression line for different humidity levels of all configurations 67
Figure 19: Normalized environmental impacts per hour of thermal protection for all packaging configurations at 50% relative humidity. Results are shown for (a) Fossil Fuel Use, (b) Freshwater Eutrophication, (c) Global Warming Potential, and (d) Water Use. Each impact value was normalized by dividing by the average of its respective impact category to improve comparability across configurations and enhance visualization of relative performance. 78
Figure 20: Comparison of environmental impacts per ISC and per hour of thermal protection for (a) fossil fuel use, (b) freshwater eutrophication, (c) global warming potential, and (d) water use across all configurations 79
Figure 21: Performance and statistical analysis of configuration 1 (Small) 84
Figure 22: Performance and statistical analysis of configuration 2 (Small) 85
Figure 23: Performance and statistical analysis of configuration 3 86

Figure 24: Performance and statistical analysis of configuration 1 (Small 35°C)....87
Figure 25: Performance and statistical analysis of configuration 1 (with product)....88
Figure 26: Environmental impact report for configuration 1 (small)....89
Figure 27: Environmental impact report for configuration 3....89
Figure 28: Environmental impact report for configuration 2 (small)....90
Figure 29: Environmental impact report for configuration 4....90
Figure 30: Environmental impact report for configuration 1 (large)....91
Figure 31: Environmental impact report for configuration 2 (large)....91

List of Tables

Table 1: Temperature requirement for different products for storage and shipping in cold chain logistics 10
Table 2: Summary of phase change temperatures and latent heat for different PCM materials. 17
Table 3: Measured average thicknesses of the materials evaluated. 38
Table 4: Measured average densities of the materials evaluated. 42
Table 5: Summary of Experimental and FEM Results for ISCs under Controlled, Uncontrolled, and ISTA 7E Heat Conditions 44
Table 6: Comparison of FEM and Experimental Results Using RMSE and MAPE Across Insulation Types and Test Conditions 49
Table 7: Construction materials for the studied shipper configurations. 57
Table 8: Outer box dimension for each shipper category 58
Table 9: Summary of the experimental design followed for the study. 61
Table 10: Result summary of the average time to reach 8°C for different configurations with their significance on humidity 63
Table 11: Significance on different humidity level change for different configurations 64
Table 12: Configuration constant with humidity effect coefficient for different configurations 68
Table 14: Material composition and mass inventory for all packaging configurations 75
Table 15: Thermal hold time at 50% Rh for all configurations 76

1 Introduction

The cold chain involves storing and transporting temperature-sensitive products using thermal or refrigerated packaging, along with carefully planned logistics, to preserve product quality and integrity throughout the entire supply process(Singh et al., 2013). Cold chain logistics is a critical component of modern supply chain management, ensuring that perishable goods such as food, pharmaceuticals, and biological products are transported and stored under controlled temperature conditions to maintain their quality and safety. The growing global demand for fresh and safe products, coupled with the rise in international trade, has heightened the need for efficient cold chain logistics systems. This necessity became even more apparent during the COVID-19 pandemic, where the distribution of temperature-sensitive vaccines underscored the importance of robust cold storage and transportation infrastructure(Fahrni et al., 2022). Demand for packaging for temperature-sensitive products is currently valued at approximately $35 billion and is projected to grow to $117 billion by 2030(Kumar Deb, 2023). According to Freedonia, e-commerce sales are expected to reach $1.4 trillion by 2026(*E-Commerce*, n.d.), , with online grocery sales increasing by 12% annually(*The Future of Grocery Report*, n.d.) and meal-kit delivery services anticipated to reach $15 billion by 2027(*Meal Kits*, n.d.). This rapid expansion of e-commerce and last-mile delivery for temperature-sensitive products, including pharmaceuticals and fresh foods, has introduced new challenges for protective packaging design(Chowdhury et al., 2023b; Raj et al., 2024a). Fluctuations in storage temperature can significantly affect the quality of perishable goods, including fresh foods and pharmaceuticals(Van Boxstael et al., 2013). To keep products safe during transport and storage, it is important to control their temperature and the environment around them(Kucharek et al., 2020). In the pharmaceutical sector, it's anticipated that the volume of temperature-sensitive products will keep rising. As an example, the Food and Drug Administration (FDA) is increasingly focused on cold chain shipping to address the growing importance of managing these temperature-sensitive products(Matsunaga et al., 2007). When referring to fresh produce, post-harvest losses for some temperature-sensitive produce can reach up to 50% due to insufficient access to cold chain logistics(UN Environment Programme, 2019). Despite advancements in cold chain technology, significant challenges remain, including temperature fluctuations, high energy consumption, infrastructure limitations, regulatory compliance, and the integration of emerging technologies(Zhang & Mohammad, n.d.). **Table 1** shows different products and the temperature requirement to store and transport them.

Table 1: Temperature requirement for different products for storage and shipping in cold chain logistics

Product	Temperature	Reference
Aquatic products, Frozen food	<-18	(Tan et al., 2022)
Poultry, Frozen meat	<-18 °C	(Carson & East, 2018)
Chilled meat	0 – 4°C	(Coombs et al., 2017)
Soy products	0 – 4°C	(Spychaj et al., 2018)
Dairy products Yogurt, Cheese, Pasteurized milk	2 – 6°C	(Mercier et al., 2017)
Western-style pastry	0 – 5 °C	(Meng et al., 2022)
Clean vegetables	0 – 6°C	(Adekomaya et al., 2016)
Beans, melons	7 – 15 °C	(Meng et al., 2022)
Drugs, Vaccines (Refrigerated)	2 – 8 °C	
Drugs, Vaccines (Frezzer)	-50 – -15 °C	
Drugs, Vaccines (Ultra Frezzer)	-90 – -60°C	

Cold chain systems include designing the insulated shipping containers (ISCs), monitoring in the distribution network and the storage to keep temperature-sensitive products safe and maintain their quality throughout the entire supply process(Kartoglu et al., 2017). Cold chain logistics systems are typically divided into two main types: active systems, which use powered refrigeration units to control temperature, and passive systems, which rely on insulated containers combined with refrigerants such as phase change materials or dry ice to maintain temperature without external power(Calati et al., 2022). Active cold chain distribution employs refrigerated storage containers to consistently maintain the required temperatures during distribution[6]. Refrigerated trucks contribute approximately 2.5% of global Greenhouse Gas (GHG) emissions by using high-Global Warming Potential (GWP) refrigerants and relying on fossil fuel-based grid or diesel-powered off-grid electricity(*Sustainable Cold Chain and Food Loss Reduction*, 2019). In recent years, the use of passive cold chain packaging has grown rapidly, driven by demand for cost-effective, energy-independent, and more sustainable solutions in pharmaceutical and food logistics(Ren et al., 2022a). Within the pharmaceutical industry, passive thermal packaging is increasingly preferred due to its simplicity and strong performance in last-mile delivery applications (Sykes, n.d.). Future Market Insights reports that passive packaging

represents roughly 72.5% of the pharmaceutical cold chain market(*Pharmaceutical Cold Chain Packaging Market Demand 2025 to 2035*, n.d.).x To better manage energy consumption and maintain proper product temperatures throughout the different supply chain stages, researchers have explored and developed phase change materials (PCMs), which leverage high energy density through phase changes between liquid and solid states at nearly constant temperatures, as replacements for traditional active cold chain designs in certain sections of product distribution, especially in the last-mile delivery where refrigeration is more expensive and less efficient(Calati et al., 2022). This strategy refers to the use of passive cooling techniques.

The performance and design of passively cooled insulated foam containers have been widely studied using both numerical and experimental methods. Multiple researchers have conducted numerical simulations validated by experimental results to understand heat transition in foam containers(Ge et al., 2014a), investigated various thermal insulation materials and found that packaging performance was significantly influenced by material type and configuration(Wang et al., 2020), examined the design of eco-efficient cold chain networks emphasizing the role of insulation strategies in reducing environmental impact(Zanoni et al., 2019). Previous research studies have also evaluated the effect of aluminium foil layers on thermal insulation performance and reported enhanced cold retention in logistic packaging(Zeng et al., 2022). Burgess(G. Burgess, 1999) developed a series of equations to calculate the thermal resistance (R-value) of packaging. These equations, derived through ice melt tests and adjusted via linear regression, considered factors such as the packing material, wall thickness, container geometry, and design. The model was used to estimate time within temperature specifications for specific packages, with estimated results falling typically within 20% of actual times measured in laboratory tests. However, this approach showed limitations that required multiple tests to build a database for various packaging models. Choi(Choi & Burgess, 2007) took a theoretical approach by developing a two-dimensional (2D) steady-state model to calculate the heat penetration rate (HPR), which measures energy transfer per degree of temperature difference. While this model accurately assesses the insulation performance of the package, it did not fully account for changes over time. Zeng et al. (Zeng et al., 2022) developed a mathematical model to study how aluminium foil affects packaging insulation in cold chain logistics. This study developed the concept of "maximum insulation time" (MIT) to measure the thermal performance of packaging. The authors showed that the addition of aluminium foil to the inner surface of insulation improved performance by over 25%, making evident the significance of radiation heat transfer even inside the packages. Singh(Singh et al., 2013) conducted a series of experiments with insulation materials of multiple densities and

thicknesses to assess their thermal resistance. By analysing different material types, Singh found that Vacuum Insulation Panels (VIPs) exhibited the highest thermal resistance of the materials and variations tested, followed by insulation constructed out of polyurethane, recycled expanded polystyrene (EPS), and virgin EPS. Specifically, for a one-inch-thick container, VIPs demonstrated a 128% and 267% improvement in thermal resistance compared to polyurethane and virgin EPS, respectively. Ge(Ge et al., 2013a) developed a Finite Element Analysis (FEA) to predict temperature changes in insulated packaging. It found partial agreement between field-measured and FEA-predicted temperatures. Both field data and FEA simulations showed that temperatures initially drop below 0°C before stabilizing above freezing. Using extruded polystyrene (XPS) foam containers, the duration of sub-zero temperatures depended on the gel packs' starting temperature, the empty space in the container, and the insulation materials. To prevent vaccines from freezing, the authors recommended to adjust the gel packs' initial temperatures and control the release of cold air.

The global cold chain packaging industry is experiencing a shift away from traditional petrochemical-based insulating materials, such as expanded polystyrene (EPS) and polyurethane (PU) foams, toward more sustainable options including biopolymers, cellulose-based insulation, and mycelium-based materials (Rahman et al., 2025). In addition, advancements in renewable feedstocks such as lignin and vegetable oils are supporting the development of bio-based polyurethane formulations, providing a more sustainable alternative to conventional fossil-derived foam insulation used in cold chain applications(Jayalath et al., 2025). When focusing specifically on the use of fibre-based insulation, research interest and development of commercial products has increased considerably(*Fiber-Based Packaging Market Size, Volume & Export Data*, n.d.). Driven by consumer preferences, the introduction of new regulations and advancements in the development of higher performance insulations, the proliferation of fibre-based and other alternative materials in the passive cold chain must be carefully studied to ensure successful adoption. As shown in previous research, most of it has been conducted using petroleum-based materials and considerations of important factors such as humidity effects have not been widely present.

Current Thermal Packaging System (TPS) evaluation standards rarely consider humidity as a key performance factor. For instance, ISO 23412:2020 outlines requirements for temperature-controlled parcel delivery but focuses mainly on temperature stability and handling practices, with no specific testing provisions for high or low humidity conditions(*ISO 23412:2020(En), Indirect, Temperature-Controlled Refrigerated Delivery Services — Land Transport of Parcels with Intermediate Transfer*, n.d.). Likewise, ISTA 7E protocols model ambient temperature profiles for

cold chain validation, but their environmental conditioning steps do not require controlled relative humidity (RH) beyond incidental variation(International Safe Transit Association (ISTA), 2010). ASTM thermal performance standards relevant to insulated shipping systems (e.g., ASTM D3103) address steady-state heat transfer, yet do not call for moisture pre-conditioning or simultaneous humidity cycling during testing(D10 Committee, n.d.). Similarly, the Parenteral Drug Association Technical Report No. 39 (PDA TR39) provides detailed guidance on temperature mapping for pharmaceutical distribution packaging but does not include humidity as a validation parameter(*PDA Technical Report No. 39 Revised 2021 (TR 39) Guidance for Temperature-Controlled Medicinal Products - Maintaining the Quality of Temperature-Sensitive Medicinal Products through the Transportation Environment (Single User Digital Version)*, n.d.).

For insulated shipping containers, thermal performance is evidently the most critical characteristic. For passive shippers we do not have any control on the environmental condition during shipment. To mitigate the risk of damage to temperature-sensitive products, companies must verify the TPS before shipping. This verification process potentially includes rigorous testing, which is time and resource intensive. Additionally, there is a need to address the effect of humidity on the fiber-based materials used to build the TPS's. To achieve this, this study was conducted in two phases.

1.1 Objectives

1. To optimize the development and validation of fiber-based cold chain packaging for insulated shipping containers.
2. To evaluate the influence of environmental humidity on the thermal performance of fiber-based and polymer-based insulation materials used in passive cold chain packaging
3. To conduct a comparative life cycle assessment of ISCs manufactured with fiber-based versus polymer-based insulation materials

2 Literature review

2.1 Passive cold chain system

The cold chain is a temperature-controlled logistics network that preserves safety and quality of perishable and temperature-sensitive goods from origin to end-use. Classic operations research and supply-chain studies frame it as a coordinated system in which stability of perishables depends on infrastructure, planning, and thermal control across nodes; more recent overviews emphasize technology and data for continuous monitoring to mitigate losses(Bogataj et al., 2005a). Passive systems maintain temperature integrity without powered refrigeration by combining structural insulation layers and thermal buffers, most commonly phase change materials (PCMs). Their adoption has accelerated in pharmaceutical and vaccine logistics because they enable long-duration thermal protection in regions with limited or unreliable access to electricity. Studies on vaccine distribution report that properly specified passive containers can preserve cold-chain conditions for multiple days as needed, supporting last-mile delivery, emergency response, and decentralized healthcare initiatives(Pambudi et al., 2022a). This operational simplicity reduces system complexity, mitigates equipment failure modes, and lowers deployment costs, making passive solutions increasingly competitive against powered transport for short- and medium-duration shipment lanes(Oró et al., 2012). Passive shippers typically include insulated enclosures made of EPS or PU foams and, increasingly, aerogels, combined with PCM packs tuned to target temperature ranges and data loggers for continuous monitoring(Oró et al., 2012).

Thermal behavior is governed by transient conduction through insulation and the latent-heat buffering effect of PCMs, which creates a temperature plateau during phase change. Models based on enthalpy and energy balance remain widely used to support system design (Sharma et al., 2009). Computational approaches integrate multi-layer conduction modeling, radiative input, and convective heat gain, enabling prediction of hold-time performance under complex ambient profiles. Reviews emphasize that thermal modeling can significantly reduce physical prototyping costs by optimizing insulation thickness, PCM mass fraction, and pack placement before laboratory qualification(Zhai et al., 2013a). Hold time depends on insulation type/thickness, PCM selection/placement, payload mass, and external profile severity. Literatures conducted on modeling insulated packages show how material choice and geometry shift time-to-threshold, supporting lane-based qualification(Wang et al., 2020). Packaging geometry also modifies internal temperature gradients, affecting local phase-transition rates and potentially driving premature warming near corner or lid regions. Consequently, lane-based qualification increasingly incorporates varied ambient profiles to reflect real transport exposures(Ren et al., 2022a).

Temperature excursions remain a key risk driver. Pharmaceutical literature outlines programmatic approaches to excursion management and quantifies mail-based variations by carrier and season, supporting the inclusion of data loggers and robust passive design margins(Ramakanth et al., 2021a). Mail-based shipment analysis further reveals that seasonal variability, carrier selection, and route dwell times significantly affect excursion probability, reinforcing the need for predictive monitoring and integrated data logging(Chowdhury et al., 2023b). As regulatory pressure intensifies, incorporating digital traceability into passive packaging is becoming standard practice(Ramakanth et al., 2021a). Reviews during and after the COVID-19 pandemic highlight passive and hybrid packaging applications for vaccine distribution, with emphasis on reliability in constrained settings and integration of advanced materials. Broader sustainability reviews catalog commercial packaging options and discuss recyclability/footprint trade-offs(Ramakanth et al., 2021a). Beyond pharmaceuticals, passive systems are increasingly used in e-commerce food logistics, biologics-research shipments, and clinical-trial transport. Sustainability literature highlights recyclability challenges associated with polymer foams and proposes circular-economy strategies, including bio-based liners and recyclable fiber composites(Ren et al., 2022a).

Current trends indicate the need of PCM optimization and heat-transfer enhancement for optimized charge/discharge, bio-based liners to reduce mass and improve performance, and digital traceability to pair passive boxes with real-time risk management(Cabeza et al., 2011). Additional work explores additive manufacturing for custom internal geometries, thermal fillers to accelerate PCM heat transfer, and multi-objective computational optimization to balance mass, cost, and duration. These emerging strategies collectively aim to extend hold time, reduce packaging volume, and improve sustainability without compromising thermal integrity(Baetens et al., 2011).

2.2 Phase Change Material (PCM)

Phase Change Materials (PCMs) are substances that absorb or release significant amounts of latent heat when they undergo a change in their physical state, such as melting from solid to liquid or freezing from liquid to solid. PCMs typically store energy through latent heat of fusion or solidification at a constant temperature, which is known as the transition temperature(Noël, 2016). Thermal energy storage is classified into three types: sensible heat storage (SHS), latent heat storage (LHS), and thermochemical storage. SHS, the simplest form, relies on the material's specific heat capacity and density but has limited energy storage capacity and experiences inevitable heat losses. LHS is more

efficient, utilizing phase change materials to transfer heat during transitions like solid to liquid, and offers higher energy density at stable temperatures. Thermochemical storage, while capable of storing substantially more energy—up to 10 times that of SHS or LHS—faces challenges with long-term stability and involves complex and expensive development processes(Ilangovan et al., 2022). The total quantity of heat (Q) that can be stored by a PCM over the temperature interval T1 to T2 is:

$$Q = \int_{T_1}^{T_{trs}} mc_{p,1}\mathrm{dT} + M\Delta_{trs}\mathrm{H} + \int_{T_{trs}}^{T_2} mc_{p,2}\,\mathrm{dT}$$

Where T_{trs} is the transition temperature; Δ_{trs}H is the transition enthalpy change; $c_{p,1}$ is the specific heat capacity of the low-temperature phase; and $c_{p,2}$ is the specific heat capacity of the high-temperature phase.

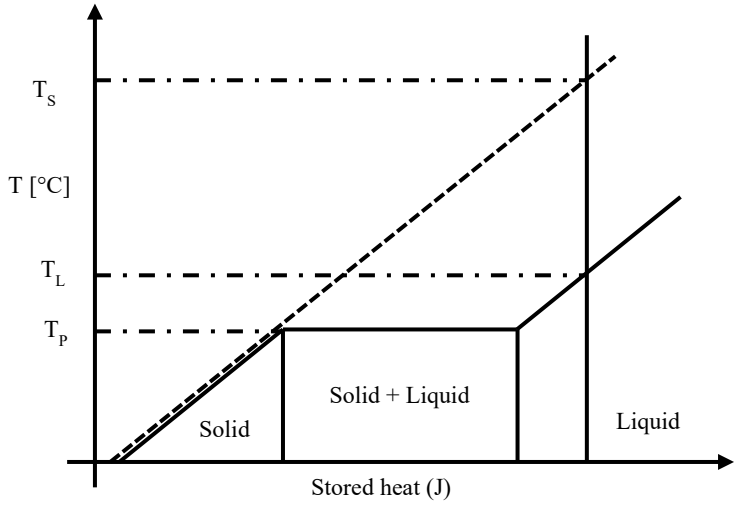

Figure 1: Comparison of sensible and latent energy storage systems during the melting process.

Figure 1 illustrates the comparative thermal storage performance of sensible and latent heat storage systems. Latent heat storage systems using PCMs perform better than traditional sensible heat systems. Both systems start at the same temperature. When the latent system (shown with a continuous line) reaches the phase change temperature (T_P), it begins to melt and stores heat at almost the same temperature. The PCM can store more heat. To store the same amount of heat, the sensible system (shown with a dotted line) heats up to a higher final sensible temperature (T_S) than the

PCM system (T_L). Keeping an optimal temperature helps the equipment last longer by reducing heat stress. This reduces the risk of damage, lowers maintenance costs, and makes the system safer and more reliable.

Phase change materials can be categorized based on phase transitions and chemical compositions. Solid-liquid phase change materials are widely used due to their availability, affordability, small volume changes, and high energy storage density. Organic phase change materials, like alkanes and fatty acids, offer a wide range of phase change temperatures but have drawbacks like low thermal conductivity and flammability. Inorganic phase change materials, including salts and metallics, are cost-effective with high thermal conductivity but suffer from subcooling issues and poor cycle stability. Figure 2 shows different types of PCMs.

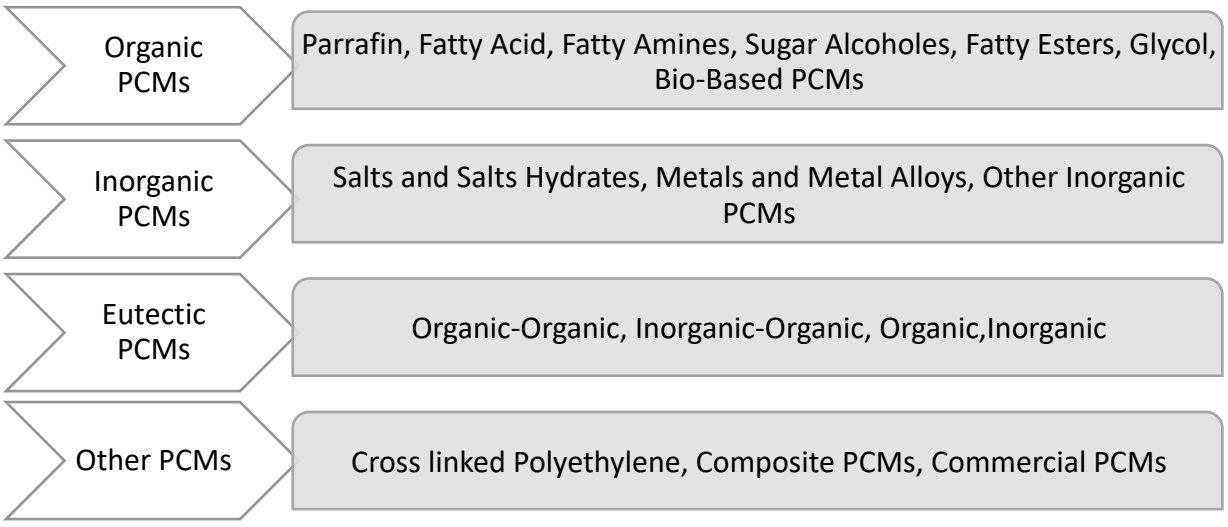

Figure 2: Different types of PCM

Composite phase change materials blend different materials to harness their combined advantages, addressing limitations of individual materials and enhancing overall performance(M. Li et al., 2024). Table 2 represents different types of PCM available with their phase change temperature and the latent heat.

Table 2: Summary of phase change temperatures and latent heat for different PCM materials.

Type	Material	Phase Change Temperature (°C)	Latent Heat (jg^{-1})	Reference
Organic	n-Nonane	-53.4	120.6	(Y. Li et al., 2021)
	n-Decane	-29.6	201.8	(Y. Li et al., 2021)

Type	Material	Phase Change Temperature (°C)	Latent Heat (jg^{-1})	Reference
	n-Undecane	-25.5	141.9	(Y. Li et al., 2021)
	Vinyl pentylcarbinol	-21.55	190.4	(Qi et al., 2022)
	Diethylene glycol	-10.4	247	(Qi et al., 2022)
	n-Dodecane	-9.6	135	(M. Li et al., 2024)
	Nonanal	-3.84	175.3	(Qi et al., 2022)
	Triethylene glycol	-7	247	(Sarkar et al., 2022)
	n-Tetradecane	5.8	227	(Y. Li et al., 2021)
	Methyl laurate	5.48	224	(Sarkar et al., 2022)
	Tetrahydrofuran	5	280	(Sarkar et al., 2022)
	Microencapsulated tetradecane	5.2	215	(Ben Taher et al., 2022a)
	Paraffin C14	5.5	228	(Ben Taher et al., 2022a)
	n-Tetradecane	5.5	215	(Ben Taher et al., 2022a)
	Formic acid	8	247	(Ben Taher et al., 2022a)
	Polyglycol E400	7.8	99.6	(Ben Taher et al., 2022a)
	Dimethyl adipate	9.7	164.6	(Y. Li et al., 2021)
	Paraffin C15	10	205	(Ben Taher et al., 2022a)
	n-Pentadecane	10	193.9	(Ben Taher et al., 2022a)
	Tetrabutyl ammonium	10	193	(Ben Taher et al., 2022a)
Inorganic	$KF{\cdot}4H_2O$	-21.2	236.1	(M. Li et al., 2024)
	H_2O	0	333	(Ben Taher et al., 2022a)
	$K_2HPO_4{\cdot}6H_2O$	4	109	(Ben Taher et al., 2022a)
	LiClO3·3H2O hydrated salt	8	253	(Ben Taher et al., 2022a)
	$LiClO_3{\cdot}3H_2O$	8	155	(Ben Taher et al., 2022a)
	$ZnCl_2{\cdot}3H_2O$	10	-	(Ben Taher et al., 2022a)

Type	Material	Phase Change Temperature (°C)	Latent Heat (jg^{-1})	Reference
Eutectic	51 wt% $ZnCl_2$-H_2O	-62	116.84	(M. Li et al., 2024)
	33.1 wt% $FeCl_3$-H_2O	-55	155.52	(M. Li et al., 2024)
	29.8 wt% $CaCl_2$-H_2O	-55	164.93	(M. Li et al., 2024)
	36 wt% $CuCl_2$-H_2O	-40	166.17	(M. Li et al., 2024)
	39.6 wt% K_2CO_3-H_2O	-36.5	165.36	(M. Li et al., 2024)
	17.1 wt% $MgCl_2$-H_2O	-33.6	221.88	(M. Li et al., 2024)
	30.5 wt% $Al(NO_3)_2$-H_2O	-30.6	207.63	(M. Li et al., 2024)
	34.6 wt% $Mg(NO_3)_2$-H_2O	-29	186.93	(M. Li et al., 2024)
	39.4 wt% $Zn(NO_3)_2$- H_2O	-29	169.88	(M. Li et al., 2024)
	32.3 wt% NH_4F-H_2O	-28.1	187.83	(M. Li et al., 2024)
	40.3 wt% NaBr-H_2O	-28	175.69	(M. Li et al., 2024)
	NaCl-$NaNO_3$-H_2O	-27	50-150	(M. Li et al., 2024)
	NaCl-KCl-H_2O	-23	260	(M. Li et al., 2024)
	21.5 wt% KF-H_2O	-21.6	227.13	(M. Li et al., 2024)
	22.4 wt% NaCl-H_2O	-21.2	228.14	(M. Li et al., 2024)
	NaCl-Na_2SO_4-H_2O	-21	200	(M. Li et al., 2024)
	25 wt% $MgCl_2$-H_2O	-19.4	223.1	(M. Li et al., 2024)
	39.7 wt% $(NH_4)_2SO_4$- H_2O	-18.5	187.75	(M. Li et al., 2024)
	36.9 wt% $NaNO_3$-H_2O	-17.7	187.75	(M. Li et al., 2024)
	8 wt% KCl-8 wt% NH_4Cl-H_2O	-17.58	280.26	(M. Li et al., 2024)
	41.2 wt% NH_4NO_3- H_2O	-17.35	186.29	(M. Li et al., 2024)
	35 wt% $Ca(NO_3)_2$-H_2O	-16	199.35	(M. Li et al., 2024)
	19.5 wt% NH_4Cl-H_2O	-16	248.44	(M. Li et al., 2024)
	36.8 wt% K_2HPO_4-H_2O	-13.5	197.79	(M. Li et al., 2024)
	30 wt% $Na_2S_2O_3$-H_2O	-11	219.86	(M. Li et al., 2024)

Type	Material	Phase Change Temperature (°C)	Latent Heat (jg^{-1})	Reference
	19.5 wt% KCl-H_2O	-10.7	253.18	(M. Li et al., 2024)
	32.2 wt% $MnSO_4$-H_2O	-10.5	213.07	(M. Li et al., 2024)
	32.4 wt% NaH_2PO_4- H_2O	-9.9	214.25	(M. Li et al., 2024)
	22.5 wt% $BaCl_2$-H_2O	-7.8	246.44	(M. Li et al., 2024)
	27.2 wt% $ZnSO_4$-H_2O	-6.5	235.75	(M. Li et al., 2024)
	24.5 wt% $Sr(NO_3)_2$- H_2O	-5.75	243.15	(M. Li et al., 2024)
	16.95 wt% $KHCO_3$-H_2O	-5.4	268.54	(M. Li et al., 2024)
	20.6 wt% $NiSO_4$-H_2O	-4.15	258.61	(M. Li et al., 2024)
	12.7 wt% Na_2SO_4-H_2O	-3.55	284.95	(M. Li et al., 2024)
	3.9 wt% NaF-H_2O	-3.5	314.09	(M. Li et al., 2024)
	19 wt% NaOH-H_2O	-2.8	265.98	(M. Li et al., 2024)
	19 wt% $MgSO_4$-H_2O	-3.9	264.42	(M. Li et al., 2024)
	9.7 wt% KNO_3-H_2O	-2.8	296.02	(M. Li et al., 2024)
	5.9 wt% Na_2CO_3-H_2O	-2.1	310.23	(M. Li et al., 2024)
	13.04 wt% $FeSO_4$-H_2O	-1.8	286.81	(M. Li et al., 2024)
	11.9 wt% $CuSO_4$-H_2O	-1.6	290.91	(M. Li et al., 2024)
	6.49 wt% K_2SO_4-H_2O	-1.55	268.8	(M. Li et al., 2024)

leading to substantial energy savings. Studies have demonstrated that PCMs can cut energy consumption in refrigerated transport systems by 35-65%, thus lowering operational costs and reducing the environmental footprint of cold chain logistics(S. Burgess et al., 2022). The ability of PCMs to store and release thermal energy also helps in stabilizing internal temperatures during power outages or equipment failures, further contributing to energy efficiency and reliability(Tan et al., 2022). Incorporating PCMs into cold chain logistics aligns with environmental sustainability goals by reducing the dependency on energy-intensive refrigeration methods. The enhanced energy efficiency provided by PCMs leads to lower greenhouse gas emissions associated with cold chain operations(Adekomaya et al., 2016). Furthermore, PCMs contribute to the development of greener logistics solutions by enabling the use of alternative energy sources and reducing the overall carbon footprint of the cold chain industry.

2.3 Insulation in Passive cold chain system

Cold chain insulation is crucial for maintaining the integrity of temperature-sensitive products, such as vaccines, pharmaceuticals, and perishable goods, during storage and transportation. Effective insulation ensures that these products remain within the required temperature ranges, preventing degradation and ensuring efficacy. This insulation helps to prevent heat exchange with the external environment, thereby preserving product quality and effectiveness. Enhancing insulation performance aims to extend the period during which products retain their potency by reducing heat transfer gradients within the insulated shipping container and minimizing heat penetration (Devrani et al., 2021a). The low heat penetration rate (HPR) enhances the packaging's insulating capabilities. One way to test the insulation performance is by ice melt test to extract heat penetration rate (Zeng et al., 2022). The most common types are non-biodegradable insulations (Zhao et al., 2020).

$$HPR = \frac{(Water\ Weight)\ X\ (Latent\ Heat\ of\ Ice)}{(Melt\ Time)\ X\ (Outside\ Temperature - PCM\ Temperature)}$$

The thermal performance of insulated shipping containers is influenced by the packaging materials, container size, and insulation(Ng et al., 2020). Insulation is a critical design parameter in passive cold chain packaging because it governs the rate of heat transfer from external environments into the payload chamber, directly affecting hold-time performance for temperature-sensitive products. Conventional passive shippers commonly utilize expanded polystyrene (EPS) and polyurethane (PU) foams due to their low thermal conductivity, ease of fabrication, and

low cost; however, their performance declines when subjected to sustained temperature gradients and prolonged exposure durations(Wang et al., 2020). Previous studies show that insulation effectiveness depends not only on thermal conductivity but also on density, cell structure, and moisture absorption, with open-cell polymer foams exhibiting sensitivity to humidity-driven conductivity increases. These limitations have motivated research into composite insulation systems and alternative materials with more stable thermal resistance profiles over time(Baetens et al., 2011). One emerging class of high-performance insulation is silica aerogel, which features nano-porous morphology and extremely low thermal conductivity (<0.020 W/m·K), enabling thinner panels and lower mass compared to polymer foams. Aerogel blankets maintain performance across broad temperature gradients, and hybrid reinforcement strategies have been proposed to improve durability in packaging contexts(Baetens et al., 2011).

However, fiber-based insulation remains attractive due to recyclability, biodegradability, and lower carbon footprint when compared to EPS and PU systems, making it a growing candidate for sustainable cold-chain packaging. Life-cycle assessments suggest that this environmental advantage may outweigh moderate performance penalties when the transport duration is predictable and ambient exposure is moderate(Ren et al., 2022a). To extend hold time without significant bulk, vacuum insulated panels (VIPs) have gained interest in pharmaceutical distribution. VIPs provide superior thermal performance, but cost, fragility, and edge-seal degradation remain barriers to large-scale adoption. Studies indicate that hybridization of VIPs with PCM-based liners can further reduce thermal ingress during transient spikes(Baetens et al., 2011).

Computational modeling demonstrates that insulation thickness and geometry strongly influence transient heat conduction, particularly in corner regions where thermal bridging accelerates warming. Numerical simulations therefore assist designers in optimizing panel configuration and prioritizing insulation placement based on heat flux patterns(Zhai et al., 2013a).

Finally, sustainability pressures are accelerating the transition away from traditional foam-based insulation toward recyclable or compostable composites. The cold chain sector increasingly evaluates not only heat-transfer efficiency but also end-of-life disposal, packaging mass, regulatory compliance, and carbon emissions. Researchers argue that next-generation insulation must balance performance, environmental impact, and cost while maintaining manufacturability and thermal reliability(Ren et al., 2022a).

2.4 Modelling of Passive cold chain system

Early research on passive cold chain systems shows that compact energy-balance models and one-dimensional conduction equations with latent-heat terms can predict the thermal behavior of insulated shippers containing phase change materials. These models are commonly applied to estimate hold time and time-to-threshold conditions because they generate meaningful results with low computational effort. One example is a two-dimensional transient model combined with steady-state elements that was validated against ice-melt experiments and produced good agreement with temperature patterns observed along common shipping profiles while remaining computationally efficient. Building on this approach, other studies have introduced simplified heat transfer models that estimate spatial and temporal temperature variations in real time. Although these models sacrifice some spatial detail, they are faster and suitable for supervisory decision-making during transport(Kucharek et al., 2020; Leungtongkum et al., 2023). Compact modelling approaches rely on the enthalpy method, often referred to as the apparent heat-capacity method, which incorporates phase change into the mathematical energy balance and forms a standard basis for passive packaging simulations(Kong et al., 2022).

In settings where extensive chamber test data are available, empirical regressions and reduced-order surrogate models are often developed. These models relate measurable variables, including ambient temperature severity, insulation type, PCM mass, and payload size, to predicted hold time. Recent work has applied artificial neural networks trained on both simulation outputs and real shipment data to forecast temperature trajectories and remaining safe time without running a full physics-based simulation(Bhatt et al., 2024a). Some studies further identify system parameters during operation to support real-time prediction, route selection, or adjustments to PCM use(Leungtongkum et al., 2023). These empirical methods are generally calibrated using chamber-controlled temperature cycles and later verified using simulated shipping lanes, making them practical tools for packaging engineers.

For more detailed design work, numerical simulations are used to resolve multi-layer heat conduction through insulation and latent-heat effects in PCMs, sometimes incorporating internal natural convection and external radiative heat transfer. Comparisons between experimental results, one-dimensional enthalpy models, and computational fluid dynamics simulations show that enthalpy-based solvers capture overall freezing and melting behavior, whereas CFD offers additional insight into localized temperature patterns that influence pack placement(Borri et al., 2020a). Reviews of thermal energy storage modelling summarize the numerical techniques used in this context, including enthalpy, effective heat-capacity, and front-tracking methods, and also provide guidance on mesh resolution, time-step selection, and convergence(Heim & Kułakowski, 2023). Modern enthalpy solvers often linearize the temperature–enthalpy curve and iterate to a stable solution, as presented in recent open-

access modelling work(Kong et al., 2022). In practice, validated simulation workflows are now used to reduce the number of environmental chamber trials required before qualification by allowing engineers to adjust insulation thickness, PCM mass, and pack placement virtually(Formato et al., 2010a).

Hybrid modelling pipelines have emerged in recent years. In this approach, high-fidelity physics-based models are used to generate synthetic thermal data that trains faster surrogate predictors or neural networks. These models can then evaluate different transport scenarios, monitor temperature conditions during shipment, and estimate remaining safe time in real time(Bhatt et al., 2024a). Cold chain monitoring literature highlights the importance of pairing modelling approaches with digital sensors and structured excursion management to limit product waste(Badia-Melis et al., 2018).

Several studies have evaluated the performance of passively cooled insulated containers(Ge et al., 2014a; Wang et al., 2020; Zanoni et al., 2019; Zeng et al., 2022). Burgess(G. Burgess, 1999) developed equations to calculate the thermal resistance (R-value) of packaging. These equations, derived through ice melt tests and adjusted via linear regression, considered factors such as the packing material, wall thickness, container geometry, and design. The model was used to estimate time within temperature specifications for specific packages, with estimated results falling typically within 20% of actual times measured in laboratory tests. However, this approach showed limitations that required multiple tests to build a database for various packaging models. Choi(Choi & Burgess, 2007) took a theoretical approach by developing a two-dimensional (2D) steady-state model to calculate the heat penetration rate (HPR), which measures energy transfer per degree of temperature difference. While this model accurately assesses the insulation performance of the package, it did not fully account for changes over time. Zeng et al. (Zeng et al., 2022) developed a mathematical model to study how aluminium foil affects packaging insulation in cold chain logistics. This study developed the concept of "maximum insulation time" (MIT) to measure the thermal performance of packaging. The authors showed that the addition of aluminium foil to the inner surface of insulation improved performance by over 25%, making evident the significance of radiation heat transfer even inside the packages. Singh(Singh et al., 2013) conducted experiments with insulation materials of varying densities and thicknesses to assess their thermal resistance. By analysing different material types, Singh found that Vacuum Insulation Panels (VIPs) exhibited the highest thermal resistance of the materials and variations tested, followed by polyurethane, recycled EPS, and virgin EPS. Specifically, for a one-inch-thick container, VIPs demonstrated a 128% and 267% improvement in thermal resistance compared to polyurethane and virgin EPS, respectively. Ge(Ge et al., 2013a) developed a Finite Element Analysis (FEA) to predict temperature changes in insulated packaging. It found partial agreement between field-measured and FEA-predicted temperatures. Both

field data and FEA simulations show that temperatures initially drop below 0°C before stabilizing above freezing. Using XPS foam containers, the duration of sub-zero temperatures depends on the gel packs' starting temperature, the empty space in the container, and the insulation materials. To prevent vaccines from freezing, the authors recommended to adjust the gel packs' initial temperatures and control the release of cold air. The risk of freezing mainly occurs during the first few hours after packing.

When focusing specifically on the use of fibre-based insulation, research interest and development of commercial products has increased considerably(*Fiber-Based Packaging Market Size, Volume & Export Data*, n.d.). Driven by consumer preferences, the introduction of new regulations and advancements in the development of higher performance insulations, the proliferation of fibre-based and other alternative materials in the passive cold chain must be carefully studied to ensure successful adoption. As shown in the past research, most of it has been conducted using petroleum-based materials and considerations of important factors such as humidity effects have not been widely present.

To address these challenges, recent advancements in cold chain logistics have focused on integrating digital technologies such as the Internet of Things (IoT), blockchain, and artificial intelligence (AI). IoT-enabled sensors provide real-time monitoring of temperature conditions, allowing for immediate corrective actions when deviations occur(Qian et al., 2022). Blockchain technology enhances traceability and transparency by creating a tamper-proof record of transactions, reducing fraud and ensuring regulatory compliance(Ren et al., 2022a). AI-based predictive analytics can further optimize logistics operations by forecasting potential disruptions and suggesting alternative transportation routes to minimize delays(Shi et al., 2024). While these technologies offer promising solutions, their widespread adoption is hindered by high implementation costs, data security concerns, and the need for industry-wide standardization(Zhang & Mohammad, n.d.). Another emerging trend in cold chain logistics is the adoption of joint distribution models, where multiple companies collaborate to share storage and transportation resources. This approach optimizes supply chain efficiency by reducing costs and minimizing carbon emissions associated with separate transportation networks(Shi et al., 2024). Additionally, smart packaging solutions, such as temperature-sensitive labels and biodegradable insulation, have been developed to enhance product protection while addressing environmental concerns(Zhang & Mohammad, n.d.). Despite these advancements, regulatory barriers, lack of industry collaboration, and economic constraints continue to pose challenges to large-scale implementation.

2.5 Standards

Thermal performance standards play a critical role in ensuring the safe storage and transport of temperature-sensitive goods throughout the passive cold chain, and several international guidance documents define expectations for packaging qualification, distribution practices, monitoring, and excursion management. ISO 23412:2020 provides service requirements for indirect temperature-controlled refrigerated delivery of parcels transported by land, outlining operational responsibilities, handover conditions, documentation, and process traceability to maintain temperature during multi-stop distribution. However, the scope is service-oriented and does not prescribe specific test profiles for insulated shipping systems(*ISO 23412:2020(En), Indirect, Temperature-Controlled Refrigerated Delivery Services — Land Transport of Parcels with Intermediate Transfer*, n.d.). ISO 21973:2020 covers the transportation of cells for therapeutic use and emphasizes chain-of-custody, monitoring responsibility, emergency contingency, and transport container qualification, which is critical for advanced therapy products sensitive to minor thermal deviations(*ISO 21973:2020(En), Biotechnology — General Requirements for Transportation of Cells for Therapeutic Use*, n.d.). Like ISO 23412, these standard addresses transport processes rather than laboratory thermal testing, requiring users to pair it with packaging qualification standards such as the International Safe Transit Association (ISTA) or ASTM. In practice, the most widely referenced thermal test profiles is published by ISTA. ISTA 7E provides standardized environmental chamber temperature profiles derived from aggregated field lane data for small-parcel distribution. These repeated hot, cold, and cyclic profiles allow consistent operational qualification of insulated shippers under controlled laboratory conditions and enable comparison among commercial solutions, although route-specific profiles may still be required when risk assessments identify unique exposure patterns(International Safe Transit Assocoation (ISTA), 2010). ISTA Standard 20 complements ISTA 7E by outlining the design, documentation, verification, calibration, and laboratory certification processes necessary to qualify insulated shipping containers. Rather than dictating temperature profiles, ISTA 20 defines the qualification workflow, data integrity requirements, and auditability necessary for pharmaceutical compliance.

ASTM standards also support thermal qualification. ASTM D3103 defines a laboratory method for quantifying the thermal insulation performance of insulated shipping containers by exposing packages to controlled external conditions and measuring internal product temperatures. This method offers versatility and allows custom temperature plateaus or steps valuable in research and development; however, users must define their own exposure schedule because the standard does not provide field-derived thermal profiles(*Standard Test Method for Thermal Insulation Performance of Distribution Packages*, n.d.). While ISTA and ASTM focus on package-level

performance, quality-system guidance documents such as PDA Technical Report 39 provide comprehensive expectations for temperature-controlled medicinal product distribution. PDA TR 39 addresses risk assessment, excursion management, qualification strategy, monitoring plans, documentation, and deviation investigation, making it foundational for quality groups seeking alignment between packaging validation and operational logistics(*PDA Technical Report No. 39 Revised 2021 (TR 39) Guidance for Temperature-Controlled Medicinal Products - Maintaining the Quality of Temperature-Sensitive Medicinal Products through the Transportation Environment (Single User Digital Version)*, n.d.). The World Health Organization further supports global cold chain operations with Technical Report Series 961 Annex 9, offering risk-based guidance for storage, transport, receipt, inspection, equipment qualification, monitoring, and operational controls for time- and temperature-sensitive pharmaceutical products. This document is widely adopted by public health authorities, humanitarian organizations, and national ministries where regulatory infrastructure is developing (*TRS 961 - Annex 9*, n.d.) Within the European Union, Good Distribution Practice (GDP) guidelines establish legal expectations for distribution of medicinal products, requiring temperature mapping of storage areas, controlled transport conditions, documentation, and oversight of third-party logistics providers. GDP outlines system-level controls but does not define laboratory temperature profiles, meaning insulated package qualification is typically demonstrated through ISTA or ASTM testing.

The United States Pharmacopeia (USP) general chapters provide additional regulatory alignment. USP <1079> addresses good storage and distribution practices, including excursion assessment, packaging controls, and risk-based strategies. USP <1079.2> describes how mean kinetic temperature can be appropriately applied to evaluate aggregate thermal stress during excursions, and USP <1079.3> defines expectations for selecting, qualifying, and calibrating monitoring devices, such as data loggers. USP <659> defines official storage conditions such as controlled room temperature, refrigerated, and frozen, and clarifies expectations for packaging used to maintain these conditions(*US Pharmacopeia (USP)*, n.d.). Air transport introduces additional regulatory layers. IATA's Temperature Control Regulations (TCR) specify handling requirements, labeling conventions, acceptance checks, and operational responsibilities for healthcare products carried by air. Aircraft ground handling poses elevated excursion risks due to tarmac exposure, and TCR provides standardized procedures to mitigate these hazards (*Temperature Control Regulations (TCR)*, n.d.). For food, plants, and other perishables, the IATA Perishable Cargo Regulations (PCR) govern recommended packaging, documentation, and transport handling, acting as the primary reference for non-pharmaceutical perishables

Taken together, these standards form a layered framework. ISTA 7E provides temperature profiles for laboratory operational qualifications, while ISTA Standard 20 defines how the qualification process should be executed. ASTM D3103 enables custom thermal testing beyond standardized profiles. PDA TR 39, WHO guidelines, and GDP chapters establish quality-system expectations for documentation, deviation management, and monitoring. USP chapters define storage terminology, excursion analysis methods, and monitoring device requirements. ISO 23412 and ISO 21973 govern process-level transport operations, while IATA regulations establish expectations for air-cargo handling. No single document is sufficient in isolation, and organizations typically combine these standards to satisfy product-label claims, regulatory expectations, risk-based transport design, and global distribution models. Collectively, these standards ensure that insulated passive shipping systems are qualified in controlled laboratory environments, monitored during distribution, and supported by documented quality systems to maintain product integrity across complex, multi-modal cold chain networks.

3 References

Adekomaya, O., Jamiru, T., Sadiku, R., & Huan, Z. (2016). Sustaining the shelf life of fresh food in cold chain – A burden on the environment. Alexandria Engineering Journal, 55(2), 1359–1365. https://doi.org/10.1016/j.aej.2016.03.024

Badia-Melis, R., Carthy, U. M., Ruiz-Garcia, L., Garcia-Hierro, J., & Villalba, J. I. R. (2018). New trends in cold chain monitoring applications—A review. Food Control, 86, 170–182. https://doi.org/10.1016/j.foodcont.2017.11.022

Baetens, R., Jelle, B. P., & Gustavsen, A. (2011). Aerogel insulation for building applications: A state-of-the-art review. Energy and Buildings, 43(4), 761–769. https://doi.org/10.1016/j.enbuild.2010.12.012

Ben Taher, M. A., Ahachad, M., Mahdaoui, M., Zeraouli, Y., & Kousksou, T. (2022). A survey of computational and experimental studies on refrigerated trucks. Journal of Energy Storage, 47, 103575. https://doi.org/10.1016/j.est.2021.103575

Bhatt, T., Baser, M., Tyagi, A., & Ng, E. Y. K. (2024). CRYOMOVE: Cold chain real-time management of vaccine delivery using PCM and deep learning. Applied Thermal Engineering, 255, 123962. https://doi.org/10.1016/j.applthermaleng.2024.123962

Bogataj, M., Bogataj, L., & Vodopivec, R. (2005). Stability of perishable goods in cold logistic chains. International Journal of Production Economics, 93–94, 345–356. https://doi.org/10.1016/j.ijpe.2004.06.032

Borri, E., Sze, J. Y., Tafone, A., Romagnoli, A., Li, Y., & Comodi, G. (2020). Experimental and numerical characterization of sub-zero phase change materials for cold thermal energy storage. Applied Energy, 275, 115131. https://doi.org/10.1016/j.apenergy.2020.115131

Burgess, G. (1999). Practical thermal resistance and ice requirement calculations for insulating packages. Packaging Technology and Science, 12(2), 75–80. https://doi.org/10.1002/(SICI)1099-1522(199903/04)12:2%253C75::AID-PTS454%253E3.0.CO;2-2

Burgess, S., Wang, X., Rahbari, A., & Hangi, M. (2022). Optimisation of a portable phase-change material (PCM) storage system for emerging cold-chain delivery applications. Journal of Energy Storage, 52, 104855. https://doi.org/10.1016/j.est.2022.104855

Cabeza, L. F., Castell, A., Barreneche, C., De Gracia, A., & Fernández, A. I. (2011). Materials used as PCM in thermal energy storage in buildings: A review. Renewable and Sustainable Energy Reviews, 15(3), 1675–1695. https://doi.org/10.1016/j.rser.2010.11.018

Calati, M., Hooman, K., & Mancin, S. (2022). Thermal storage based on phase change materials (PCMs) for refrigerated transport and distribution applications along the cold chain: A review. International Journal of Thermofluids, 16, 100224. https://doi.org/10.1016/j.ijft.2022.100224

Carson, J. K., & East, A. R. (2018). The cold chain in New Zealand – A review. International Journal of Refrigeration, 87, 185–192. https://doi.org/10.1016/j.ijrefrig.2017.09.019

Choi, S.-J., & Burgess, G. (2007). Practical Mathematical Model to Predict the Performance of Insulating Packages. Packaging Technology and Science, 20(6), 369–380. https://doi.org/10.1002/pts.762

Chowdhury, D. A., Jeong, M. S., Vyas, L., Kim, J., Cosler, L. E., Lash, D. J., Barone, J. A., Toscani, M., & Volino, L. R. (2023). Evaluation of temperature excursions from USP recommendations during mail transit. Journal of the American Pharmacists Association, 63(3), 847–852. https://doi.org/10.1016/j.japh.2023.02.002

Coombs, C. E. O., Holman, B. W. B., Friend, M. A., & Hopkins, D. L. (2017). Long-term red meat preservation using chilled and frozen storage combinations: A review. Meat Science, 125, 84–94. https://doi.org/10.1016/j.meatsci.2016.11.025

D10 Committee. (n.d.). Test Method for Thermal Insulation Performance of Distribution Packages. ASTM International. https://doi.org/10.1520/D3103-14

Devrani, S., Tiwari, R., Khan, N., Sankar, K., Patil, S., & Sridhar, K. (2021). Enhancing the insulation capability of a vaccine carrier box: An engineering approach. Journal of Energy Storage, 36, 102182. https://doi.org/10.1016/j.est.2020.102182

E-Commerce: United States - Unbiased Analysis, Market Size, Industry Output, Segment-By-Segment Forecasts, Market Leaders, Leading Brands, Market Drivers, Market Trends, US and World Topics, Data Visualization, Easy-To-Use Knowledge Center. (n.d.). The Freedonia Group. Retrieved November 3, 2025, from https://www.freedoniagroup.com/freedonia-focus/e-commerce-united-states-ff90043.htm

Fahrni, M. L., Ismail, I. A.-N., Refi, D. M., Almeman, A., Yaakob, N. C., Saman, K. M., Mansor, N. F., Noordin, N., & Babar, Z.-U.-D. (2022). Management of COVID-19 vaccines cold chain logistics: A scoping review. Journal of Pharmaceutical Policy and Practice, 15(1), 16. https://doi.org/10.1186/s40545-022-00411-5

Fiber-based Packaging Market Size, Volume & Export Data. (n.d.). Retrieved December 1, 2024, from https://www.towardspackaging.com/insights/fiber-based-packaging-market-sizing

Formato, R. M., Potami, R., & Ahmed, I. (2010). Use of Advanced Modeling Techniques To Optimize Thermal Packaging Designs. PDA Journal of Pharmaceutical Science and Technology, 64(6), 545.

Ge, C., Cheng, Y., & Li, B. (2014). Numerical simulation and experimental study of the heat transition in a foam container. Journal of Cellular Plastics, 50(1), 15–36. https://doi.org/10.1177/0021955X13503846

Ge, C., Cheng, Y., & Shen, Y. (2013). Application of the Finite Elemental Analysis to Modeling Temperature Change of the Vaccine in an Insulated Packaging Container during Transport. PDA Journal of Pharmaceutical Science and Technology, 67(5), 544–552. https://doi.org/10.5731/pdajpst.2013.00937

Heim, D., & Kułakowski, T. (2023). Thermal model of heat transfer in a PCM multilayer construction using Moving Mushy Volume Approach – verification, validation and sensitivity analysis. Journal of Building Performance Simulation, 16(3), 308–326. https://doi.org/10.1080/19401493.2022.2138548

Ilangovan, A., Hamdane, S., Silva, P. D., Gaspar, P. D., & Pires, L. (2022). Promising and Potential Applications of Phase Change Materials in the Cold Chain: A Systematic Review. Energies, 15(20), 7683. https://doi.org/10.3390/en15207683

International Safe Transit Assocoation (ISTA). (2010). ISTA 7E - Testing Standard for Thermal Transport Packaging Used in Parcel Delivery System Shipment [Standard]. https://ista.org/thermal_standards.php

ISO 21973:2020(en), Biotechnology—General requirements for transportation of cells for therapeutic use. (n.d.). Retrieved November 2, 2025, from https://www.iso.org/obp/ui/en/#iso:std:iso:21973:ed-1:v1:en

ISO 23412:2020(en), Indirect, temperature-controlled refrigerated delivery services—Land transport of parcels with intermediate transfer. (n.d.). Retrieved August 11, 2025, from https://www.iso.org/obp/ui/es/#iso:std:iso:23412:ed-1:v1:en

Jayalath, P., Ananthakrishnan, K., Jeong, S., Shibu, R. P., Zhang, M., Kumar, D., Yoo, C. G., Shamshina, J. L., & Therasme, O. (2025). Bio-Based Polyurethane Materials: Technical, Environmental, and Economic Insights. Processes, 13(5), 1591. https://doi.org/10.3390/pr13051591

Kartoglu, U., Vesper, J., Teräs, H., & Reeves, T. (2017). Experiential and authentic learning approaches in vaccine management. Vaccine, 35(17), 2243–2251. https://doi.org/10.1016/j.vaccine.2016.11.104

Kong, W., Wang, G., Englmair, G., Nielsen, E. N. N., Dragsted, J., Furbo, S., & Fan, J. (2022). A simplified numerical model of PCM water energy storage. Journal of Energy Storage, 55, 105425. https://doi.org/10.1016/j.est.2022.105425

Kucharek, M., Yang, L., & Wang, K. (2020). Assessment of insulating package performance by mathematical modelling. Packaging Technology and Science, 33(2), 65–73. https://doi.org/10.1002/pts.2492

Kumar Deb, R. (2023). Temperature Sensitive Packaging Market Share, Size and Forecast 2030 (No. 19375). Credence Research, Inc. https://www.credenceresearch.com/report/temperature-sensitive-packaging-market

Leungtongkum, T., Laguerre, O., & Flick, D. (2023). Simplified heat transfer model for real-time temperature prediction in insulated boxes equipped with a phase change material. International Journal of Refrigeration, 149, 286–298. https://doi.org/10.1016/j.ijrefrig.2023.02.009

Li, M., Xie, B., Li, Y., Cao, P., Leng, G., & Li, C. (2024). Emerging phase change cold storage technology for fresh products cold chain logistics. Journal of Energy Storage, 88, 111531. https://doi.org/10.1016/j.est.2024.111531

Li, Y., Yang, D., Xie, J., & Wang, J. (2021). Review on research and application of phase change materials in cold storage refrigerator. IOP Conference Series: Earth and Environmental Science, 766(1), 012094. https://doi.org/10.1088/1755-1315/766/1/012094

Matsunaga, K., Burgess, G., & Lockhart, H. (2007). Two methods for calculating the amount of refrigerant required for cyclic temperature testing of insulated packages. Packaging Technology and Science, 20(2), 113–123. https://doi.org/10.1002/pts.747

Meal Kits: United States - Unbiased Analysis, Market Size, Industry Output, Segment-By-Segment Forecasts, Market Leaders, Leading Brands, Market Drivers, Market Trends, US and World Topics, Data Visualization, Easy-To-Use Knowledge Center. (n.d.). The Freedonia Group. Retrieved November 3, 2025, from https://www.freedoniagroup.com/freedonia-focus/meal-kits-united-states-ff10060.htm

Meng, B., Zhang, X., Hua, W., Liu, L., & Ma, K. (2022). Development and application of phase change material in fresh e-commerce cold chain logistics: A review. Journal of Energy Storage, 55, 105373. https://doi.org/10.1016/j.est.2022.105373

Mercier, S., Villeneuve, S., Mondor, M., & Uysal, I. (2017). Time–Temperature Management Along the Food Cold Chain: A Review of Recent Developments. Comprehensive Reviews in Food Science and Food Safety, 16(4), 647–667. https://doi.org/10.1111/1541-4337.12269

Ng, C. Z., Lean, Y. L., Yeoh, S. F., Lean, Q. Y., Lee, K. S., Suleiman, A. K., Liew, K. B., Kassab, Y. W., Al-Worafi, Y. M., & Ming, L. C. (2020). Cold chain time- and temperature-controlled transport of vaccines: A simulated experimental study. Clinical and Experimental Vaccine Research, 9(1), 8. https://doi.org/10.7774/cevr.2020.9.1.8

Noël, J. A. (2016). Chapter 13—Phase Change Materials. In Storing Energy. https://doi-org.ezproxy.lib.vt.edu/10.1016/B978-0-12-803440-8.00013-0

Oró, E., De Gracia, A., Castell, A., Farid, M. M., & Cabeza, L. F. (2012). Review on phase change materials (PCMs) for cold thermal energy storage applications. Applied Energy, 99, 513–533. https://doi.org/10.1016/j.apenergy.2012.03.058

Pambudi, N. A., Sarifudin, A., Gandidi, I. M., & Romadhon, R. (2022). Vaccine cold chain management and cold storage technology to address the challenges of vaccination programs. Energy Reports, 8, 955–972. https://doi.org/10.1016/j.egyr.2021.12.039

PDA Technical Report No. 39 Revised 2021 (TR 39) Guidance for Temperature-Controlled Medicinal Products—Maintaining the Quality of Temperature-Sensitive Medicinal Products through the Transportation Environment (single user digital version). (n.d.). Default. Retrieved August 11, 2025, from https://www.pda.org/bookstore/product-detail/6280-tr-39-revised-2021

Pharmaceutical Cold Chain Packaging Market Demand 2025 to 2035. (n.d.). Retrieved October 21, 2025, from https://www.futuremarketinsights.com/reports/pharmaceutical-cold-chain-packaging-market

Qi, T., Ji, J., Zhang, X., Liu, L., Xu, X., Ma, K., & Gao, Y. (2022). Research progress of cold chain transport technology for storage fruits and vegetables. Journal of Energy Storage, 56, 105958. https://doi.org/10.1016/j.est.2022.105958

Qian, J., Yu, Q., Jiang, L., Yang, H., & Wu, W. (2022). Food cold chain management improvement: A conjoint analysis on COVID-19 and food cold chain systems. Food Control, 137, 108940. https://doi.org/10.1016/j.foodcont.2022.108940

Rahman, M., Sikandar, M. U., Chowdhury, P., Roy, S., & Khrystoslavenko, O. (2025). Toward Sustainable Cold Chain Packaging: A Systematic Review of Insulating Materials and Green Alternatives for Temperature-Sensitive Logistics.

Raj, R., Singh, A., Kumar, V., De, T., & Singh, S. (2024). Assessing the e-commerce last-mile logistics' hidden risk hurdles. Cleaner Logistics and Supply Chain, 10, 100131. https://doi.org/10.1016/j.clscn.2023.100131

Ramakanth, D., Singh, S., Maji, P. K., Lee, Y. S., & Gaikwad, K. K. (2021). Advanced packaging for distribution and storage of COVID-19 vaccines: A review. Environmental Chemistry Letters, 19(5), 3597–3608. https://doi.org/10.1007/s10311-021-01256-1

Raval, A. H., Solanki, S. C., & Yadav, R. (2013). A simplified heat transfer model for predicting temperature change inside food package kept in cold room. Journal of Food Science and Technology, 50(2), 257–265. https://doi.org/10.1007/s13197-011-0342-z

Ren, T., Ren, J., Matellini, D. B., & Ouyang, W. (2022). A Comprehensive Review of Modern Cold Chain Shipping Solutions. Sustainability, 14(22), 14746. https://doi.org/10.3390/su142214746

Sarkar, S., Mestry, S., & Mhaske, S. T. (2022). Developments in phase change material (PCM) doped energy efficient polyurethane (PU) foam for perishable food cold-storage applications: A review. Journal of Energy Storage, 50, 104620. https://doi.org/10.1016/j.est.2022.104620

Sharma, A., Tyagi, V. V., Chen, C. R., & Buddhi, D. (2009). Review on thermal energy storage with phase change materials and applications. Renewable and Sustainable Energy Reviews, 13(2), 318–345. https://doi.org/10.1016/j.rser.2007.10.005

Shi, H., Zhang, Q., & Qin, J. (2024). Cold Chain Logistics and Joint Distribution: A Review of Fresh Logistics Modes. Systems, 12(7), 264. https://doi.org/10.3390/systems12070264

Singh, J., Jaggia, S., & Saha, K. (2013). The Effect of Distribution on Product Temperature Profile in Thermally Insulated Containers for Express Shipments. Packaging Technology and Science, 26(6), 327–338. https://doi.org/10.1002/pts.1985

Spychaj, A., Pospiech, E., Iwańska, E., & Montowska, M. (2018). Detection of allergenic additives in processed meat products. Journal of the Science of Food and Agriculture, 98(13), 4807–4815. https://doi.org/10.1002/jsfa.9083

Standard Test Method for Thermal Insulation Performance of Distribution Packages. (n.d.). Retrieved November 2, 2025, from https://store.astm.org/d3103-20.html

Sustainable Cold Chain and Food Loss Reduction. (2019). UN-environmantal programme. https://ozone.unep.org/system/files/documents/MOP31-Sustainable-HL_Briefing_Note.pdf

Sykes, C. (n.d.). Time- and Temperature-Controlled Transport: Supply Chain Challenges and Solutions.

Tan, M., Ding, Z., Yang, D., & Xie, J. (2022). The quality properties of frozen large yellow croaker fillets during temperature fluctuation cycles: Improvement by cellobiose and carboxylated cellulose nanofibers. International Journal of Biological Macromolecules, 194, 499–509. https://doi.org/10.1016/j.ijbiomac.2021.11.093

Temperature Control Regulations (TCR). (n.d.). Retrieved November 2, 2025, from https://www.iata.org/en/publications/manuals/temperature-control-regulations/

The Future of Grocery Report: Online Grocery, Meal Kits, & Direct-to-Consumer Food | Packaged Facts. (n.d.). The Freedonia Group. Retrieved November 3, 2025, from https://www.freedoniagroup.com/packaged-facts/future-of-grocery-online-grocery-meal-kits-direct-to-consumer-food

TRS 961 - Annex 9: Model guidance for the storage and transport of time and temperature sensitive pharmaceutical products. (n.d.). Retrieved November 2, 2025, from https://www.who.int/publications/m/item/trs961-annex9-modelguidanceforstoragetransport

UN Environment Programme. (2019, November). Sustainable Cold Chain and Food Loss Reduction. https://ozone.unep.org/system/files/documents/MOP31-Sustainable-HL_Briefing_Note.pdf

US Pharmacopeia (USP). (n.d.). Retrieved November 2, 2025, from https://www.usp.org/

Van Boxstael, S., Habib, I., Jacxsens, L., De Vocht, M., Baert, L., Van De Perre, E., Rajkovic, A., Lopez-Galvez, F., Sampers, I., Spanoghe, P., De Meulenaer, B., & Uyttendaele, M. (2013). Food safety issues in fresh produce: Bacterial pathogens, viruses and pesticide residues indicated as major concerns by stakeholders in the fresh produce chain. Food Control, 32(1), 190–197. https://doi.org/10.1016/j.foodcont.2012.11.038

Wang, K., Yang, L., & Kucharek, M. (2020). Investigation of the effect of thermal insulation materials on packaging performance. Packaging Technology and Science, 33(6), 227–236. https://doi.org/10.1002/pts.2500

Zanoni, S., Mazzoldi, L., & Ferretti, I. (2019). Eco-efficient cold chain networks design. International Journal of Sustainable Engineering, 12(5), 349–364. https://doi.org/10.1080/19397038.2018.1538268

Zeng, T., Jiang, H., & Hao, F. (2022). Study on the effect of aluminium foil on packaging thermal insulation performance in cold chain logistics. Packaging Technology and Science, 35(5), 395–403. https://doi.org/10.1002/pts.2637

Zhai, X. Q., Wang, X. L., Wang, T., & Wang, R. Z. (2013). A review on phase change cold storage in air-conditioning system: Materials and applications. Renewable and Sustainable Energy Reviews, 22, 108–120. https://doi.org/10.1016/j.rser.2013.02.013

Zhang, B., & Mohammad, J. (n.d.). Sustainability of Perishable Food Cold Chain Logistics: A Systematic Literature Review. SAGE Open.

Zhao, Y., Zhang, X., Xu, X., & Zhang, S. (2020). Research progress of phase change cold storage materials used in cold chain transportation and their different cold storage packaging structures. Journal of Molecular Liquids, 319, 114360. https://doi.org/10.1016/j.molliq.2020.114360

4 Chapter 1: Predicting the thermal performance of bio-based cold chain packaging systems through finite element modelling for passively cooled containers

Abstract: This study investigates the performance of insulated shipping containers (ISCs) for temperature-sensitive products through the development of a finite element model (FEM) to optimize the verification processes. ISCs are critical for transporting sensitive goods such as pharmaceuticals and perishable foods, yet traditional preliminary performance evaluation methods are both time-consuming and resource intensive. Additionally, the extensive use of non-biodegradable insulation materials exacerbates environmental concerns, emphasizing the need for sustainable alternatives. This research establishes a material analysis foundation for FEM-based heat transfer modelling by characterizing the thermal properties of ISC components. Differential Scanning Calorimetry (DSC) and the Heat Flow Meter methods were used to characterize the thermal properties of the components used to build the ISCs. This characterization provides critical input parameters for FEM simulations to replicate the thermal performance across various supply chain scenarios. This study includes analysis of corrugated packaging components, and Phase Change Materials (PCMs) while exploring the integration of eco-friendly insulation alternatives to ensure optimal shipment conditions and sustainability. Results demonstrate strong correlation between FEM simulations and experimental validations, with mean prediction deviations ranging from 4% (double-wall corrugated insulation) to 8% (honeycomb insulation) when maintaining temperatures below critical thresholds (8°C). These results confirm that FEM-based predictions provide high accuracy for bio-based insulated shipping container performance, significantly reducing prototyping and verification resources compared to traditional methods. Furthermore, the incorporation of biodegradable insulation materials addresses environmental challenges by promoting eco-friendly cold chain packaging solutions. This research provides a robust framework for material analysis and thermal modelling, offering practical and scalable solutions to enhance cold chain efficiency while minimizing environmental impact.

Keywords: cold chain, insulated shipping container, insulation, phase change material (PCM), finite element modelling.

4.1 Introduction

Fluctuations in storage temperature can significantly affect the quality of perishable goods, including fresh foods and pharmaceuticals(Van Boxstael et al., 2013). To keep products safe during transport and storage, it is important to control their temperature and the environment around them(Kucharek et al., 2020). In the pharmaceutical sector, it's anticipated that the volume of temperature-sensitive products will keep rising. As an example, the Food and Drug Administration (FDA) is increasingly focused on cold chain shipping to address the growing importance of managing these temperature-sensitive products(Matsunaga et al., 2007). When referring to fresh produce, post-harvest losses for some temperature-sensitive produce can reach up to 50% due to insufficient access to cold chain logistics(*Sustainable Cold Chain and Food Loss Reduction*, 2019).

Cold chain systems include designing the insulated shipping containers (ISCs), monitoring in the distribution network and the storage to keep temperature-sensitive products safe and maintain their quality throughout the entire supply process(Kartoglu et al., 2017). Active cold chain distribution employs refrigerated storage containers to consistently maintain the required temperatures during distribution[6]. Refrigerated trucks contribute approximately 2.5% of global Greenhouse Gas (GHG) emissions by using high-Global Warming Potential (GWP) refrigerants and relying on fossil fuel-based grid or diesel-powered off-grid electricity(*Sustainable Cold Chain and Food Loss Reduction*, 2019). Furthermore, the entire refrigeration sector is responsible for approximately 30% of global energy consumption(Ben Taher et al., 2022a). To better manage energy consumption and maintain proper product temperatures throughout the different supply chain stages, researchers have explored and developed phase change materials (PCMs), which leverage high energy density through phase changes between liquid and solid states at nearly constant temperatures, as replacements for traditional active cold chain designs in certain sections of product distribution, especially in the last-mile delivery where refrigeration is more expensive

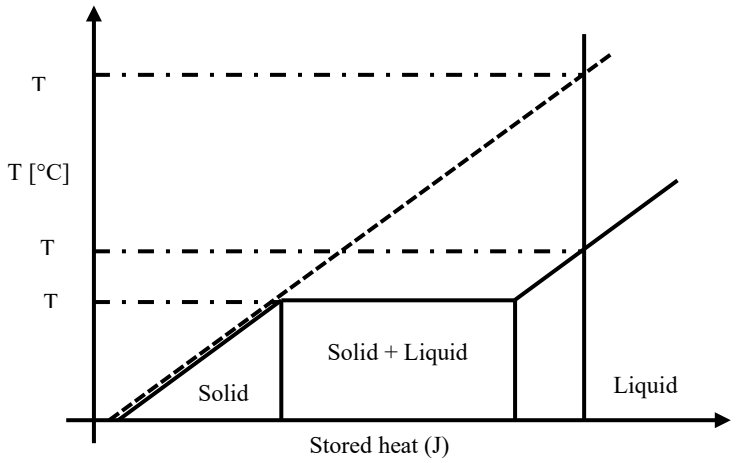

and less efficient(Calati et al., 2022). This refers to the use of passive cooling techniques.

Figure 3: Comparison of sensible and latent energy storage systems during the melting process.

Figure 3 illustrates the comparative thermal storage performance of sensible and latent heat storage systems. Latent heat storage systems using PCMs perform better than traditional sensible heat systems. Both systems start at the same temperature. When the latent system (shown with a continuous line) reaches the phase change temperature (T_P), it begins to melt and stores heat at almost the same temperature. The PCM can store more heat. To store the same amount of heat, the sensible system (shown with a dotted line) heats up to a higher final sensible temperature (T_S) than the PCM system (T_L). Keeping an optimal temperature helps the equipment last longer by reducing heat stress. This reduces the risk of damage, lowers maintenance costs, and makes the system safer and more reliable.

The thermal performance of insulated shipping containers is influenced by packaging materials, container size, and insulation(Ng et al., 2020). The performance and design of passively cooled insulated foam containers have been widely studied using both numerical and experimental methods. Ge et al. conducted numerical simulations validated by experimental results to understand heat transition in foam containers, demonstrating partial alignment with field data(Ge et al., 2014a). Wang et al. investigated various thermal insulation materials and found that packaging performance was significantly influenced by material type and configuration(Wang et al., 2020). Zanoni et al. examined the design of eco-efficient cold chain networks and emphasized the role of insulation strategies in reducing environmental impact(Zanoni et al., 2019). Zeng et al. evaluated the effect of aluminium foil layers on thermal insulation performance and reported enhanced cold retention in logistic packaging(Zeng et al., 2022). Burgess(G. Burgess, 1999) developed equations to calculate the thermal resistance (R-value) of packaging. These equations, derived through ice melt tests and adjusted via linear regression, considered factors such as the packing material, wall thickness, container geometry, and design. The model was used to estimate time within temperature specifications for specific packages, with estimated results falling typically within 20% of actual times measured in laboratory tests. However, this approach showed limitations that required multiple tests to build a database for various packaging models. Choi(Choi & Burgess, 2007) took a theoretical approach by developing a two-dimensional (2D) steady-state model to calculate the heat penetration rate (HPR), which measures energy transfer per degree of temperature difference. While this model accurately assesses the insulation performance of the package, it did not fully account for changes over time. Zeng et al. (Zeng et al., 2022) developed a mathematical model to study how aluminium foil affects packaging insulation in cold chain logistics. This study developed the concept of "maximum insulation time" (MIT) to measure the thermal performance of packaging. The authors showed that the addition of aluminium foil to the inner surface of insulation improved performance by over 25%, making evident the significance of radiation heat transfer even inside the packages. Singh(Singh et al., 2013) conducted experiments with insulation materials of varying densities and thicknesses to assess their thermal resistance. By analysing different material types, Singh found that Vacuum Insulation Panels (VIPs) exhibited the highest thermal resistance of the materials and variations tested, followed by insulation constructed out of polyurethane, recycled EPS, and virgin EPS. Specifically, for a one-inch-thick container, VIPs demonstrated a 128% and 267% improvement in thermal resistance compared to polyurethane and virgin EPS, respectively. Ge(Ge et al., 2013a) developed a Finite Element Analysis (FEA) to predict temperature changes in insulated packaging. It found partial agreement between field-measured and FEA-predicted temperatures. Both field data and FEA simulations show that temperatures initially drop below 0°C before stabilizing above freezing.

Using extruded polystyrene (XPS) foam containers, the duration of sub-zero temperatures depends on the gel packs' starting temperature, the empty space in the container, and the insulation materials. To prevent vaccines from freezing, the authors recommended to adjust the gel packs' initial temperatures and control the release of cold air.

When focusing specifically on the use of fibre-based insulation, research interest and development of commercial products has increased considerably(*Fiber-Based Packaging Market Size, Volume & Export Data*, n.d.). Driven by consumer preferences, the introduction of new regulations and advancements in the development of higher performance insulations, the proliferation of fibre-based and other alternative materials in the passive cold chain must be carefully studied to ensure successful adoption. As shown in the past research, most of it has been conducted using petroleum-based materials and considerations of important factors such as humidity effects have not been widely present.

For insulated shipping containers, thermal performance is evidently the most critical characteristic. To mitigate the risk of temperature excursions for temperature-sensitive products, it is important to verify the ISCs before shipping them. The verification process includes rigorous testing, which is time and resource intensive. The objective of this paper is to develop a framework for computer simulation models to accurately predict the thermal performance of the ISCs when using fibre-based insulation materials. The verification process was optimized through a systematic thermal property analysis of the materials used and building a finite element model to replicate the thermal condition of the ISCs experienced in a laboratory environment.

4.2 Methodology

The overall workflow was divided into three stages to ensure accurate thermal performance assessment and model validation. First, a controlled experiment was conducted in an environmental chamber to evaluate the performance of the insulated shipping container (ISC) under laboratory conditions. This provided a reliable dataset for benchmarking. In the second stage, material properties of all components were carefully analyzed and characterized to support accurate numerical modeling. Finally, a detailed finite element model (FEM) was developed based on the experimental setup, incorporating temperature-dependent properties and the phase change behavior. The simulation results were then validated against the experimental data to confirm the accuracy of the model.

4.2.1 Experimental simulation

A generic ISC design was developed, consisting of an outer box, an insulation layer, water-based gel packs as the phase-change material (PCM), and an empty payload box. Two types of shippers were created by varying only the insulation material: configuration 1 using two layers of BC double-wall corrugated board, and configuration 2 using ½" nominal honeycomb board. All other components remained identical between the two designs. The external dimensions of the ISCs were kept constant at 185 mm (length) × 185 mm (width) × 240 mm (height). The inner dimensions of the outer box were adjusted based on the insulation thickness to maintain a consistent internal volume across both shipper types. **Table *3*** summarizes the thickness of the component analysed.

Table 3: Measured average thicknesses of the materials evaluated.

Material	Component Used	Thickness (mm)
Two-layers of BC doublewall corrugated board	Insulation	13.96
½" Honeycomb board	Insulation	14.70
C-flute	Outer Box	4.20
30-Pt SBS Paperboard	Payload Box	0.72

Each ISC was loaded with a total of seven 340 grams, 0 °C gel packs. Four gel packs were placed at the bottom of the payload box, while the remaining three were positioned on top of it. To ensure proper sealing and insulation, the manufacturer's joints of both the outer box and the payload box were sealed using 3M™ Hot Melt Adhesive 3762 (3M Corporation, Saint Paul, MN, USA). Additionally, all edges and flaps of the outer box were sealed with 3M™ packing tape to minimize air leakage. A Dayton T-type 24 AWG thermocouple was positioned at the geometric centre of the payload box to monitor internal temperature. The study was conducted under an empty payload box condition to isolate the thermal behaviour of the packaging system. A cross-sectional view of the packout construction and insulation orientation is shown in **Figure 4.**

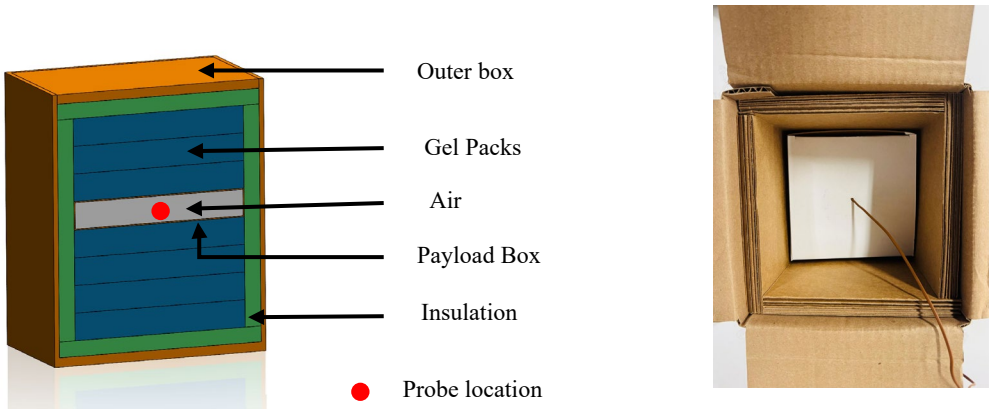

Figure 4: Cross-sectional view for the modelled insulated shipping container with the probe location (right) and a top-view picture of the partially assembled unit.

Temperature readings were collected using an Omega OM-CP-TCTempX Series data logger (Omega Engineering, Norwalk, Connecticut), with Omega T-type miniature male connectors used to complete the setup. All the fiber-based materials except the gel packs were preconditioned for 36 hours at 25°C ± 1°C and 50% ± 2% relative humidity (RH) before conducting the test. The gel packs were frozen individually at -20°C C ± 3°C for a minimum of 48 hours. The ISCs were placed inside a walk-in environmental chamber (Temperature Product Solutions, New Columbia, PA), in a covered rack used to minimize forced air convection. Forced air convection is not expected in traditional dry delivery vans, thus the research simulates a stagnant air flow.

Three different temperature profiles were evaluated; one followed the 72 hours heat profile of ISTA 7E(International Safe Transit Assocoation (ISTA), 2010) , a constant 25°C ± 1°C (controlled) and an uncontrolled ambient room temperature simulation (uncontrolled). Each profile maintained 50% ± 2% RH and stagnant air throughout the whole study. A convection coefficient of 5 $W/m^2 \cdot °C$ was assumed for the stagnant air environment. Five replicates were tested for controlled and uncontrolled environments, and three replicates were tested for ISTA 7E. **Figure 5** shows the three temperature conditions and the time steps applied in this study.

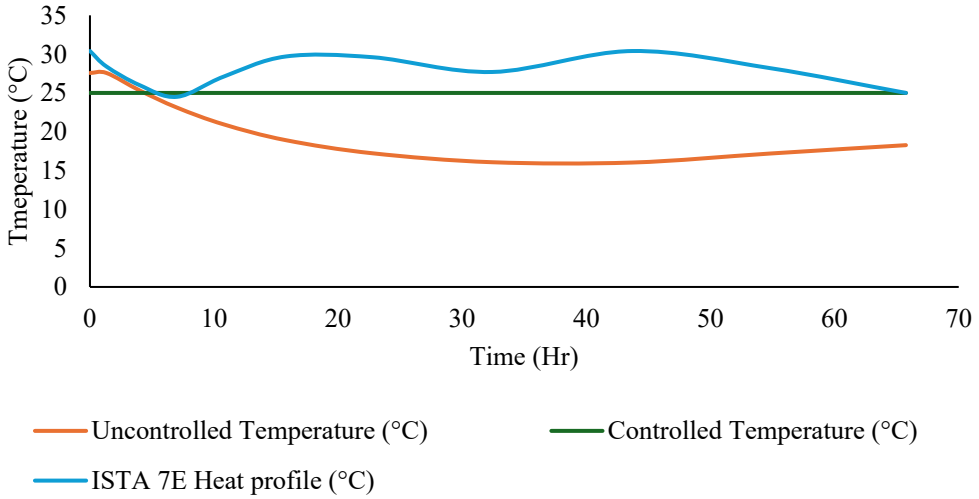

Figure 5: Temperature profiles followed for the shipping container evaluation

4.2.2 Material Property Analysis

Equivalent thermal resistance (TR) of all the materials except the PCMs was measured by using a Heat Flow Meter (HFM) with the steady state method (ASTMC518)(ASTM International, 2021). The gel pack's thermal resistance was also directly measured by placing a single pack inside the HFM using the ASTM C1784 method(ASTM International, 2020). TR measurements were performed at four temperature points: -10°C, 0°C, 25°C, and 35°C. These points were selected to accurately build the finite element model and analyse TR trends across the temperature range of interest. **Figure 6**shows the measured thermal resistivity of the materials.

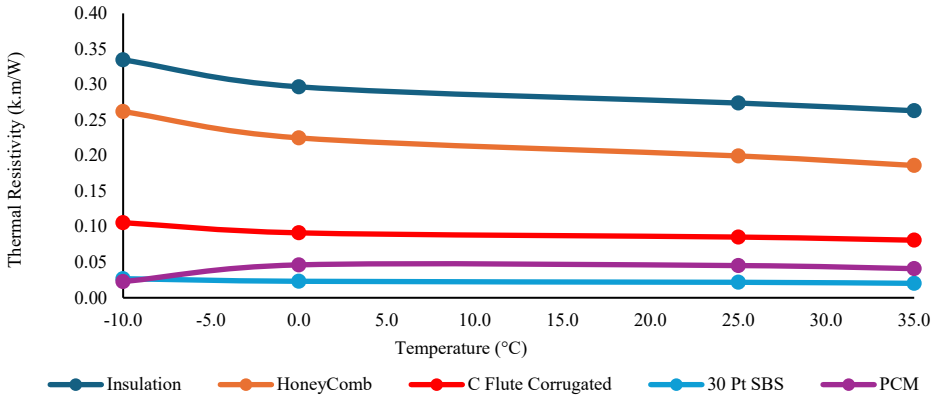

Figure 6: Thermal resistivity of the materials

The phase change material (PCM) used in this study was formulated to undergo phase transition at 0 °C. The PCM composition consisted of 98% water and 2% Carboxy Methyl Cellulose (CMC), which acts as a thickening agent to

enhance thermal stability and prevent phase separation. Differential Scanning Calorimetry (DSC) was used to measure the enthalpy of the phase change material (PCM). Testing was conducted using a TA Instruments Q20 DSC system (TA Instruments, DE) following ASTM E2716-09(ASTM International, 2014) standard procedures. A modulation amplitude of ±1 °C and a modulation period of 120 seconds were used to enhance resolution and separate reversing and non-reversing heat flows. The PCM sample was subjected to a controlled heating rate of 3 °C per minute over a temperature range of −30 °C to 45 °C. This method allowed accurate quantification of the latent heat associated with the PCM's phase transition. Three different test samples were tested with a enthalpy value COV of 0.3 %. **Figure 7** shows the enthalpy measurements from DSC. The integrated area under the heat flow curve is the total stored latent heat of the PCM. The enthalpy change during the phase change for this material is represented in the integrated peak area of heat flow curve, which is approximately 270.4 J/g.

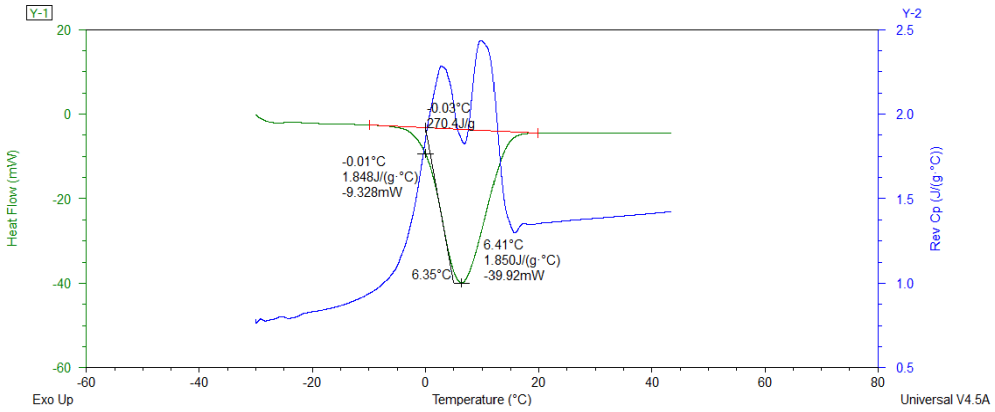

Figure 7: Representative example of a Differential Scanning Calorimetry enthalpy characterization testing result for the phase change material.

To use the DSC results in the thermal model, the enthalpy of the PCM was expressed as a function of temperature using a simple piecewise formulation. Four characteristic temperatures were defined:

- T_0: reference temperature below the onset of melting
- T_{solid}: temperature at which the solid–liquid transition begins
- T_{liquid}: temperature at which the material is fully melted
- T_{high}: any temperature above $T_{\text{liquid}}$where the PCM behaves as a sensible liquid

The latent heat obtained from DSC (L_{fusion}, J/kg) was distributed over the measured transition interval $\Delta T_{\text{transition}} = T_{\text{liquid}} - T_{\text{solid}}$. An effective specific heat in the transition region, C^*, was then defined as

$$C^* = C_{p,\text{avg}} + \frac{L_{\text{fusion}}}{\Delta T_{\text{transition}}}$$

where $C_{p,\text{avg}}$is the average sensible specific heat capacity is over the transition range. This approach allows the latent heat to be included as an apparent increase in heat capacity over the melting interval.

Taking the enthalpy at the reference temperature T_0as H_0, the enthalpy at the start of melting (T_{solid}) is

$$H_{\text{solid}} = H_0 + C_{p,\text{solid}} \, (T_{\text{solid}} - T_0)$$

where $C_{p,\text{solid}}$is the specific heat of the solid PCM below the transition.

Across the phase change region, the enthalpy increases according to the effective heat capacity C^*. The enthalpy at the end of melting (T_{liquid}) is therefore

$$H_{\text{liquid}} = H_{\text{solid}} + C^* \, (T_{\text{liquid}} - T_{\text{solid}})$$

For temperatures above the transition, the PCM behaves as a liquid with specific heat $C_{p,\text{liquid}}$. The enthalpy at a higher temperature $T_{\text{high}} > T_{\text{liquid}}$is given by

$$H_{\text{high}} = H_{\text{liquid}} + C_{p,\text{liquid}} \, (T_{\text{high}} - T_{\text{liquid}})$$

Together, these expressions provide a continuous enthalpy–temperature relationship that incorporates both sensible and latent heat effects derived from the DSC measurements and can be directly implemented in the thermal model. Corrugated board has a specific heat of 1.52 J/g°C(Khan et al., 2008). The density of all materials was determined using a precision scale and consistent sample dimensioning. Due to the presence of air bubbles in the gel packs caused by their viscous nature, the volume fraction method was used to more accurately determine their density. **Table 4** represents the density of the materials used.

Table 4: Measured average densities of the materials evaluated.

Material	Density (kg/m3)
Two-layers of BC doublewall corrugated board	150
½” Honeycomb board	48
C-flute Outer Box	142
Payload Box	1212
Gel pack	1016 [calculated]

4.2.3 Finite Element Model (FEM)

A finite element model (FEM) was developed using ANSYS 2024 R1 to simulate the transient thermal behavior of ISCs. The geometry was built and imported from SolidWorks, and a two-step analysis was conducted: a steady-state thermal simulation to establish initial conditions, and a transient thermal simulation using a full nonlinear formulation. The PCM was modelled using a temperature-dependent enthalpy-based formulation to accurately capture latent heat effects during phase transition. Thermal conductivity, density, and specific heat capacity for all materials were input

as functions of temperature where applicable. This comprehensive material input setup allowed the simulation to closely replicate realistic thermal behaviour and match experimental results.

A probe was placed at the geometric center of the payload box to track internal temperature. Heat transfer was modeled purely through conduction with perfect thermal contact between components. The temperature field was governed by the heat conduction equation with temperature-dependent properties as shown in (1).

$$\rho(T)Cp(T)\frac{\delta T}{\delta t} = \nabla.\ (k(T)\nabla T) \qquad (1)$$

where ρ is density, Cp is specific he(at capacity, and k is thermal conductivity of the material (all generally functions of temperature T). This equation applies within each material domain (insulation, phase-change material (PCM) gel, and air payload), assuming no internal heat generation and perfect thermal contact at interfaces (continuous temperature and heat flux).

For the PCM, latent heat was considered using an enthalpy-based method as shown in (2).

$$\rho\frac{\delta H(T)}{\delta t} = \nabla.\ (k(T)\nabla T) \qquad (2)$$

The FEM formulation led to (3) and (4):

$$[M]\frac{dT}{dt} + [K]T = F \qquad (3)$$

$$[M]\frac{T^{n+1}-T^n}{\nabla t} + [K]T^{n+1} = F^{n+1} \qquad (4)$$

where $[M]$is the heat capacity matrix, $[K]$ is the conductivity matrix, and F is the load vector. With backward-Euler time integration and time step ∇t, the fully discrete equation becomes (4). Temperature-dependent properties were updated at each step, and nonlinearities were resolved using Newton-Raphson iteration. The 3D geometry was discretized in ANSYS Mechanical using an unstructured tetrahedral mesh. Mesh sizing was program-controlled, with an average element size of 7.0×10^{-3} m, and edge lengths ranging from 1.02×10^{-3} m to 2.00×10^{-2} m. A mapped mesh was applied to selected faces, while the remaining volume was meshed using default solid element formulation. No inflation layers or manual biasing were applied. The final mesh consisted of 28,757 elements and 189,725 nodes.

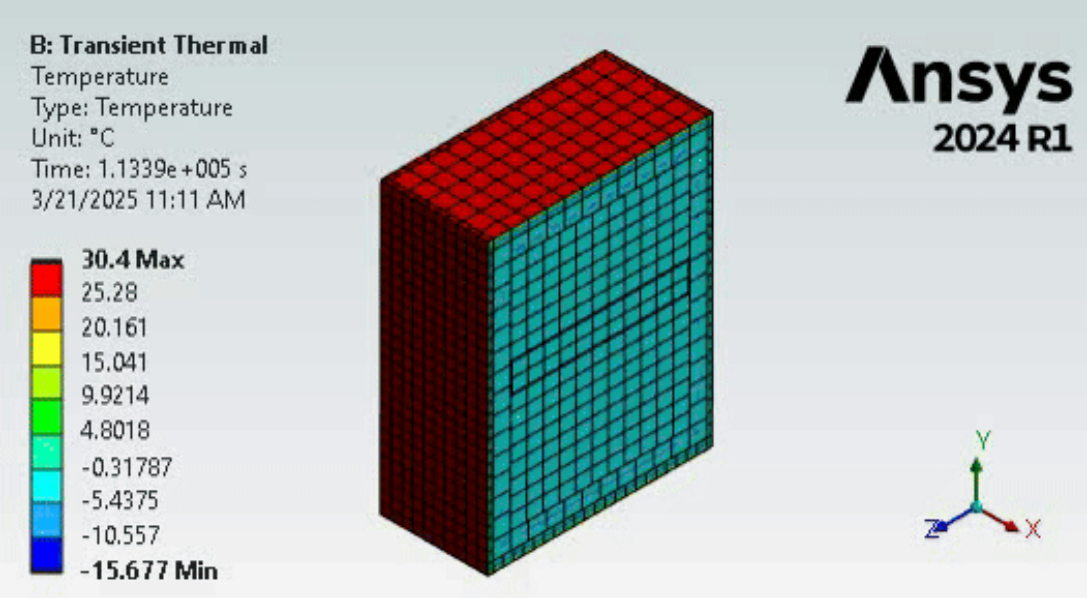

Figure 8: Cross-sectional view and temperature gradient of transient thermal solution

Figure 8 represents the cross-sectional view of the ISC in transient thermal simulation. of the mesh was designed to accurately capture thermal gradients, especially near material interfaces and within the phase change material (PCM) zones. This mesh configuration ensured a balance between computational efficiency and numerical accuracy for transient thermal simulations.

4.3 Results and Discussion

Table 5 summarizes the results of the laboratory experimental testing and the finite element model predictions for all the material and environmental conditions tested. The experimental and FEM results were compared based on the time required for the internal temperature at the probe location to surpass 8.0 °C.

Table 5: Summary of Experimental and FEM Results for ISCs under Controlled, Uncontrolled, and ISTA 7E Heat Conditions

Metric	BC Controlled (25 °C)	Honeycomb Controlled (25 °C)	BC Uncontrolled (Room Temp)	Honeycomb Uncontrolled (Room Temp)	BC ISTA 7E Heat Profile	Honeycomb ISTA 7E Heat Profile
Avg. Time to Reach 8 °C; COV % (Experimental)	40.90 hr (2.40%)	36.70 hr (2.10%)	60.00 hr (2.70%)	53.40 hr (1.80%)	36.20 hr (1.00%)	31.10 hr (2.00%)

Metric	BC Controlled (25 °C)	Honeycomb Controlled (25 °C)	BC Uncontrolled (Room Temp)	Honeycomb Uncontrolled (Room Temp)	BC ISTA 7E Heat Profile	Honeycomb ISTA 7E Heat Profile
FEM Predicted Time to Reach 8 °C	43.50 hr	36.30 hr	62.20 hr	51.10 hr	38.90 hr	32.50 hr
FEM Absolute Prediction Error (%)	6.40 %	0.90 %	3.70 %	4.40 %	7.40 %	4.20 %
Exp vs. FEM Pearson Correlation*	0.84	0.99	0.90	0.95	N/A	N/A
ISC Replicates Pearson Correlation Range ^	0.99 – 1.00	0.99 – 1.00	0.98 – 1.00	0.99 – 1.00	N/A	N/A

* The Pearson Correlation coefficient determines the fit of the predicted model throughout the timeframe evaluated, not just the time to reach the temperature threshold. ^ISC Replicates Pearson Correlation refers to the correlation between each of the pairs of replicates, summarizing appropriate alignment among replicates.

Thermal behaviour across different temperature ranges was analysed to distinguish between sensible and latent heat effects, particularly within the refrigerant's phase change interval. The correlation between experimental measurements and FEM predictions was quantified across the full temperature range studied to assess the model's accuracy in capturing both transient heat conduction and phase change phenomena. The quantification was conducted calculating the Pearson Correlation coefficient throughout the timeframe studied.

The temperature–time graphs (Figure 7 to 11) present the thermal behaviour of insulated shipping containers (ISCs) under various insulation types and ambient conditions. In each plot, the x-axis represents time in hours, while the y-axis shows the temperature at the internal probe location. A horizontal dashed line at 8 °C denotes the critical threshold for cold chain integrity. Multiple experimental curves are displayed to demonstrate repeatability across test samples, with the finite element method (FEM) prediction overlaid as a single continuous line. The PCM phase change behaviour is evident in the flat plateau near 0 °C, where latent heat absorption delays temperature rise. The shape and

alignment of the FEM curve relative to the experimental data reveal the model's accuracy in capturing both sensible and latent heat effects. In cases with dynamic ambient profiles, such as the ISTA 7E test, stepwise variations in temperature can be observed in both the experiment and simulation, highlighting the model's ability to track real-world boundary changes. Overall, the graphs visually support the quantitative performance metrics presented in the summary

Figure 9 presents the experimental and FEM results for ISCs using BC double-wall corrugated board insulation, while **Figure 10** shows the corresponding results for ISCs with honeycomb board insulation at constant 25°C.

Figure 11 presents the experimental and FEM results for ISCs using BC double-wall corrugated board insulation, while **Figure 12** shows the corresponding results for ISCs with honeycomb board insulation at uncontrolled temperature condition.

Figure 13 presents the experimental and FEM results for ISCs using BC double-wall corrugated board insulation, while **Figure 14** shows the corresponding results for ISCs with honeycomb board insulation at ISTA 7E heat profile condition.

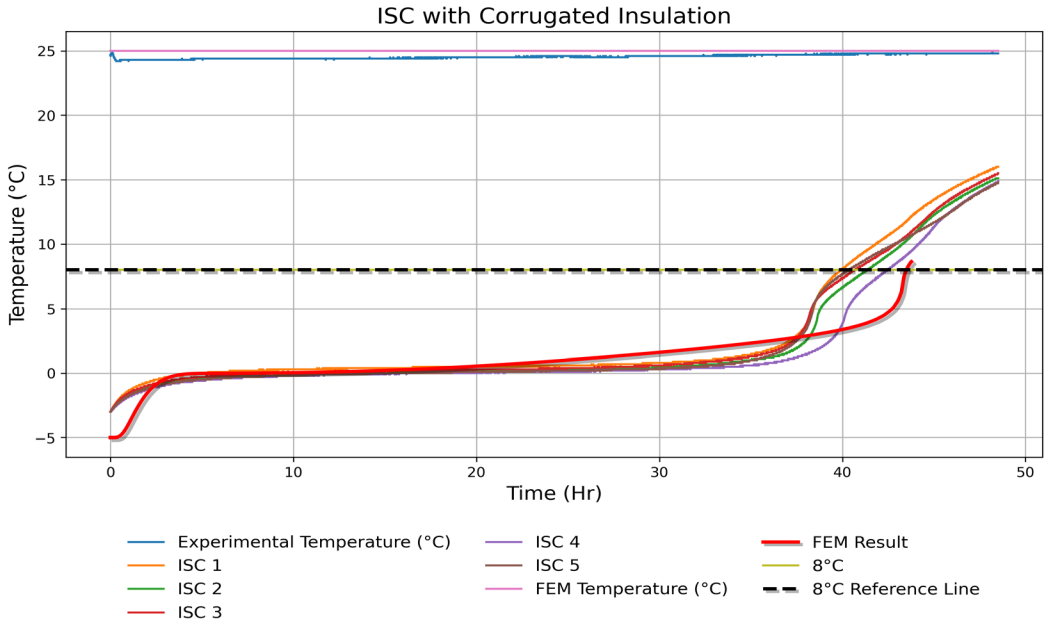

Figure 9: Internal temperature versus time of the shipping container with BC double wall corrugated board insulation at constant 25 ° C.

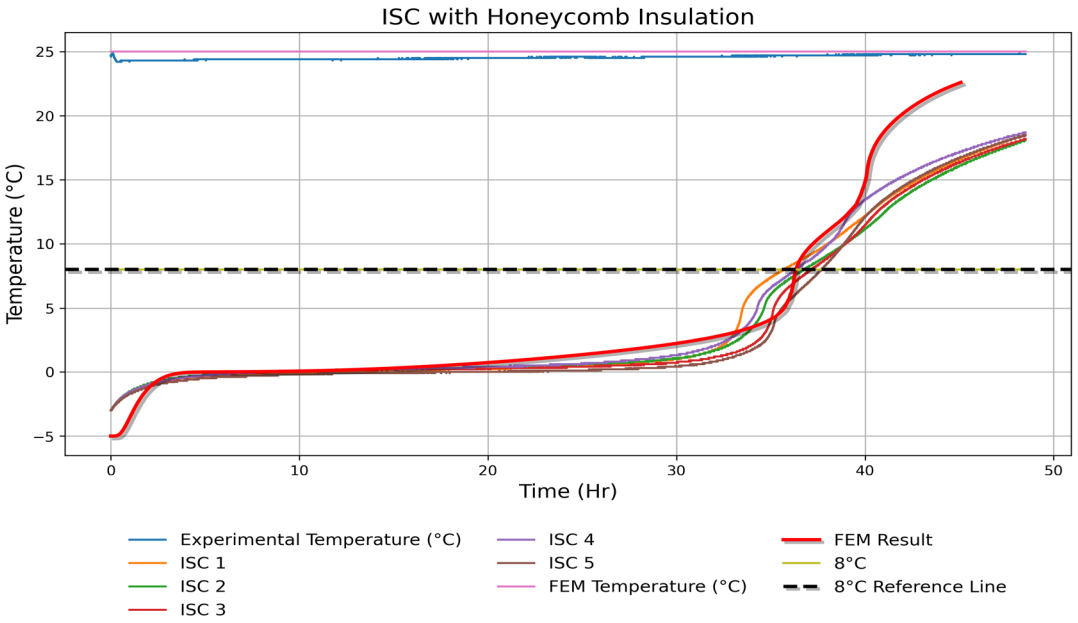

Figure 10: Internal temperature versus time of the shipping container with Honeycomb board insulation at constant 25 ° C.

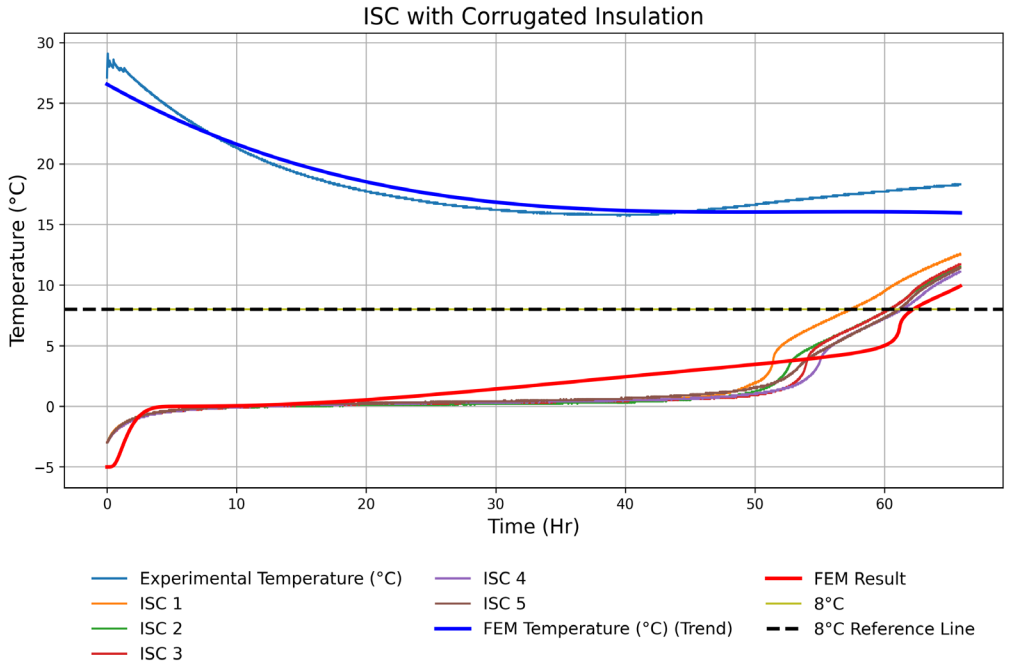

Figure 11: Internal temperature versus time of the shipping container with BC double wall corrugated board insulation at uncontrolled temperature

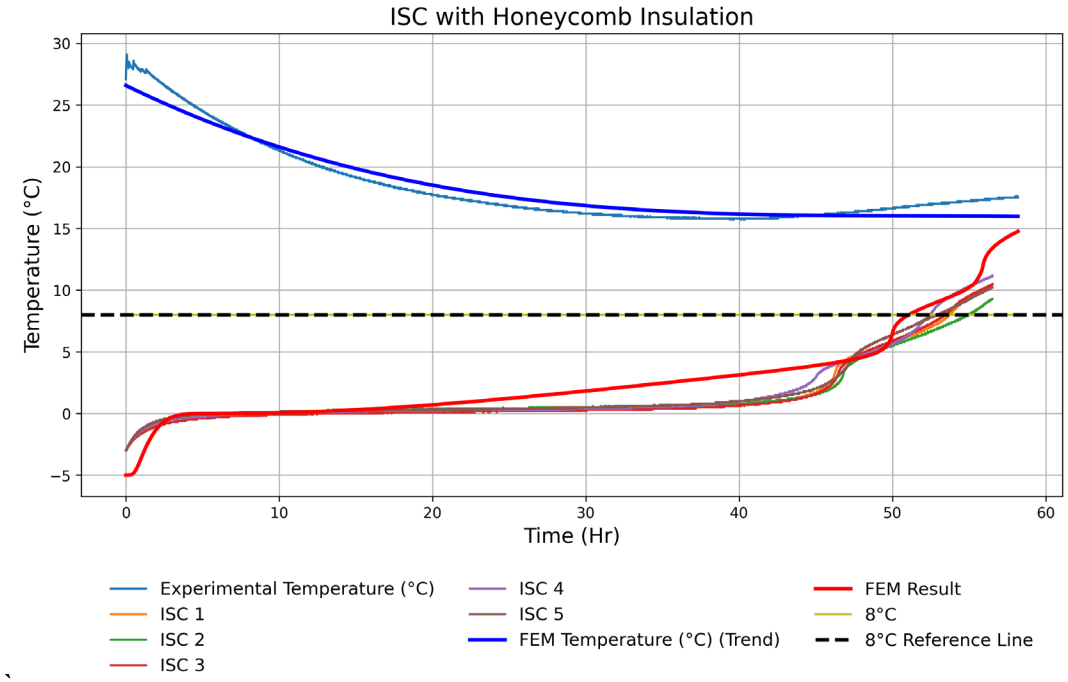

Figure 12: Internal temperature versus time of the shipping container with Honeycomb board insulation at uncontrolled temperature

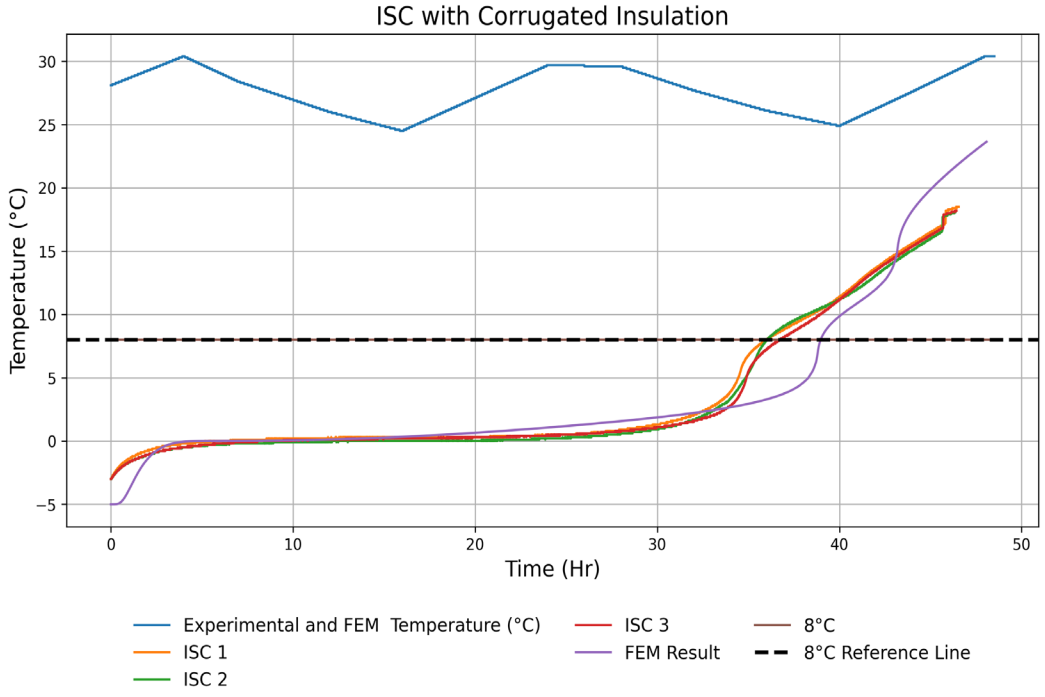

Figure 13: Internal temperature versus time of the shipping container with BC double wall corrugated insulation at ISTA 7E Heat Profile

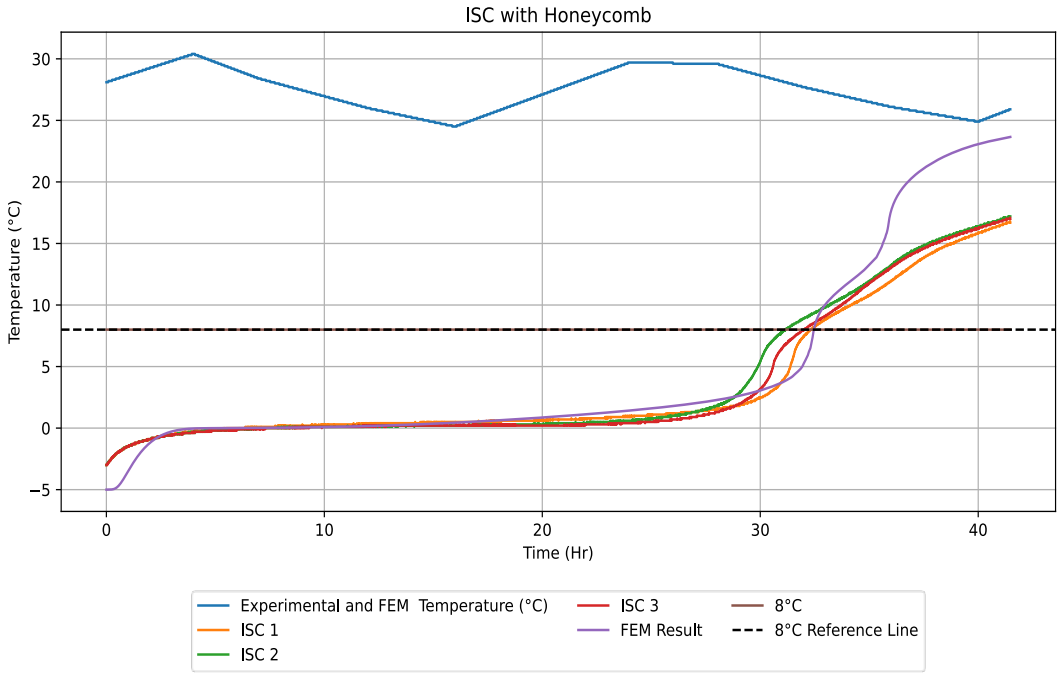

Figure 14: Internal temperature versus time of the shipping container with Honeycomb board insulation at ISTA 7E Heat Profile

To evaluate the fidelity of the FEM model, Root Mean Square Error (RMSE) and Mean Absolute Percentage Error (MAPE) were calculated for each insulation and test condition by comparing the FEM-predicted time to reach 8 °C with corresponding experimental results. The lowest RMSE was observed for the Honeycomb Controlled (25 °C) configuration at 0.77 hr, indicating minimal absolute deviation from experimental data, while the highest RMSE occurred in the BC Controlled (25 °C) case at 2.76 hr, suggesting slightly greater spread in prediction error. Similarly, the MAPE values ranged from a minimum of 1.73% (Honeycomb Controlled) to a maximum of 7.47% (BC ISTA 7E Heat Profile), demonstrating that model performance was more consistent under steady-state boundary conditions. The relatively larger MAPE under ISTA 7E conditions reflects the challenges associated with transient heat profiles and dynamic external environments. These error metrics, along with the corresponding test configurations and thermal classifications, are summarized in**Table 6** . Overall, the FEM model exhibits strong predictive accuracy across all configurations, with all MAPE values remaining below 8%, and a consistent alignment between predicted and experimental thermal behavior.

Table 6: Comparison of FEM and Experimental Results Using RMSE and MAPE Across Insulation Types and Test Conditions

Test Configuration	No. of Samples	FEM Prediction (hr)	RMSE (hr)	MAPE (%)
BC Controlled (25°C)	5	43.5	2.76	6.46
Honeycomb Controlled (25°C)	5	36.3	0.77	1.73
BC Uncontrolled (Room Temp)	5	62.2	2.59	3.66
Honeycomb Uncontrolled (Room Temp)	5	51.1	2.49	4.35
BC ISTA 7E Heat Profile	3	38.9	2.72	7.47
Honeycomb ISTA 7E Heat Profile	3	32.5	0.87	2.23

Fiber-based insulation materials are a promising option for cold chain applications due to their sustainability and thermal performance. However, their use requires careful evaluation of several technical challenges. One major issue is the high variability between products. Differences in fiber density, type, and surface coatings can affect thermal conductivity and moisture resistance. These differences make it difficult to generalize performance across all fiber-based materials.

Another key concern is the effect of humidity. Fiber-based materials are often hygroscopic, meaning they absorb moisture from the environment. This moisture can increase the material's thermal conductivity and reduce its insulation effectiveness. Over time, exposure to high humidity can also damage the structure of the insulation. To capture this behavior, models should include the effects of moisture and how it interacts with heat flow.

To improve accuracy, thermal models must also consider radiative heat transfer and forced convection. These effects become important during real transport conditions. Simulations should represent the entire cold chain, from warehouse storage to final delivery, so that the results reflect actual use cases.

Future studies should perform sensitivity analyses to understand how changes in key variables affect performance. These include the properties of phase change materials (PCMs), insulation thickness, ambient temperature profiles, shipper size, and refrigerant mass. Models should be validated against different combinations of these variables to identify their limits and improve reliability. By addressing these factors, more accurate and dependable thermal models can be developed for fiber-based insulation systems in cold chain logistics.

4.4 Conclusion

This study successfully developed and validated a finite element model (FEM) to predict the thermal performance of bio-based insulated shipping containers (ISCs) for passive cold chain applications. The research addressed the limitations of traditional performance verification methods, such as resource and time constraints, by introducing an efficient computational approach.

The following key conclusions can be drawn:

- Thermal properties of bio-based materials, including multi-layer double-wall corrugated board and honeycomb insulation, were accurately measured using standardized methods for thermal conductivity and specific heat analysis. The measured thermal conductivity and density values were critical inputs for the FEM.
- Experimental validation demonstrated strong agreement with FEM predictions, with errors of 4% for BC insulation and 8% for honeycomb insulation. This highlights the reliability and precision of the developed model.
- ISCs with double-wall insulation-maintained temperatures below the critical threshold of 8°C for 40.9 hours, while the honeycomb insulation lasted 36.7 hours. These results confirmed that both configurations are viable solutions for passive cooling applications, with performance differences attributed to material thermal conductivity and insulation thickness.
- The phase-change properties of gel packs played a significant role in prolonging the cooling duration, demonstrating the efficacy of latent heat storage systems for passive cold chain logistics.
- The FEM provided accurate thermal performance predictions under stagnant air conditions, reducing the need for extensive environmental chamber testing. This approach offers a scalable solution for optimizing insulated packaging designs with various materials and boundary conditions.
- The developed FEM framework can be easily adapted for other bio-based materials or modified ISCs, enabling faster evaluation of design changes without compromising accuracy.
- By utilizing bio-based and recyclable insulation materials, this study promotes sustainable alternatives to petroleum-based insulation, aligning with the growing demand for environmentally friendly cold chain solutions.
- The optimized FEM workflow not only reduces product development time and costs but also enhances the reliability of ISCs for transporting temperature-sensitive products such as pharmaceuticals and fresh produce.

Further studies should incorporate humidity effects on fibre-based materials to simulate real-world conditions more comprehensively. Including radiative heat transfer and exploring forced convection effects could enhance the accuracy

of thermal predictions. Sensitivity analyses on gel pack phase-change properties and insulation configurations could provide insights for further improving ISC designs.

In conclusion, this research establishes a consistent and repeatable methodology for predicting and optimizing the thermal performance of insulated shipping containers using finite element modelling. This work contributes to the development of cost-effective, sustainable, and high-performing solutions for passive cold chain packaging systems.

4.5 References

ASTM International. (2014). Standard Test Method for Determining Specific Heat Capacity by Sinusoidal Modulated Temperature Differential Scanning Calorimetry (No. ASTM E2716-09(2014)). https://doi.org/10.1520/E2716-09R14

ASTM International. (2020). Standard Test Method for Using a Heat Flow Meter Apparatus for Measuring Thermal Storage Properties of Phase Change Materials and Products (No. ASTM C1784-20). https://doi.org/10.1520/C1784-20

ASTM International. (2021). Standard Test Method for Steady-State Thermal Transmission Properties by Means of the Heat Flow Meter Apparatus (No. ASTM C518-21). https://doi.org/10.1520/C0518-21

Ben Taher, M. A., Ahachad, M., Mahdaoui, M., Zeraouli, Y., & Kousksou, T. (2022). A survey of computational and experimental studies on refrigerated trucks. Journal of Energy Storage, 47, 103575. https://doi.org/10.1016/j.est.2021.103575

Burgess, G. (1999). Practical thermal resistance and ice requirement calculations for insulating packages. Packaging Technology and Science, 12(2), 75–80. https://doi.org/10.1002/(SICI)1099-1522(199903/04)12:2%253C75::AID-PTS454%253E3.0.CO;2-2

Calati, M., Hooman, K., & Mancin, S. (2022). Thermal storage based on phase change materials (PCMs) for refrigerated transport and distribution applications along the cold chain: A review. International Journal of Thermofluids, 16, 100224. https://doi.org/10.1016/j.ijft.2022.100224

Choi, S.-J., & Burgess, G. (2007). Practical Mathematical Model to Predict the Performance of Insulating Packages. Packaging Technology and Science, 20(6), 369–380. https://doi.org/10.1002/pts.762

Fiber-based Packaging Market Size, Volume & Export Data. (n.d.). Retrieved December 1, 2024, from https://www.towardspackaging.com/insights/fiber-based-packaging-market-sizing

Ge, C., Cheng, Y., & Li, B. (2014). Numerical simulation and experimental study of the heat transition in a foam container. Journal of Cellular Plastics, 50(1), 15–36. https://doi.org/10.1177/0021955X13503846

Ge, C., Cheng, Y., & Shen, Y. (2013). Application of the Finite Elemental Analysis to Modeling Temperature Change of the Vaccine in an Insulated Packaging Container during Transport. PDA Journal of Pharmaceutical Science and Technology, 67(5), 544–552. https://doi.org/10.5731/pdajpst.2013.00937

International Safe Transit Assocoation (ISTA). (2010). ISTA 7E - Testing Standard for Thermal Transport Packaging Used in Parcel Delivery System Shipment [Standard]. https://ista.org/thermal_standards.php

Kartoglu, U., Vesper, J., Teräs, H., & Reeves, T. (2017). Experiential and authentic learning approaches in vaccine management. Vaccine, 35(17), 2243–2251. https://doi.org/10.1016/j.vaccine.2016.11.104

Khan, M., De Ris, J., & Ogden, S. (2008). Effect of Moisture on Ignition Time of Cellulosic Materials. Fire Safety Science, 9, 167–178. https://doi.org/10.3801/IAFSS.FSS.9-167

Kucharek, M., Yang, L., & Wang, K. (2020). Assessment of insulating package performance by mathematical modelling. Packaging Technology and Science, 33(2), 65–73. https://doi.org/10.1002/pts.2492

Matsunaga, K., Burgess, G., & Lockhart, H. (2007). Two methods for calculating the amount of refrigerant required for cyclic temperature testing of insulated packages. Packaging Technology and Science, 20(2), 113–123. https://doi.org/10.1002/pts.747

Ng, C. Z., Lean, Y. L., Yeoh, S. F., Lean, Q. Y., Lee, K. S., Suleiman, A. K., Liew, K. B., Kassab, Y. W., Al-Worafi, Y. M., & Ming, L. C. (2020). Cold chain time- and temperature-controlled transport of vaccines: A simulated experimental study. Clinical and Experimental Vaccine Research, 9(1), 8. https://doi.org/10.7774/cevr.2020.9.1.8

Raval, A. H., Solanki, S. C., & Yadav, R. (2013). A simplified heat transfer model for predicting temperature change inside food package kept in cold room. Journal of Food Science and Technology, 50(2), 257–265. https://doi.org/10.1007/s13197-011-0342-z

Singh, J., Jaggia, S., & Saha, K. (2013). The Effect of Distribution on Product Temperature Profile in Thermally Insulated Containers for Express Shipments. Packaging Technology and Science, 26(6), 327–338. https://doi.org/10.1002/pts.1985

Sustainable Cold Chain and Food Loss Reduction. (2019). UN-environmantal programme. https://ozone.unep.org/system/files/documents/MOP31-Sustainable-HL_Briefing_Note.pdf

Van Boxstael, S., Habib, I., Jacxsens, L., De Vocht, M., Baert, L., Van De Perre, E., Rajkovic, A., Lopez-Galvez, F., Sampers, I., Spanoghe, P., De Meulenaer, B., & Uyttendaele, M. (2013). Food safety issues in fresh produce: Bacterial pathogens, viruses and pesticide residues indicated as major concerns by stakeholders in the fresh produce chain. Food Control, 32(1), 190–197. https://doi.org/10.1016/j.foodcont.2012.11.038

Wang, K., Yang, L., & Kucharek, M. (2020). Investigation of the effect of thermal insulation materials on packaging performance. Packaging Technology and Science, 33(6), 227–236. https://doi.org/10.1002/pts.2500

Zanoni, S., Mazzoldi, L., & Ferretti, I. (2019). Eco-efficient cold chain networks design. International Journal of Sustainable Engineering, 12(5), 349–364. https://doi.org/10.1080/19397038.2018.1538268

Zeng, T., Jiang, H., & Hao, F. (2022). Study on the effect of aluminium foil on packaging thermal insulation performance in cold chain logistics. Packaging Technology and Science, 35(5), 395–403. https://doi.org/10.1002/pts.2637

5 Chapter 2: Effect of relative humidity on the performance of passive thermal cold chain packaging systems

Abstract: This study examines how environmental humidity affects the thermal performance of insulated shipping containers used in cold-chain logistics. Controlled laboratory experiments were conducted on several insulation types, including fiber based corrugated fiberboard, honeycomb paperboard, and polymeric foams, to evaluate temperature evolution and hold-time behavior under varying relative humidity conditions from 30% to 80%. The results showed that higher humidity levels substantially accelerated the warming process inside the containers and reduced the time for the payload region to reach the critical threshold of 8 °C. The effect was particularly evident in fiber-based insulation systems, where moisture absorption increased the effective thermal conductivity, while polymer-based materials such as expanded polystyrene (EPS) and polyurethane (PU) remained relatively stable. Complementary energy-balance modeling supported these observations, confirming that humidity acts as a key external driver of heat transfer in porous insulation materials. The findings underscore the importance of integrating humidity control into standardized thermal performance test procedures such as ISO 23412, ISTA 7E, and ASTM D3103. Beyond thermal behavior, the study highlights the environmental advantages of fiber-based packaging, which offers renewable sourcing and end-of-life recyclability despite its higher humidity sensitivity. These insights emphasize the need for future design strategies that balance thermal reliability with material sustainability and encourage the inclusion of humidity considerations in standardized thermal testing protocols.

Keywords: cold chain, insulation, relative humidity, phase change material, EPS

5.1 Introduction

The cold chain refers to the transportation and storage of temperature-sensitive products using thermal or refrigerated packaging systems, combined with strategic logistical planning, to ensure the integrity and quality of the products throughout the supply chain(Singh et al., 2013). Cold chain logistics systems are generally classified into two main categories: active systems, which employ powered refrigeration units to regulate temperature, and passive systems, which maintain thermal conditions using insulated containers in combination with refrigerants such as phase change materials or dry ice, without the need for external power sources(Calati et al., 2022). In recent years, the adoption of passive cold chain packaging has accelerated significantly, driven by the growing need for cost-effective, energy-independent, and sustainable solutions for pharmaceutical and food logistics(Ren et al., 2022b). Passive thermal packaging has become increasingly favored in the pharmaceutical sector due to its operational simplicity and effectiveness in last-mile delivery scenarios(Sykes, n.d.). According to Future Market Insights, passive packaging accounts for approximately 72.5% of the pharmaceutical cold chain market(*Pharmaceutical Cold Chain Packaging Market Demand 2025 to 2035*, n.d.). Demand for packaging for temperature sensitive products is currently valued around $35 billion and expected to grow to 117 billion by 2030(Kumar Deb, 2023). According to Freedonia, e-commerce sales are projected to reach $1.4 trillion by 2026(Freedonia Group, 2022), with online grocery sales growing 12% annually(Rasch, 2025) and meal kit delivery services reaching $15 billion by 2027(Freedonia Group, 2023). This exponential growth of e-commerce and last-mile delivery of temperature-sensitive products, such as pharmaceuticals

and fresh foods, has created unprecedented challenges for protective packaging design(Chowdhury et al., 2023a; Raj et al., 2024a). The global cold chain packaging industry is undergoing a strategic transition from conventional petrochemical-based insulating materials, such as expanded polystyrene (EPS) and polyurethane (PU) foams, toward more sustainable alternatives, such as biopolymers, cellulose-based insulation, and mycelium-derived materials(Rahman et al., 2025). Advancements in renewable feedstocks, such as lignin and vegetable oils are further driving the development of bio-based polyurethane formulations, offering sustainable alternatives to traditional fossil-derived foam insulation used in cold chain applications(Jayalath et al., 2025).

Current Thermal Packaging System (TPS) evaluation standards rarely address humidity as a critical performance variable. For example, ISO 23412:2020 outlines service requirements for temperature-controlled parcel delivery but focuses primarily on temperature maintenance and handling procedures, without explicit test provisions for high- or low-humidity conditions(*ISO 23412:2020(En), Indirect, Temperature-Controlled Refrigerated Delivery Services — Land Transport of Parcels with Intermediate Transfer*, n.d.). Similarly, ISTA 7E protocols simulate ambient temperature profiles for cold chain validation, yet their environmental conditioning steps do not mandate relative humidity (RH) control beyond incidental variation(International Safe Transit Assocoation (ISTA), 2010). ASTM thermal performance standards relevant to insulated shipping systems (e.g., ASTM D3103) define steady-state heat transfer measurements but do not require moisture pre-conditioning or concurrent humidity cycling during testing(D10 Committee, n.d.). Likewise, the Parenteral Drug Association Technical Report No. 39 (PDA TR39), which provides comprehensive guidance on design qualification (DQ), operational qualification (OQ), and performance qualification (PQ) for pharmaceutical distribution packaging, addresses temperature mapping in detail but omits humidity as a validation or controllable parameter(*PDA Technical Report No. 39 Revised 2021 (TR 39) Guidance for Temperature-Controlled Medicinal Products - Maintaining the Quality of Temperature-Sensitive Medicinal Products through the Transportation Environment (Single User Digital Version)*, n.d.).

While fiber-based materials for cold chain packaging offer promising environmental advantages, their performance can be significantly influenced by environmental conditions, particularly humidity. Cellulose-based insulation experiences a substantial increase in thermal conductivity, up to 40% as relative humidity rises from 35% to 95%(Kendzierawska & Trochonowicz, 2024). In addition to reduced thermal performance, moisture absorption also leads to dimensional instability and a heightened risk of microbial growth, further compromising the material's

reliability in humid environments(Dombek et al., 2020). Fiber-based insulation materials like cellulose fiber insulation (CFI) exhibit strong hygroscopic behavior, meaning they absorb and release moisture in response to ambient humidity. As humidity increases, moisture uptake leads to significant changes in water content, which not only affects thermal conductivity but also raises the risk of interstitial condensation(Lee et al., 2020). Furthermore, the hygroscopic nature of cellulose causes its mechanical properties, such as stiffness, strength, and dimensional stability to degrade significantly with increasing humidity, largely due to moisture-induced plasticization and weakening of inter-fiber bonds(Spiewak et al., 2022). Assaad et al. reported that moisture migration during testing significantly increased the measured thermal conductivity of biobased insulation materials, indicating that dry-state testing may underestimate heat gain under realistic humid conditions(El Assaad et al., 2024). Gordeyeva et al. examined cellulose nanofibril-based foams and found a pronounced rise in thermal conductivity with increasing RH, confirming that cellulose-based materials are particularly sensitive to moisture(Apostolopoulou-Kalkavoura et al., 2018). Furthermore, environmental humidity in the United States exhibits significant spatial and seasonal variability, which has direct implications for cold chain packaging performance. According to a national climatological analysis, the average daytime relative humidity across the U.S. is approximately 59%, while nighttime averages reach around 75%, reflecting diurnal moisture accumulation(Gaffen & Ross, 1999).

Passive cold chain systems play an increasingly vital role in the global distribution of temperature-sensitive products, yet their performance is inherently dependent on the thermal insulation materials used. While fiber-based insulation materials such as cellulose, paper composites, and other hygroscopic bio-based products are known to be highly sensitive to ambient humidity, non-fiber/polymer-based materials, including expanded polystyrene (EPS) and polyurethane (PU) foams, are generally assumed to be less affected. However, current thermal packaging system (TPS) evaluation standards focus almost exclusively on temperature maintenance under controlled laboratory conditions and rarely account for the potential performance variation caused by different humidity levels. This omission creates a critical knowledge gap in understanding how real-world humidity fluctuations may influence the comparative performance of different insulation types in passive cold chain systems. The objective of this work is to systematically evaluate the impact of varying environmental humidity on the thermal performance of both fiber-based and non-fiber/polymer-based insulation materials used in passive cold chain packaging. Specifically, the study aims to:

1. Quantify the change in thermal performance of representative fiber-based and polymer-based TPS materials across a range of controlled relative humidity conditions.
2. Identify potential differences in sensitivity to humidity between the two material categories and assess the implications for passive cold chain system reliability.
3. Provide evidence-based recommendations for integrating humidity considerations into TPS qualification protocols and performance standards.

By addressing these objectives, this study seeks to bridge the gap between laboratory-based TPS testing and the environmental realities of cold chain logistics, ensuring that both fiber-based and polymer-based passive systems are evaluated and optimized for the full range of humidity conditions they may encounter in service.

5.2 Methodology

5.2.1 Materials and Packout Construction

This study investigates the effect of environmental humidity on the thermal performance of insulated shipping containers (ISCs) using different bio-based and petroleum-based insulation materials. The experiment was designed to systematically compare the behavior of commonly used packaging insulation materials under controlled conditions. The insulation materials were carefully selected to represent two distinct categories: paper-based materials that are usually susceptible to moisture absorption, and petroleum-based foams that exhibit minimal hygroscopic behavior. The experimental approach focuses on evaluating how variations in ambient humidity influence the capacity of the ISCs to maintain a required temperature during simulated shipping conditions.

A generic shipper design was developed, consisting of a Regular Slotted Container (RSC) style outer box, an insulation layer, water-based gel packs as the phase-change material (PCM), and a payload box. Four (4) different insulation materials were selected for the construction of the shippers. All the shippers have the same material for the outer box and the payload box. The materials used for different configurations are listed in Table 7 with their respective insulation thickness.

Table 7: Construction materials for the studied shipper configurations.

Shipper Configuration	Outer box	Insulation Material	Thickness (mm)	Payload box	Gel pack
1	Nominal 40 lb/in. ECT	Two-layers of BC double-wall corrugated board	13.96	30 pt SBS paperboard	98% water+2% Carboxy Methyl Cellulose
2		Honeycomb board	14.7		

3	C-Flute	EPS molded cooler	38.1	(CMC), 0°C PCM
4		Metallized roll (PU)	12.5	

Shipper configurations 1 and 2 were built in two sizes, small and large, while configurations 3 and 4 had different dimensions. Table 8 summarizes the outer box dimensions and the quantity of refrigerants used for each configuration.

Table 8: Outer box dimension for each shipper category

Shipper Configuration	Subcategory	Dimensions (L x W x H) (mm)	Gel pack quantity
1	Small	185x185x240	7 x (340 g)
	Small (with product)	185x185x240	7 x (340 g)
	Large	185x185x290	9 x (340 g)
2	Small	185x185x240	7 x (340 g)
	Large	185x185x290	9 x (340 g)
3	One size	280x229x254	6 x (227 g)
4	One size	305x305x305	10 x (340 g)

A structured packing procedure to ensure consistent assembly was followed for the shipper construction (known as pack-out). This allows for controllable thermal performance and accurate temperature monitoring during testing. In Shipper Configurations 1 and 2, the insulated shipping container (ISC) assembly begins with the placement of five insulation panels inside the outer corrugated box to ensure full internal coverage and thermal protection. The sixth panel was placed towards the end of the assembly to close the container. Gel pack pouches were placed inside the shipper subject to the shipper size and type. The Shipper configurations with 7 gel packs have a bottom layer of four PCM gel packs are positioned to provide cooling beneath the payload box. The payload box was then placed directly on top of the bottom PCM layer. Three additional PCM gel packs were arranged on top of the payload box to maintain a stable thermal environment. For the subcategory Small (with product), four (4) 1 oz. glass vials filled with glycol were placed inside the payload box. The Shipper configurations with 9 gel packs have 1 added gel pack on the bottom and 1 on the top of payload box with similar pack-out construction. Finally, the box was sealed using packing tape in an H-pattern to secure all flaps and prevent air leakage. Figure 15 represents how the insulations are placed for configurations 1 and 2.

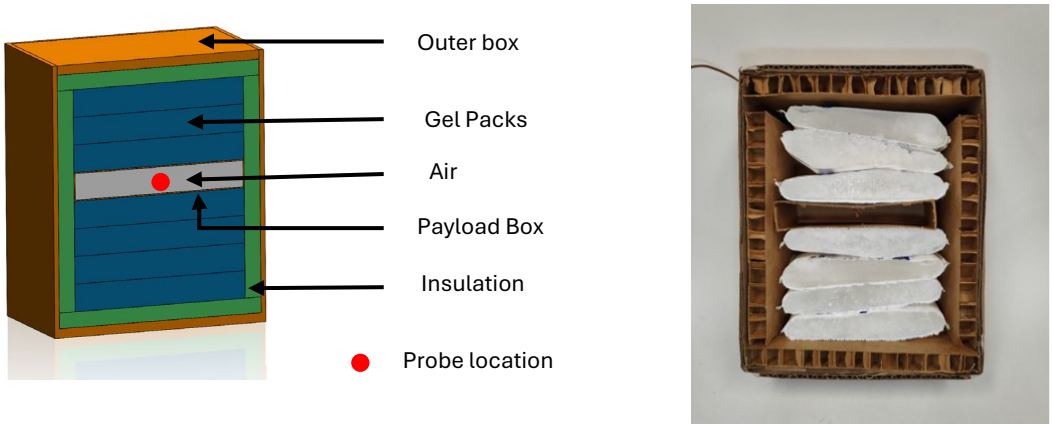

Figure 15: Schematic and representative picture of configuration 1 and 2 small shippers.

Shipper Configuration 3 was a two-piece molded Expanded Polystyrene (EPS) shipper, commonly adopted in the industry for their effective insulation properties (Uline, Pleasant Prairie, WI, US). The assembly started by placing 2 gel packs at the bottom of the molded EPS box to provide a foundational cooling layer. The payload box was then positioned directly on top of these bottom gel packs. Additionally, four gel packs were placed directly on top of the payload box. To minimize internal shifting during transport, a strip of 203 mm-long paper void fill (Ranpak, Concord Twp., OH, US) filler material was inserted on top and along the sides of the payload. Finally, the EPS lid was placed, and the cooler was sealed inside the designated outer box with packing tape.

Shipper Configuration 4 utilized a Polyurethane (PU) roll pouch encased in a metallized poly bag as the primary insulation layer. The pack-out process started with the placement of 2 gel packs at the base of the PU pouch to establish an initial cooling layer. Then, 6 gel packs were arranged along the four vertical sides of the pouch to ensure uniform thermal coverage. Once the bottom and side gel packs were in place, paper void-fill was added to create a stable cavity for the payload. The payload box was then positioned centrally within the pouch, followed by the addition of more filler on top. Two additional gel packs were placed on the top layer, bringing the total to ten gel packs used in this configuration. Finally, the PU pouch was sealed, inserted into the designated outer corrugated box, and secured with tape, completing the assembly for environmental chamber testing

The payload box was the same size for all the configurations (150mmx150mmx25mm). To ensure proper sealing and insulation, the manufacturer's joints of both the outer box and the payload box were sealed using 3M™ Hot Melt

Adhesive 3762 (3M Corporation, Saint Paul, MN, USA). Additionally, all edges and flaps of the outer box were sealed with 3M™ packing tape to minimize air leakage. A Dayton T-type 24 AWG thermocouple was positioned at the geometric center of the payload box to monitor internal temperature.

5.2.2 Preconditioning and Experimental Simulation

To ensure consistency and repeatability in the testing methodology, all the materials for the insulated shipping container were pre-conditioned prior to placement in the environmental test chamber. This includes allowing insulation materials, gel packs, outer box, and payload to equilibrate to the desired starting temperature and humidity levels. Proper pre-conditioning ensures thermal consistency, minimizes initial temperature differentials, and eliminates any transient effects that could compromise the accuracy and repeatability of the test results. This step was critical for simulating real-world pre-shipment handling and ensuring the reliability of the thermal performance evaluation. All the materials except gel packs were preconditioned at 25± 1 °C with 50 ± 2% relative humidity (RH) for 36 hours. The gel packs were conditioned at -20 ± 3°C for 48 hours.

The experiment was designed to analyze the effect of humidity on the thermal performance of insulated shipping containers (ISCs) under varying ambient conditions, specifically across different relative humidity(RH) and temperature levels. RH levels of 30%, 50%, and 80% were selected to represent typical to extreme environmental conditions, while test temperatures were maintained at either 25 °C or 35 °C depending on the configuration. For Shipper Configuration 1, which uses two layers of BC double-wall corrugated fiberboard as insulation, multiple subcategories were tested. The small, small (with product), and large variations were tested at a temperature of 25 °C and tested under all three humidity levels. Specifically, six samples were tested per humidity level for the small category, while two samples were tested at 30% and 80% RH for the small (with product) category. Configuration 1 small subcategory was also tested at 35 °C with three samples for each humidity level. Configuration 2, which used honeycomb board insulation, included both small and large subcategories. All shippers were tested at 25 °C across all humidity levels, with three samples per condition. Configuration 3, featuring the EPS molded cooler, and Configuration 4, using a metallized roll made of Polyurethane (PU) foam, were tested in a single size. Both configurations were subjected to 25 °C across 30%, 50%, and 80% relative humidity conditions, with three samples per humidity level.

Table 9 shows experimental design and the boundary condition for the environmental chamber testing. This comprehensive testing matrix ensured that the influence of humidity on all insulation materials can be rigorously compared, providing insights into their performance stability and suitability for cold chain applications under varying environmental conditions.

Table 9: Summary of the experimental design followed for the study.

Shipper	Subcategory	Insulation Material	Temperature (°C)	Relative Humidity		
				30%	50%	80%
Configuration 1	Small	Two layers of BC Double-Wall fiberboard	25	5 samples	5 samples	5 samples
	Small (with product)			2 samples	N/A	2 samples
	Large			3 samples	3 samples	3 samples
	Small		35	3 samples	N/A	3 samples
Configuration 2	Small	Honeycomb board	25	3 samples	3 samples	3 samples
	Large			3 samples	3 samples	3 samples
Configuration 3	One Size	EPS molded cooler		3 samples	3 samples	3 samples
Configuration 4	One Size	Metallized Roll (PU)		2 samples	3 samples	3 samples

Temperature readings were collected using an Omega OM-CP-TCTempX Series data logger (Omega Engineering, Norwalk, Connecticut), with Omega T-type miniature male connectors used to complete the setup. The sample frequency was set to 30 seconds. Then, the ISCs were placed inside a reach-in environmental chamber (Temperature Product Solutions, New Columbia, PA) according to their boundary conditions.

The study was carried out until the internal probe temperature of each insulated shipping container (ISC) reached a temperature of 8 °C or higher, which is a common maximum limit used to assess cold chain performance. It was out of scope for the research to control for a minimum temperature. Although all ISCs were prepared under similar conditions, it was difficult to achieve the exact same starting temperature due to handling and environmental differences. To reduce this variation, all gel packs were left at room temperature for 15 minutes before being packed to help them reach a stable condition. For consistency in calculating the time taken to reach 8 °C, a starting temperature of -3 °C was used. This value was chosen as it closely represented the average starting temperature across the samples. Since similar ISC configurations were expected to perform similarly, using this common starting point helped provide a fair and consistent comparison between different setups and humidity conditions. Following the pack-out procedure,

the containers were placed inside a calibrated environmental chamber (Temperature Product Solutions, New Columbia, PA) to begin thermal performance testing. Each test was conducted under predefined boundary conditions specific to the target temperature and relative humidity levels for that configuration. The environmental chamber provided precise control over both temperature and humidity, ensuring consistent and repeatable conditions throughout the duration of the experiment.

5.3 Results and Discussion

This section presents experimental findings on how varying environmental humidity levels impact the thermal performance of ISCs. Specifically, the study evaluated the duration required for internal temperatures to rise from −3 °C to 8 °C under three relative humidity conditions: 30%, 50%, and 80%. To assess whether the observed differences in thermal performance across humidity levels were statistically significant, a one-way analysis of variance (ANOVA) was first performed on the duration data. This test evaluated whether the mean time to reach 8 °C differed significantly among the different configuration groups. If the configuration confirms that humidity is a significant factor, then three humidity groups for the significant configurations evaluated. Following a significant ANOVA result, Tukey's Honestly Significant Difference (HSD) post-hoc test was applied to identify specific pairwise differences between humidity levels. This approach is particularly suitable for controlling the family-wise error rate when making multiple comparisons. If the pairwise comparison between different humidity levels results in a p-value greater than 0.05, it indicates that the difference in mean values is not statistically significant at the 95% confidence level. In such cases, it can be concluded that relative humidity does not have a significant effect on the thermal performance under those specific conditions, and any observed differences may be due to random variation. Conversely, if the p-value is less than 0.05, the difference in means is considered statistically significant, suggesting that relative humidity has a measurable and meaningful impact on the duration required for the internal temperature to reach the critical threshold. This confirms that humidity is a significant influencing factor in the thermal behavior of the packaging system. After that, a regression analysis has been conducted across different configurations to identify how different insulation reacts to environmental humidity change.

Table 10: Result summary of the average time to reach 8°C for different configurations with their significance on humidity.

Configuration	Subcategory / Condition	Humidity Level	Average Time to Reach 8 °C (hrs), COV%	Tukey HSD^		Humidity Effect ANOVA p-Value
1	Small	30%	38.00 (7%)	A		<.0001*
		50%	36.77 (4%)	A		
		80%	30.77 (1%)		B	
	Large	30%	41.24 (3%)	C		0.0026*
		50%	42.01 (3%)	C		
		80%	29.93 (9%)		D	
1 (With Product)	Small – Loaded Condition	30%	36.09 (2%)	E		0.0049*
		80%	30.07 (6%)		F	
1 (35 °C)	Small – High Ambient Temp	30%	25.7 (2%)	G		0.0016*
		80%	21.19 (4%)		H	
2	Small	30%	24.88 (5%)	I		0.8065
		50%	31.47 (7%)		J	
		80%	26.39 (2%)		J	
	Large	30%	37.65 (4%)	K		0.0312*
		50%	42.01 (3%)		L	
		80%	29.62 (1%)			M
3	—	30%	45.01 (3%)	N		0.1748
		50%	46.82 (2%)	N		
		80%	43.4 (2%)	N		
4	—	30%	53.9 (3%)	P		0.6039
		50%	57.51 (3%)	P		
		80%	55.7 (0%)	P		

^ Subgroups connected by the same letter; * is significant. ANOVA was conducted independently for each configuration and subcategory grouping.

Table 10 presents the average time required for different shipper configurations to reach 8 °C under varying humidity levels. The results show a clear distinction between fiber-based and polymer-based insulation systems in their response to humidity. For the fiber-based configurations, particularly those using BC double-wall paper (Configuration 1), humidity had a strong influence on thermal performance. As relative humidity increased from 30 % to 80 %, the time to reach 8 °C generally decreased, indicating that higher moisture content in the insulation accelerated heat transfer. The small and large versions of Configuration 1, as well as the loaded and high-temperature conditions, all showed statistically significant differences ($p < 0.01$). For example, the large shipper's duration decreased from about 42 h at 30 % humidity to under 30 h at 80 %, confirming that absorbed moisture reduced the material's insulating capacity. Configuration 2, which used honeycomb board, exhibited a more moderate response. The small version did not show any significant effect ($p = 0.81$), suggesting better moisture resistance, while the large version still displayed a

noticeable reduction in cold-retention time ($p = 0.03$). By contrast, the polymer-based systems (Configurations 3 and 4) demonstrated stable performance across all humidity levels. The EPS molded cooler, and the metallized PU roll maintained average durations between 43 h and 56 h, with no statistically significant changes ($p > 0.17$). Their hydrophobic and closed-cell nature prevents water vapor absorption, preserving thermal resistance even under humid conditions.

Table 11: Significance on different humidity level change for different configurations

Configuration	Subcategory / Condition	Relative Humidity Comparison	Mean Difference to reach 8C (hrs)	p-Value	Humidity Factor
1	Small	30–50 %	1.22	0.5239	Not Significant
		30–80 %	7.23	0.0001	Significant
		50–80 %	6.01	0.0004	Significant
	Large	30–50 %	0.76	0.8545	Not Significant
		30–80 %	11.31	0.0005	Significant
		50–80 %	12.08	0.0004	Significant
1 (With Product)	Small – Loaded Condition	30–80 %	6.02	0.0048	Significant
1 (35 °C)	Small – High Ambient Temp	30–80 %	4.5	0.0016	Significant
2	Small	30–50 %	6.59	Overall configuration not significant	
		30–80 %	1.51		
		50–80 %	5.08		
	Large	30–50 %	4.36	0.0057	Significant
		30–80 %	8.03	0.00022	Significant
		50–80 %	12.39	0.00002	Significant
3	—	30–50 %	1.82	Overall configuration not significant	
		30–80 %	1.61		
		50–80 %	3.42		
4	—	30–50 %	3.61	Overall configuration not significant	
		30–80 %	1.8		
		50–80 %	1.81		

Table 11 provides a detailed assessment of how different humidity ranges affected the time required for the shippers to reach 8 °C within configuration level. Overall, the results confirm that humidity plays a critical role in determining thermal performance, particularly for materials that are hygroscopic or porous in nature. As relative humidity increases, absorbed moisture tends to elevate the effective thermal conductivity of the insulation, leading to faster heat transfer and a shorter duration to reach the target temperature. In general, the influence of humidity becomes more pronounced at higher levels. Comparisons between 30 % and 50 % relative humidity show only minor differences,

and most of these changes are statistically insignificant. This suggests that moderate humidity variations have a limited effect on insulation performance, as the materials can still retain much of their dry thermal resistance. However, the differences observed in the 50–80 % and 30–80 % comparisons are consistently larger and statistically significant across most cases. This indicates that high humidity conditions cause a more substantial deterioration in insulation effectiveness, likely due to increased moisture absorption. The overall trend across all configurations shows that once humidity exceeds 50 %, the system's ability to maintain low internal temperatures begins to decline rapidly. In contrast, transitions between 30 % and 50 % humidity generally produce smaller changes, highlighting a threshold effect where materials remain relatively stable under moderate moisture exposure but degrade quickly beyond that point.

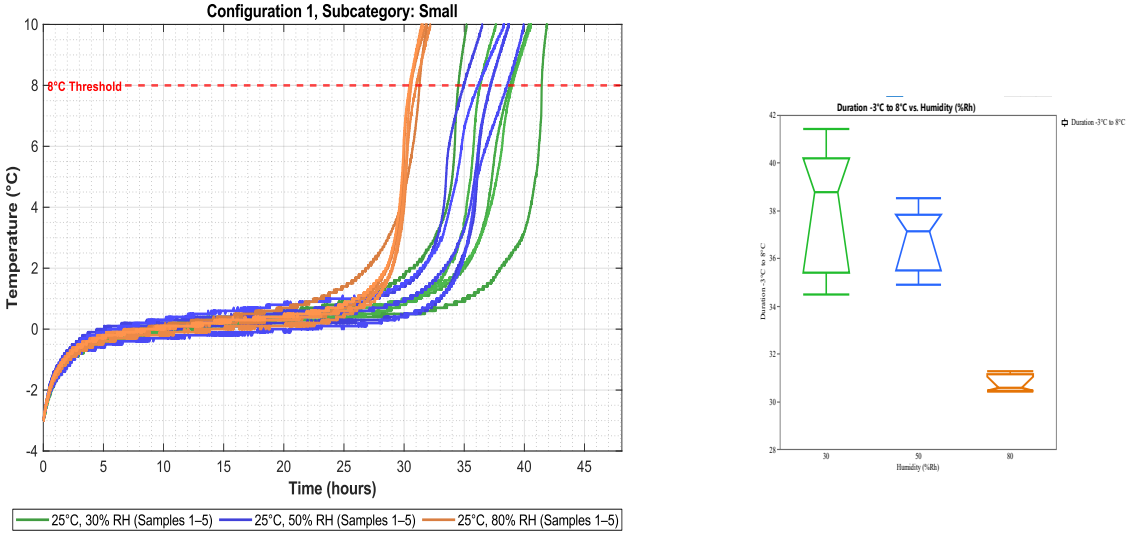

Figure 16: Thermal performance of configuration 1, Subcategory: Small

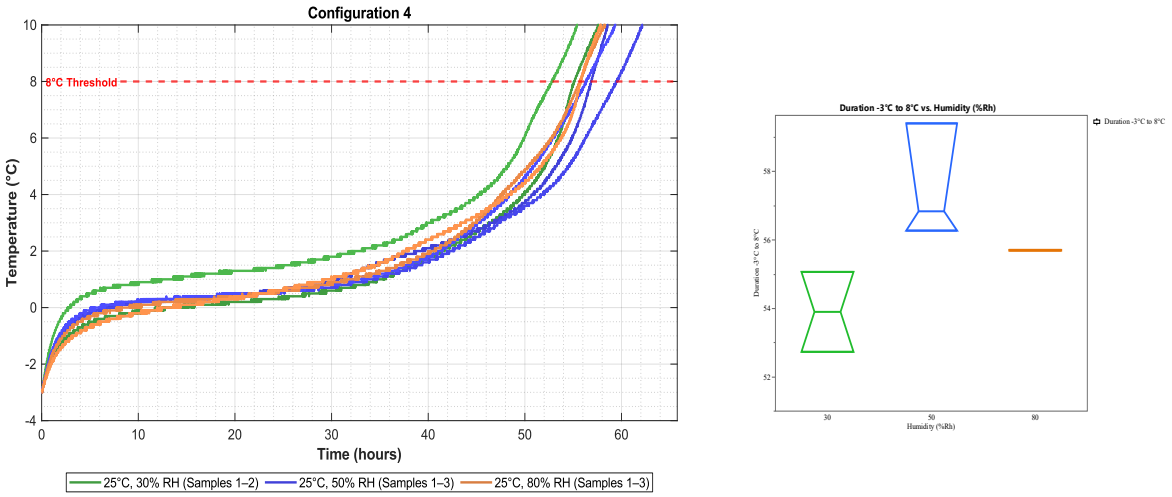

Figure 17: Thermal performance of configuration 4

Figure 16 and Figure 17 illustrate the thermal performance of Configuration 1 (Small) and Configuration 4 under different relative humidity levels. Both figures depict the transient temperature response of the packages during the warming process from the initial subzero condition up to the 8 °C threshold, highlighting the distinct phase change behavior of the PCM gel packs and the influence of insulation type and humidity on the overall temperature evolution. In Figure 16, corresponding to Configuration 1 with a fiber-based double-wall corrugated insulation, the temperature curves show a characteristic three-stage pattern typical of PCM systems. Initially, there is a rapid temperature rise during the sensible heating phase as the PCM warms from approximately −5 °C to near 0 °C. This is followed by an extended plateau region where the temperature remains nearly constant for several hours. This plateau represents the phase change region, during which the PCM absorbs latent heat while transitioning from solid to liquid, effectively delaying further temperature increase inside the shipper. Once the phase change is complete, the temperature rises sharply again as the PCM enters the post-melting sensible heating phase. The duration of this plateau region is a direct measure of the PCM's thermal buffering capacity. Under higher humidity (80 % RH), the plateau period is noticeably shorter, and the 8 °C threshold is reached sooner. This behavior reflects the detrimental effect of moisture absorption on the insulation's performance. The surrounding corrugated paper insulation becomes thermally conductive when humid, allowing more external heat to penetrate and accelerating PCM melting. In contrast, samples at 30 % RH exhibit a slower rise and longer plateau, maintaining temperatures below 8 °C for a longer period. The adjacent box plot reinforces these observations. It shows a clear downward shift in cold-retention time as humidity increases, with significantly lower median and narrower spread at 80 % RH compared to 30 % and 50 %. The smaller interquartile

range at high humidity indicates more uniform yet poorer performance, as all samples warm more quickly. This statistical distribution aligns with the earlier numerical findings, confirming that fiber-based systems are highly sensitive to humidity variations.

In Figure 17, representing Configuration 4 with a polymer-based metallized PU insulation, the general thermal trend remains similar in shape but with noticeably extended duration before reaching 8 °C. The PCM exhibits the same distinct phase change plateau, yet the curves for 30 %, 50 %, and 80 % RH nearly overlap, indicating minimal influence of humidity. The longer plateau period demonstrates effective latent heat utilization, and the smaller divergence between curves confirms the excellent moisture resistance of polymer-based insulation. The corresponding box plot for Configuration 4 further supports this observation. The mean times to reach 8 °C remain relatively consistent across humidity levels, and the variation between samples is small. This suggests that the closed-cell structure and metallized surface of the PU material effectively block moisture ingress, maintaining stable thermal insulation and consistent PCM behavior regardless of environmental humidity.

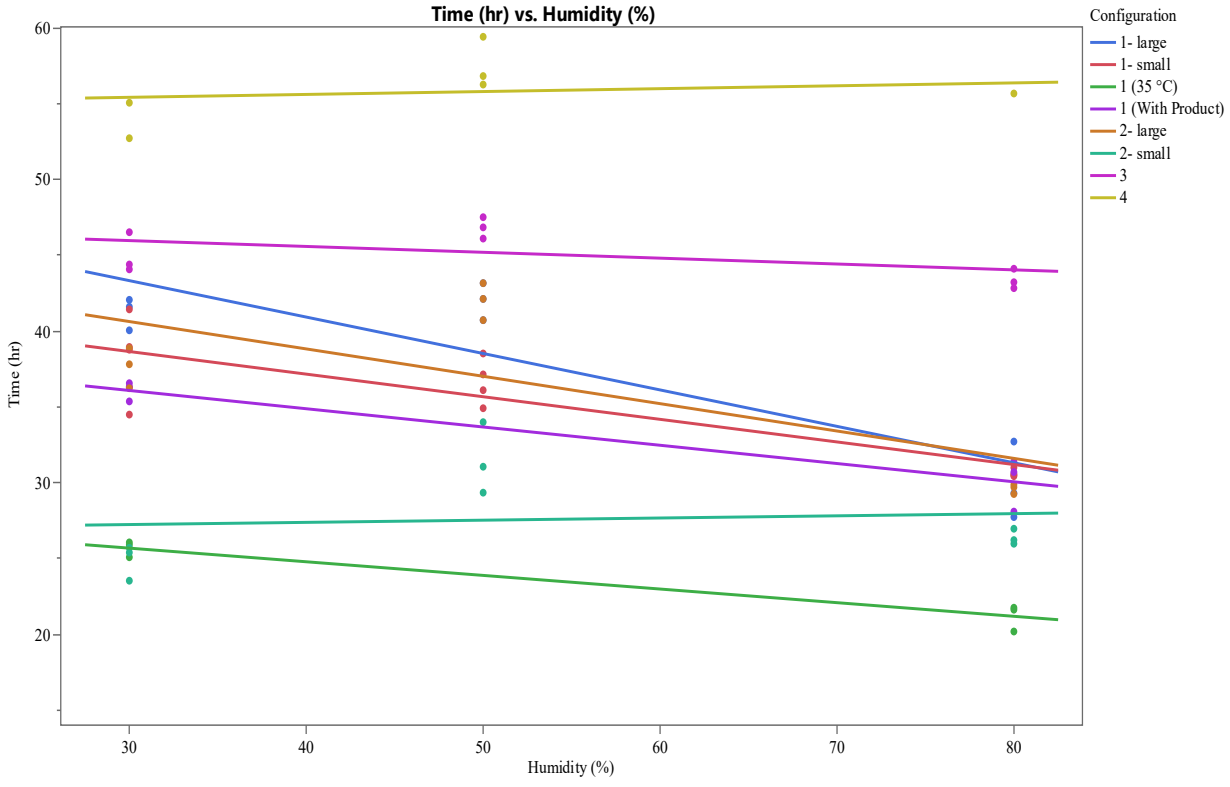

Figure 18: Scatter plot with regression line for different humidity levels of all configurations

Table 12: Configuration constant with humidity effect coefficient for different configurations

Configuration	Material Type	Configuration Constant	Slope (Humidity effect Coefficient)
1 – Large	Fiber-based	50.55	– 0.24
1 – Small	Fiber-based	43.13	– 0.15
1 (35 °C)	Fiber-based	28.39	– 0.09
1 (With Product)	Fiber-based	39.7	– 0.12
2 – Large	Fiber-based	46.05	– 0.18
2 – Small	Fiber-based	26.81	0.01 *
3	Polymer-based	47.14	– 0.04 *
4	Polymer-based	54.86	0.02*

* Humidity effect was not significant for these configurations.

Figure 18 illustrates the relationship between relative humidity and the time required for different configurations to reach 8 °C, with regression lines plotted for each system. Most fiber-based configurations show a downward slope, meaning that as humidity increases, the duration to reach 8 °C decreases. This pattern indicates that moisture in the surrounding environment gradually compromises the insulation's ability to resist heat transfer. When the humidity rises beyond 50 %, the hygroscopic insulation materials begin to absorb water vapor, which increases their thermal conductivity and accelerates heat penetration. As a result, hold time is shortened, and the PCM transitions through its melting phase more rapidly. The polymer-based configurations, on the other hand, demonstrate almost flat or slightly positive slopes, suggesting that their performance remains largely unaffected by humidity. This stability can be attributed to the closed-cell structure and low permeability of EPS and PU insulation, which minimize moisture uptake. These materials maintain their designed thermal resistance even under elevated humidity, preserving consistent PCM phase change behavior and extending temperature control duration.

Table 12 provides a quantitative summary of these trends through regression constants and slope coefficients, representing the humidity effect on each configuration. The configuration constant reflects the baseline duration at low humidity, while the slope value captures how strongly performance changes with increasing humidity. Larger negative slopes indicate greater effect due to humidity changes. For instance, the slope of −0.24 for Configuration 1–Large and −0.18 for Configuration 2–Large clearly shows a strong reduction in retention time as humidity rises. In contrast, polymer-based systems such as Configuration 3 (−0.04) and Configuration 4 (+0.02) exhibit minimal or negligible humidity dependence.

The results across all configurations indicate that humidity has a measurable impact on thermal performance, particularly for systems using fiber based insulation materials. In Configuration 1, where the shipper was insulated

with two layers of BC double-wall paper, humidity was found to be a significant factor in most subcategories, including small, small with product. Even in the presence of product load representing real-world use humidity continued to significantly influence the time required to reach 8°C. Configuration 2, which used honeycomb board, also demonstrated significant sensitivity to humidity at both subcategories tested. In contrast, polymer-based insulation systems showed mixed responses. While Configuration 3 (EPS molded cooler) exhibited significant effects, Configuration 4 (metallized PU) did not show statistically significant sensitivity to humidity. These findings reinforce that material type plays a critical role in how humidity influences thermal behavior, with biodegradable systems being more susceptible to humidity-driven performance changes.

Although EPS (Expanded Polystyrene) is generally considered a moisture-resistant material due to its closed-cell structure, it is not entirely impermeable to water vapor. Over time, small pores and interstitial voids between beads can allow for limited moisture absorption, especially under high humidity conditions. This absorbed moisture may accumulate along micro-channels or bead interfaces, increase localized thermal conductivity and slightly reduce the overall insulation effectiveness. While the bulk EPS material resists water ingress, capillary condensation in fine pores and imperfect fusion between beads can create subtle thermal pathways. These effects may not drastically alter thermal resistance in the short term, but they can contribute to measurable differences in heat transfer rate, particularly during prolonged exposure to humid environments. This mechanism helps explain why EPS systems, despite being polymer-based, may still show statistically significant sensitivity to humidity in controlled experiments.

5.4 Conclusion

This study provides clear and comprehensive evidence that environmental humidity significantly influences the thermal performance of insulated shipping containers (ISCs). Through a series of controlled experiments across various configurations, temperatures, and insulation materials, it was consistently observed that increasing relative humidity accelerates the warming process and reduces the time required for internal temperatures to reach 8 °C. The effect was most pronounced in systems using biodegradable insulation materials such as paper-based boards and honeycomb structures, which are inherently more sensitive to moisture. Even polymer-based systems, like EPS, exhibited some performance variation under high humidity, likely due to surface moisture effects, pore interactions, or system-level thermal bridging.

Statistical analysis, including Tukey's HSD and percent change comparisons, reinforced these observations. In most configurations, particularly those exposed to 80% RH, the differences in thermal response were not only visible but statistically significant. For configurations that included a payload, the presence of the product altered the thermal mass but did not eliminate the influence of humidity, demonstrating that the effect persists even under realistic loading conditions.

Given these findings, it is evident that humidity should not be treated as a secondary variable in cold chain packaging design. Instead, it must be integrated into performance evaluation protocols, insulation selection criteria, and environmental chamber testing standards.

Recommendations for Future Research:

1. Future studies should investigate the moisture absorption behavior of different insulation materials in real-time and correlate this with thermal conductivity changes to develop predictive models.

2. For reusable packaging systems, it is important to assess how repeated exposure to high humidity affects material degradation, insulation performance, and microbial susceptibility over time.

3. There is scope to develop or incorporate humidity-resistant coatings or adaptive insulation layers that respond dynamically to moisture changes and maintain consistent thermal performance.

4. Conducting tests under climate-specific humidity and temperature profiles (e.g., tropical, arid, temperate zones) can provide insight into how packaging performs across diverse geographic supply chains.

5.5 References

Apostolopoulou-Kalkavoura, V., Gordeyeva, K., Lavoine, N., & Bergström, L. (2018). Thermal conductivity of hygroscopic foams based on cellulose nanofibrils and a nonionic polyoxamer. Cellulose, 25(2), 1117–1126. https://doi.org/10.1007/s10570-017-1633-y

Calati, M., Hooman, K., & Mancin, S. (2022). Thermal storage based on phase change materials (PCMs) for refrigerated transport and distribution applications along the cold chain: A review. International Journal of Thermofluids, 16, 100224. https://doi.org/10.1016/j.ijft.2022.100224

Chowdhury, D. A., Jeong, M. S., Vyas, L., Kim, J., Cosler, L. E., Lash, D. J., Barone, J. A., Toscani, M., & Volino, L. R. (2023). Evaluation of temperature excursions from USP <659> recommendations during mail transit. Journal of the American Pharmacists Association, 63(3), 847–852. https://doi.org/10.1016/j.japh.2023.02.002

D10 Committee. (n.d.). Test Method for Thermal Insulation Performance of Distribution Packages. ASTM International. https://doi.org/10.1520/D3103-14

Dombek, G., Nadolny, Z., Przybylek, P., Lopatkiewicz, R., Marcinkowska, A., Druzynski, L., Boczar, T., & Tomczewski, A. (2020). Effect of Moisture on the Thermal Conductivity of Cellulose and Aramid Paper Impregnated with Various Dielectric Liquids. Energies, 13(17), 4433. https://doi.org/10.3390/en13174433

El Assaad, M., Plantec, Y., Colinart, T., & Lecompte, T. (2024). Influence of moisture transfer on thermal conductivity measurement by HFM: Measurement accuracy on insulation materials and consequences on building energy assessments. Energy and Buildings, 320, 114635. https://doi.org/10.1016/j.enbuild.2024.114635

Freedonia Group. (2022). E-Commerce: United States. E-Commerce: United States. www.freedoniafocusreports.com

Freedonia Group. (2023). Meal Kits: United States (Freedonia Focus Reports, pp. 1–28).

Gaffen, D. J., & Ross, R. J. (1999). Climatology and Trends of U.S. Surface Humidity and Temperature. https://journals.ametsoc.org/view/journals/clim/12/3/1520-0442_1999_012_0811_catous_2.0.co_2.xml

International Safe Transit Assocoation (ISTA). (2010). ISTA 7E - Testing Standard for Thermal Transport Packaging Used in Parcel Delivery System Shipment [Standard]. https://ista.org/thermal_standards.php

ISO 23412:2020(en), Indirect, temperature-controlled refrigerated delivery services—Land transport of parcels with intermediate transfer. (n.d.). Retrieved August 11, 2025, from https://www.iso.org/obp/ui/es/#iso:std:iso:23412:ed-1:v1:en

Jayalath, P., Ananthakrishnan, K., Jeong, S., Shibu, R. P., Zhang, M., Kumar, D., Yoo, C. G., Shamshina, J. L., & Therasme, O. (2025). Bio-Based Polyurethane Materials: Technical, Environmental, and Economic Insights. Processes, 13(5), 1591. https://doi.org/10.3390/pr13051591

Kendzierawska, W. A., & Trochonowicz, M. (2024). Effect of temperature and Humidity on the Thermal Conductivity λ of Insulation Materials. Civil and Environmental Engineering Reports, 33(4), 42–49. https://doi.org/10.59440/ceer/178976

Kumar Deb, R. (2023). Temperature Sensitive Packaging Market Share, Size and Forecast 2030 (No. 19375). Credence Research, Inc. https://www.credenceresearch.com/report/temperature-sensitive-packaging-market

Lee, H., Ozaki, A., Lee, M., & Yamamoto, T. (2020). Humidity control effect of vapor-permeable walls employing hygroscopic insulation material. Indoor Air, 30(2), 346–360. https://doi.org/10.1111/ina.12622

PDA Technical Report No. 39 Revised 2021 (TR 39) Guidance for Temperature-Controlled Medicinal Products—Maintaining the Quality of Temperature-Sensitive Medicinal Products through the Transportation Environment (single user digital version). (n.d.). Default. Retrieved August 11, 2025, from https://www.pda.org/bookstore/product-detail/6280-tr-39-revised-2021

Pharmaceutical Cold Chain Packaging Market Demand 2025 to 2035. (n.d.). Retrieved October 21, 2025, from https://www.futuremarketinsights.com/reports/pharmaceutical-cold-chain-packaging-market

Rahman, M., Sikandar, M. U., Chowdhury, P., Roy, S., & Khrystoslavenko, O. (2025). Toward Sustainable Cold Chain Packaging: A Systematic Review of Insulating Materials and Green Alternatives for Temperature-Sensitive Logistics.

Raj, R., Singh, A., Kumar, V., De, T., & Singh, S. (2024). Assessing the e-commerce last-mile logistics' hidden risk hurdles. Cleaner Logistics and Supply Chain, 10, 100131. https://doi.org/10.1016/j.clscn.2023.100131

Rasch, C. (2025). The Future of Grocery: Online Grocery, Meal Kits, & Direct-to-Consumer Food, 3rd Edition (Packaged Facts). The Freedonia Group.

Ren, T., Ren, J., Matellini, D. B., & Ouyang, W. (2022). A Comprehensive Review of Modern Cold Chain Shipping Solutions. Sustainability, 14(22), 14746. https://doi.org/10.3390/su142214746

Singh, J., Jaggia, S., & Saha, K. (2013). The Effect of Distribution on Product Temperature Profile in Thermally Insulated Containers for Express Shipments. Packaging Technology and Science, 26(6), 327–338. https://doi.org/10.1002/pts.1985

Spiewak, R., Vankayalapati, G. S., Considine, J. M., Turner, K. T., & Purohit, P. K. (2022). Humidity dependence of fracture toughness of cellulose fibrous networks. Engineering Fracture Mechanics, 264(1), 108330. https://doi.org/10.1016/j.engfracmech.2022.108330

Sykes, C. (n.d.). Time- and Temperature-Controlled Transport: Supply Chain Challenges and Solutions.

6 Chapter 3: Environmental Analysis of Passive Cold-Chain Packaging Systems Using a Performance-Based Functional Unit

Abstract: This chapter assesses the environmental impact of four passive cold-chain packaging systems by comparing their life cycle impacts per hour of thermal protection. Environmental burdens from EcoImpact-COMPASS were divided by the hold-time values measured in Chapter 2 at 50% relative humidity. The fiber-based configurations had lower material impacts but shorter cooling duration, which resulted in moderate impact-per-hour values. The EPS and PU systems showed higher impacts per unit but much longer thermal performance, giving them the lowest environmental impact per hour. The results show that thermal duration plays a stronger role than material burden when evaluating the environmental performance of insulated shippers.

Keywords: environmental impact, life cycle assessment, cold chain packaging, thermal performance, and insulation materials.

6.1 Introduction

Sustainability considerations are becoming increasingly central to cold-chain packaging design as pharmaceutical and food distribution systems expand worldwide. Traditional polymer-based insulations such as expanded polystyrene (EPS) and polyurethane (PU) have historically dominated the market due to their strong thermal performance and low cost; however, their fossil-derived feedstocks, limited recyclability, and end-of-life challenges have raised concerns regarding long-term environmental impacts (Jayalath et al., 2025). In response, fiber-based alternatives such as corrugated fiberboard, molded pulp, and honeycomb structures are increasingly being explored for passive temperature-controlled shipping applications (Rahman et al., 2025). These materials offer recyclability and lower embodied energy but often exhibit higher material mass and greater sensitivity to environmental conditions such as humidity.

Life Cycle Assessment (LCA) provides a systematic and quantitative means to compare these materials by evaluating the environmental burdens associated with their entire life cycle. However, in thermal packaging systems, conventional mass- or unit-based functional units do not fully capture performance differences rooted in thermal behavior. Because temperature hold time is a primary functional requirement for passive cold-chain packaging, environmental impacts must be interpreted relative to the duration of thermal protection provided.

To address this, the present analysis uses a performance-based functional unit, defined as the environmental impact per insulated shipping container (ISC) per hour of thermal protection. This approach aligns environmental evaluation with experimentally measured time-to-8 °C (“hold time”), thereby linking sustainability directly to functional cold-chain performance. This chapter builds on the thermal experiments presented in Chapter 2, where hold-time duration was measured for each configuration, and uses those results directly as the functional unit for evaluating environmental

performance. The analysis integrates these hold-time values with LCA outputs to provide a clear, performance-normalized comparison across all packaging configurations. Specifically, this study aims to evaluate a small-scale environmental impact assessment for fiber based and polymer based TPS.

6.2 Methodology

6.2.1 Goal and Scope Definition

The goal of this analysis is to evaluate the environmental efficiency of alternative passive cold-chain packaging designs when normalized to their achieved thermal performance. Environmental impacts were determined for each ISC using EcoImpact-COMPASS and then divided by the experimentally measured time required for the internal payload to reach 8 °C at 50 % RH (the standard condition used across samples). This performance normalization isolates the environmental "cost" of delivering one hour of compliant thermal protection, allowing direct comparison across configurations with different masses, geometries, and material compositions.

6.2.2 System Boundary

A cradle-to-grave system boundary was applied, including:

- Raw material extraction and feedstock processing for corrugated fiberboard, honeycomb board, EPS, PU foam, PCM, and 30-pt paperboard
- Material fabrication and conversion
- Shipper assembly
- End-of-life treatment using U.S. MSW statistics (high recycling rates for corrugated components and predominant landfilling for polymer foams)

The system boundary description aligns with the earlier LCA scope applied in Chapter 2 and throughout the thesis. Transportation, reuse, facility energy, and capital infrastructure were intentionally excluded, consistent with screening-level LCA practice.

6.2.3 Inventory Data

Material masses for corrugated insulation (Configuration 1), honeycomb insulation (Configuration 2), EPS (Configuration 3), and PU (Configuration 4) were obtained from experimentally measured packaging inventories. PCM loading, payload box masses, and corrugated outer box components were included for each configuration. These inventories were consistent with the datasets used for earlier thermal performance analysis. Table 14 represents the material composition and the mass used for all the packaging configuration used in this study.

Table 13: Material composition and mass inventory for all packaging configurations

Component / Material	Config 1 Small (BC)	Config 1 Large (BC)	Config 2 Small (Honeycomb)	Config 2 Large (Honeycomb)	Config 3 (EPS)	Config 4 (PU)
Total package mass (PS)	2,980 g	3,896 g	2,735 g	3,616 g	2,737 g	3,852 g
Payload box – 30 pt paperboard (gm)	32 g	32 g	32 g	32 g	32 g	32 g
Outer box – C-flute corrugated (gm)	188 g	244 g	188 g	244 g	430 g	285 g
Insulation material	380 g (BC board)	560 g (BC board)	135 g (honeycomb)	280 g (honeycomb)	235 g (EPS)	135 g (PU)
PCM (gel packs)	2,380 g	3,060 g	2,380 g	3,060 g	2,040 g	3,400 g

6.2.4 Impact Assessment Methods

Environmental burdens were quantified using EcoImpact-COMPASS midpoint indicators, which represent commonly applied metrics in packaging-focused life cycle assessments. The indicators included:

- Climate change (kg CO_2-eq)
- Fossil fuel use (MJ deprived)
- Freshwater eutrophication (kg PO_4-eq)
- Water consumption (m^3 world-eq)

These impact categories were selected because they provide a balanced view of emissions, resource use, and environmental loading relevant to insulated packaging systems.

6.2.5 Functional Unit: Environmental Impact per Hour of Thermal Protection

The functional unit applied was:

$$\text{Impact per hour} = \frac{\text{Impact per ISC (COMPASS)}}{\text{Hold time (h)}}$$

Hold times were derived from experimental data collected at 50 % RH under controlled 25 °C ambient conditions. Using a performance-based FU eliminates the confounding influence of volumetric efficiency or mass-driven scaling, allowing the analysis to focus purely on how material intensity and thermal duration interact to shape environmental outcomes. Table 15 represents thermal hold time to reach 8°C at 50% Rh.

Table 14: Thermal hold time at 50% Rh for all configurations

Configuration	Subcategory	Hold Time at 50% RH (hrs)	COV (%)
1 – Small (BC)	Small	36.77	4%
1 – Large (BC)	Large	42.01	3%
2 – Small (Honeycomb)	Small	31.47	7%
2 – Large (Honeycomb)	Large	42.01	3%
3 – EPS	—	46.82	2%
4 – PU	—	57.51	3%

For reporting purposes, the environmental impacts were normalized by dividing each configuration's impact value by the overall average for that specific impact category. This normalization approach was used to enhance comparability across indicators and improve the clarity of the graphical presentation.

6.3 Results and Discussion

Figure 19 presents the normalized environmental impacts per hour of thermal protection for all packaging configurations at 50% relative humidity. Normalization was performed by dividing each configuration's impact value by the average of its respective impact category to allow direct comparison across indicators and to improve

visualization of relative differences. When evaluated on a per-hour basis rather than per-unit mass, several notable trends emerge.

Fiber-based configurations (1 and 2) show relatively low per-unit material burdens but also exhibit the shortest hold times, particularly in the small formats. As a result, their impact-per-hour values fall near the mid-range of the evaluated systems. Increasing the package size for fiber-based systems (1-Large and 2-Large) adds substantial insulation mass but yields only modest improvements in thermal duration. This leads to higher normalized impacts and highlights the diminishing environmental returns of increasing material use without proportionally enhancing insulation effectiveness.

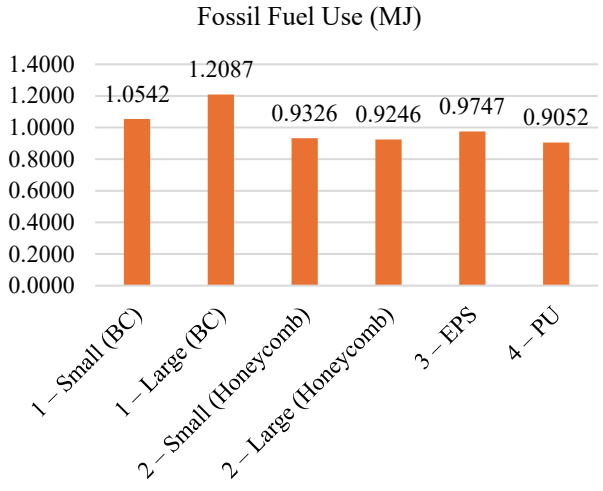

(a)

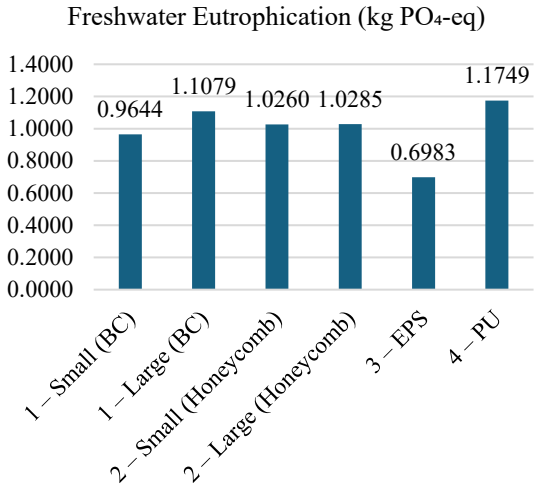

(b)

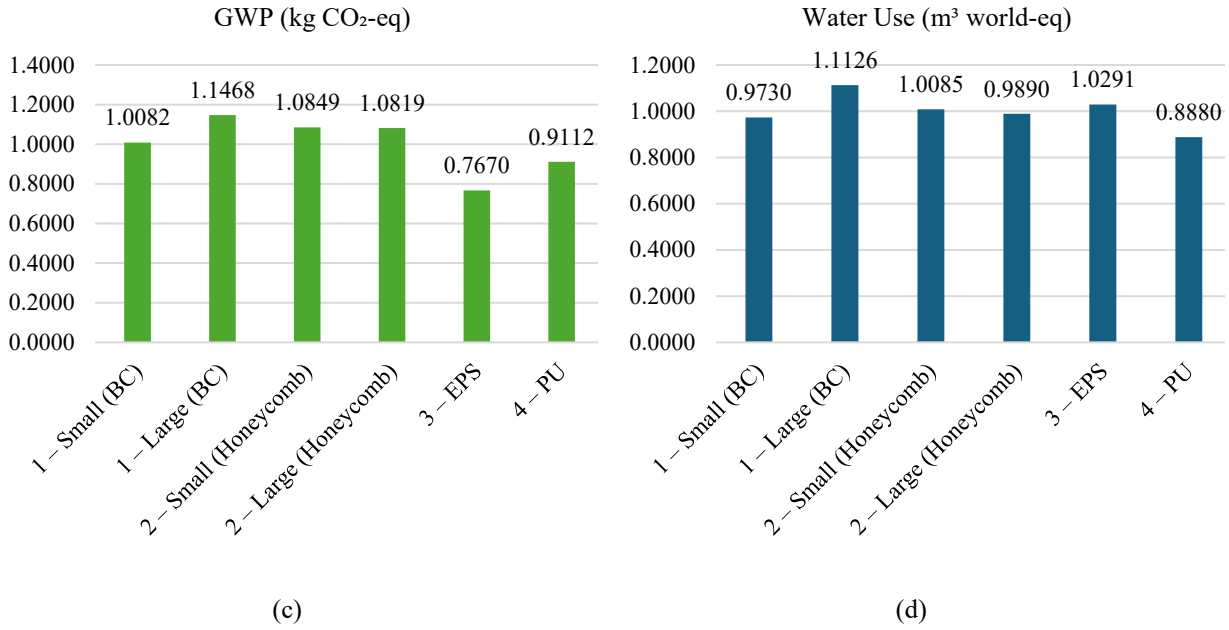

Figure 19: Normalized environmental impacts per hour of thermal protection for all packaging configurations at 50% relative humidity. Results are shown for (a) Fossil Fuel Use, (b) Freshwater Eutrophication, (c) Global Warming Potential, and (d) Water Use. Each impact value was normalized by dividing by the average of its respective impact category to improve comparability across configurations and enhance visualization of relative performance.

In contrast, polymer-based configurations (3 – EPS and 4 – PU) demonstrate longer thermal durations, with hold times of approximately 47 h and 58 h respectively. Despite having higher total environmental burdens per ISC, their extended cooling performance reduces their impact on a per-hour basis. PU, in particular, carries the highest insulation burden but also provides the longest thermal protection, resulting in one of the lowest normalized impact values. This illustrates how strong thermal performance can offset material intensity within a performance-aligned functional unit.

These findings emphasize that thermal duration is a key determinant of environmental efficiency when impacts are expressed per hour of protection. Under this functional unit, material mass alone is not a reliable indicator of sustainability; rather, the balance between insulation design and achieved thermal performance governs overall environmental outcomes.

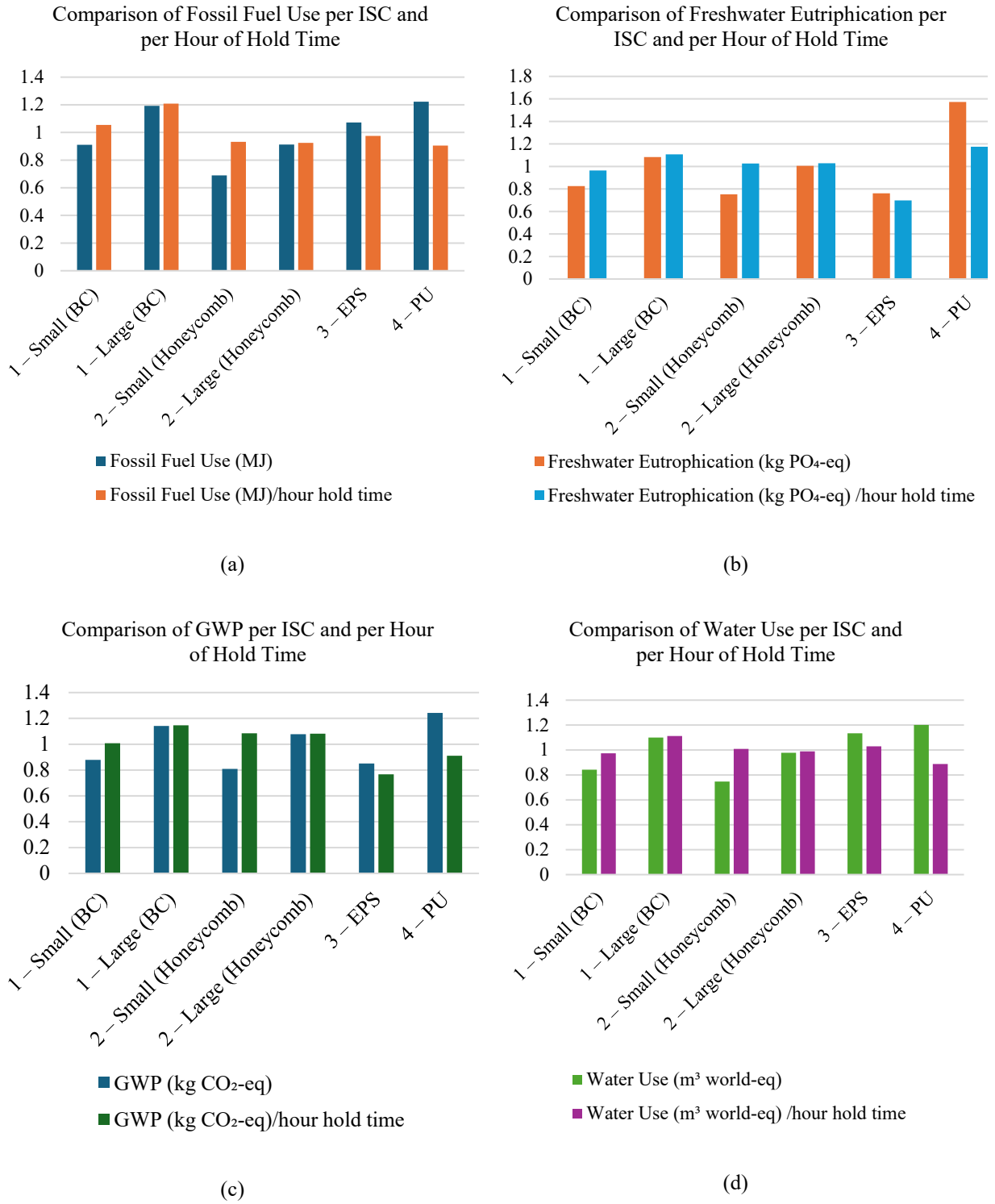

Figure 20: Comparison of environmental impacts per ISC and per hour of thermal protection for (a) fossil fuel use, (b) freshwater eutrophication, (c) global warming potential, and (d) water use across all configurations

Figure 20 illustrates how expressing environmental burdens on both a per-ISC and a per-hour basis reveals the central role of thermal performance in determining overall sustainability outcomes. Across all four indicators fossil fuel use, freshwater eutrophication, global warming potential, and water use the configurations with shorter hold times consistently show higher normalized impacts, even when their absolute per-unit impacts are comparatively low. This pattern is evident for the smaller fiber-based systems (1-Small and 2-Small), where limited thermal duration amplifies the per-hour environmental burden. Conversely, configurations with longer hold times, particularly 3 (EPS) and 4 (PU), demonstrate substantially reduced normalized impacts despite having higher material intensities. Their extended thermal performance distributes the environmental burden over more hours of protection, producing lower impact-per-hour values. These results highlight that thermal duration acts as a performance multiplier: improvements in insulation effectiveness directly enhance environmental efficiency, while reductions in hold time magnify per-hour impacts. Overall, the figure reinforces that the functional unit selection strongly affects comparative outcomes, and that thermal performance is a decisive factor in environmental sustainability for passive cold-chain packaging.

Overall, the performance-normalized LCA reveals important insights:

- Material burden alone does not determine environmental efficiency. Fiber-based materials have lower embodied impacts but shorter thermal durations, which can elevate impact-per-hour values.
- Thermal performance can outweigh material intensity. Polymer-based systems, despite higher impacts per ISC, perform more favorably when assessed on a per-hour basis.
- Humidity sensitivity indirectly influences environmental outcomes. Since fiber-based systems exhibited humidity-driven reductions in hold time in Chapter 2, their environmental efficiency is likely more variable in real-world conditions than that of EPS or PU.
- Performance-adjusted metrics reveal different sustainability conclusions than mass-based or logistics-based indicators. This reinforces why functional unit selection is critical in LCA.

6.3 Conclusion

Using a performance-based functional unit centered on impact per hour of thermal protection provides a clearer, functionally relevant understanding of the environmental trade-offs among passive cold-chain packaging systems. Fiber-based systems offer advantages in recyclability and moderate material impacts but exhibit shorter thermal durations, resulting in moderate environmental efficiency when normalized per hour. In contrast, polymer-based systems EPS and especially PU achieve long thermal durations that substantially offset their higher per-unit environmental burdens.

This analysis demonstrates that no single insulation type is universally superior; instead, sustainability depends on the balance between material impacts and achieved thermal performance. For applications requiring longer-duration protection, polymer-based systems may offer lower performance-normalized impacts, whereas fiber-based systems remain strong candidates for short-duration, high-recyclability applications. These findings reinforce the need for performance-aligned functional units in LCA, support the ongoing development of improved fiber-based insulation technologies, and highlight thermal duration as a critical parameter in sustainable cold-chain packaging design.

Recommendations for Future Research:

1. Investigate performance under more realistic distribution conditions, including fluctuating temperatures and wider humidity ranges.
2. Evaluate different payload types and masses to understand how product characteristics influence thermal behavior and environmental performance.
3. Incorporate transportation impacts and detailed end-of-life scenarios to capture the full life cycle more accurately.
4. Assess the long-term durability and potential reuse of insulation materials to determine their suitability for multi-use cold-chain systems.

6.4 References

Jayalath, P., Ananthakrishnan, K., Jeong, S., Shibu, R. P., Zhang, M., Kumar, D., Yoo, C. G., Shamshina, J. L., & Therasme, O. (2025). Bio-Based Polyurethane Materials: Technical, Environmental, and Economic Insights. Processes, 13(5), 1591. https://doi.org/10.3390/pr13051591

Rahman, M., Sikandar, M. U., Chowdhury, P., Roy, S., & Khrystoslavenko, O. (2025). Toward Sustainable Cold Chain Packaging: A Systematic Review of Insulating Materials and Green Alternatives for Temperature-Sensitive Logistics.

7 Summary

Chapter 1 focused on predicting the thermal performance of bio-based cold-chain packaging using finite element modeling (FEM) combined with laboratory characterization (DSC, Heat Flow Meter) to validate thermal properties and simulation accuracy. It demonstrated that FEM can accurately replicate experimental results (within ~8 % deviation), proving it as an efficient alternative to traditional performance testing. The chapter also emphasized the potential of fiber-based materials such as corrugated and honeycomb boards as renewable, biodegradable alternatives to polymer foams for passive cooling.

Chapter 2 investigated how environmental humidity affects the thermal behavior of passive insulated shipping containers. Controlled experiments at relative humidity levels from 30 % to 80 % revealed that high humidity accelerates internal warming, especially in fiber-based materials, because moisture absorption increases thermal conductivity. Polymer-based insulation like EPS and PU remained comparatively stable. The study confirmed humidity as a key driver of heat transfer in porous media and recommended integrating humidity control into standard testing procedures (ISO 23412, ISTA 7E, ASTM D3103).

Chapter 3 applied a performance-based Life Cycle Assessment (LCA) to evaluate the environmental impacts of four insulated shipping container (ISC) configurations constructed from fiber-based (BC and honeycomb) and polymer-based (EPS and PU) materials. Unlike conventional LCAs that use mass- or unit-based functional units, this chapter normalized environmental burdens by the measured hold time from Chapter 2 to express impacts per hour of thermal protection. This approach directly links sustainability to functional cold-chain performance. Results showed that although polymer-based systems have higher material impacts per container, their longer hold times substantially reduce impacts on an hourly basis. Fiber-based systems, while lighter and more recyclable, exhibited greater humidity-sensitive performance losses, resulting in higher impact-per-hour values under elevated RH conditions. Overall, the performance-normalized LCA highlighted thermal duration as a critical determinant of environmental efficiency and demonstrated the value of functional performance-based metrics in cold-chain packaging evaluation.

8 Conclusion

This research investigated the thermal and environmental performance of passive cold chain packaging systems, focusing on both predictive modeling and real-world environmental effects. The work combined finite element simulations, laboratory experiments, and material characterization to better understand how insulation and humidity conditions influence the temperature control capability of insulated shipping containers. The findings provide a strong foundation for designing cold chain systems that are not only thermally efficient but also sustainable and adaptable to diverse climatic conditions.

- The finite element modeling (FEM) framework accurately predicted temperature evolution within insulated containers, showing strong agreement with experimental data (average deviation ≈ 4–8%).
- Material characterization using Differential Scanning Calorimetry (DSC) and Heat Flow Meter testing provided reliable thermal property inputs that strengthened simulation accuracy.
- FEM proved to be a cost and time efficient alternative to repeated physical prototyping, enabling faster design optimization of insulation thickness, PCM volume, and geometry.
- Fiber-based insulation materials such as corrugated fiberboard and paper honeycomb exhibited promising thermal performance when combined with phase change materials (PCMs).
- Increasing relative humidity (30–80%) significantly reduced cooling duration and accelerated the warming rate, especially in fiber-based insulation systems.
- The moisture absorption behavior of porous materials increased their effective thermal conductivity, demonstrating humidity as a major driver of heat transfer in cold chain systems.
- Polymer-based foams (EPS, PU) remained thermally stable across humidity levels, highlighting the contrast between performance stability and sustainability.
- The results reveal a clear trade-off between environmental benefits and humidity sensitivity. Fiber-based materials are renewable and recyclable but require improved moisture protection.
- Humidity controlled testing should be integrated into standard protocols such as ISO 23412, ISTA 7E, and ASTM D3103 to more accurately represent real-world shipping environments.
- Future development should explore hybrid or coated fiber-based systems that combine the sustainability of paper materials with enhanced resistance to moisture and thermal degradation.

In summary, this study establishes an integrated framework that links modeling, experimentation, and environmental analysis to guide the design of next generation cold chain packaging. The outcomes demonstrate that it is possible to achieve a balance between thermal reliability and environmental sustainability, advancing the global shift toward more eco-efficient temperature-controlled logistics.

Appendix

Appendix A. Statistical Analysis summary of humidity tests

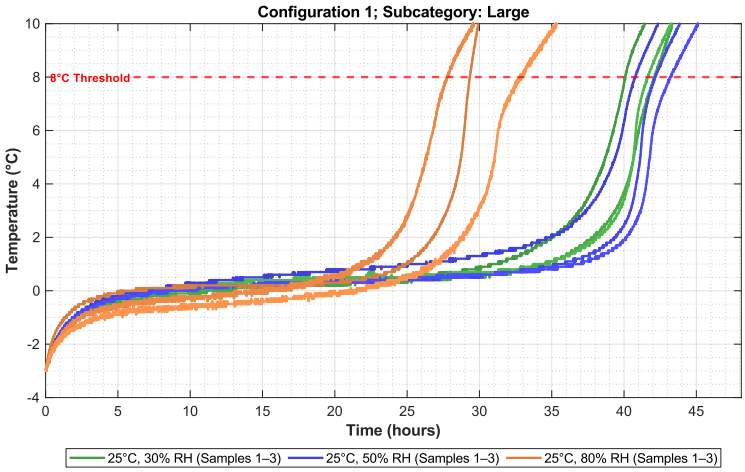

`Humidity Level	Average Time to Reach 8°C (hrs.)
30%	41.24
50%	42.01
80%	29.93

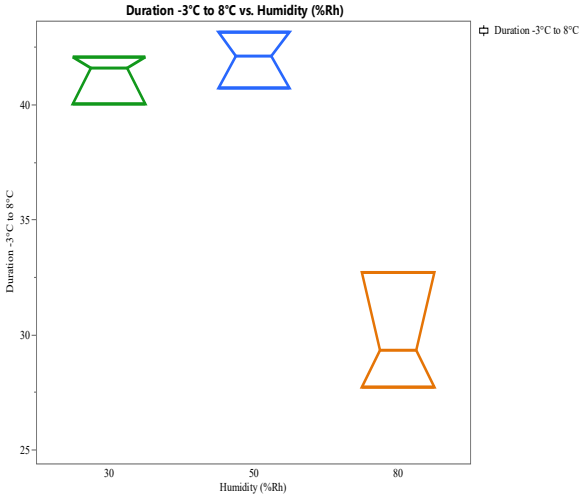

Relative Humidity Comparison	Mean Difference (Hrs)	p Value	Humidity factor
30% - 50%	0.76	0.8545	Not Significant
30% - 80%	11.31	0.0005	Significant
50% - 80%	12.08	0.0004	Significant

Figure 21: Performance and statistical analysis of configuration 1 (Small)

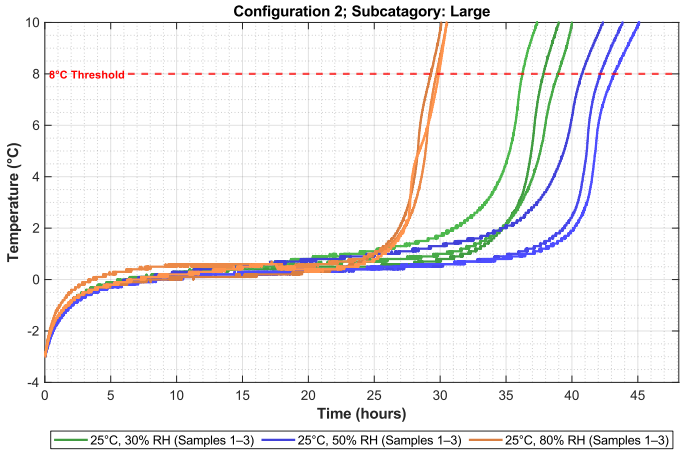

Humidity Level	Average Time to Reach 8°C (hrs.)
30%	37.65
50%	42.01
80%	29.62

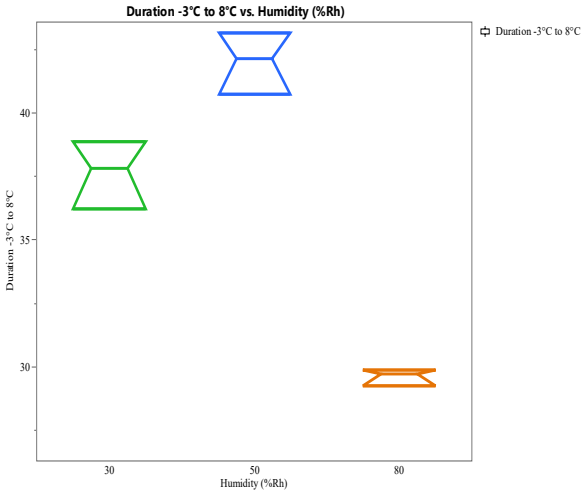

Relative Humidity Comparison	Mean Difference (Hrs)	p Value	Humidity factor
30% - 50%	4.36	0.00565	Significant
30% - 80%	8.03	0.00022	Significant
50% - 80%	12.39	0.00002	Significant

Figure 22: Performance and statistical analysis of configuration 2 (Small)

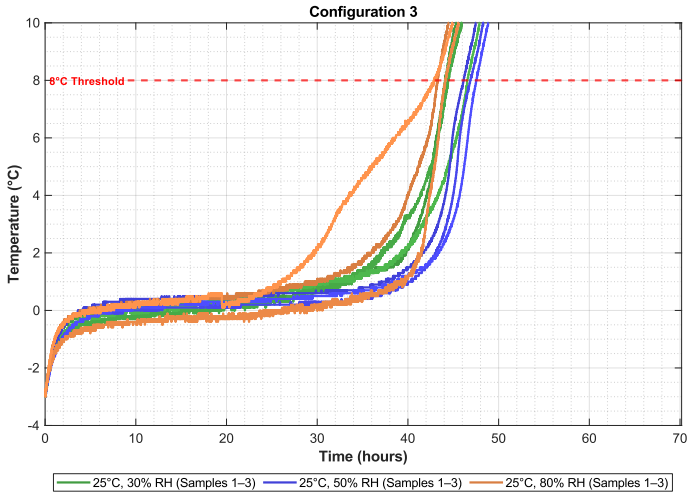

Humidity Level	Average Time to Reach 8°C (hrs.)
30%	45.01
50%	46.82
80%	43.40

Figure 23: Performance and statistical analysis of configuration 3

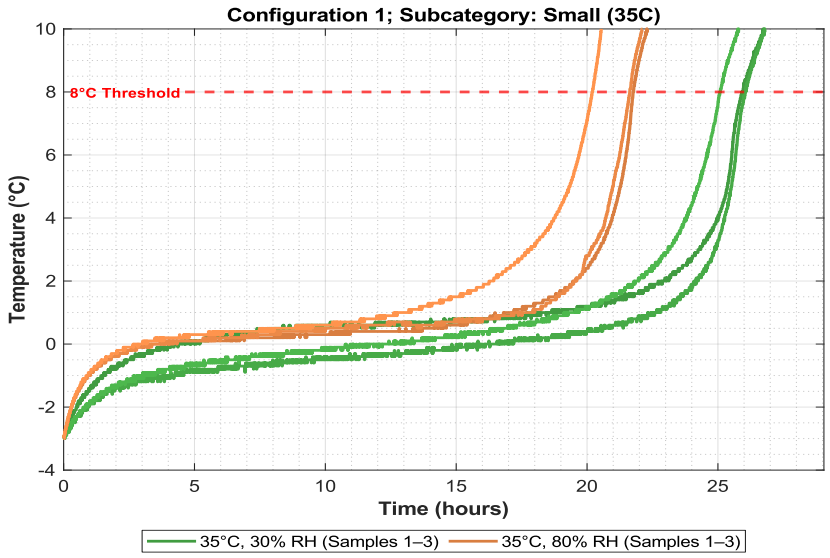

Relative Humidity Comparison	Mean Difference (Hrs)	p Value	Humidity factor
30%-80%	4.5	0.0016	Significant

Relative Humidity`	Average Time to Reach 8°C (hrs.)
30%	25.70
80%	21.19

Figure 24: Performance and statistical analysis of configuration 1 (Small 35°C)

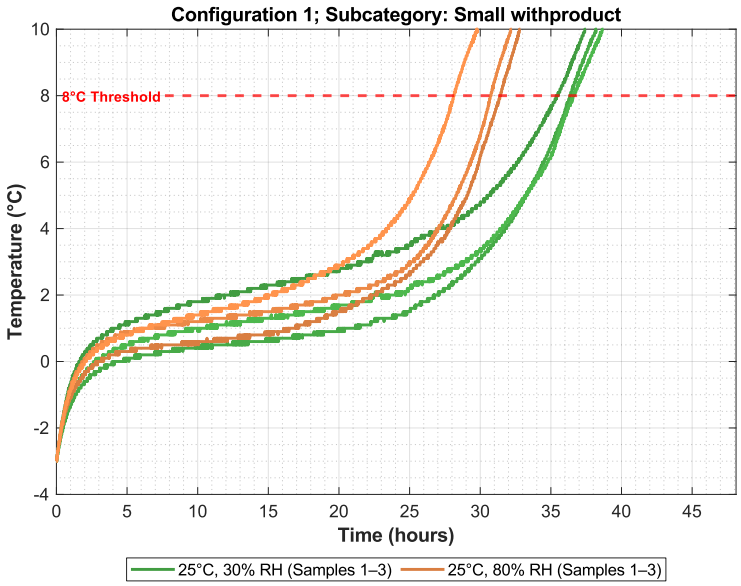

Relative Humidity Comparison	Mean Difference (Hrs)	p Value	Humidity factor
30%-80%	6.02	0.0048	Significant

Humidity Level	Average Time to Reach 8°C (hrs.)
30%	36.09
80%	30.07

Figure 25: Performance and statistical analysis of configuration 1 (with product)

Appendix B. Detailed reports of Environmental Impact Analysis

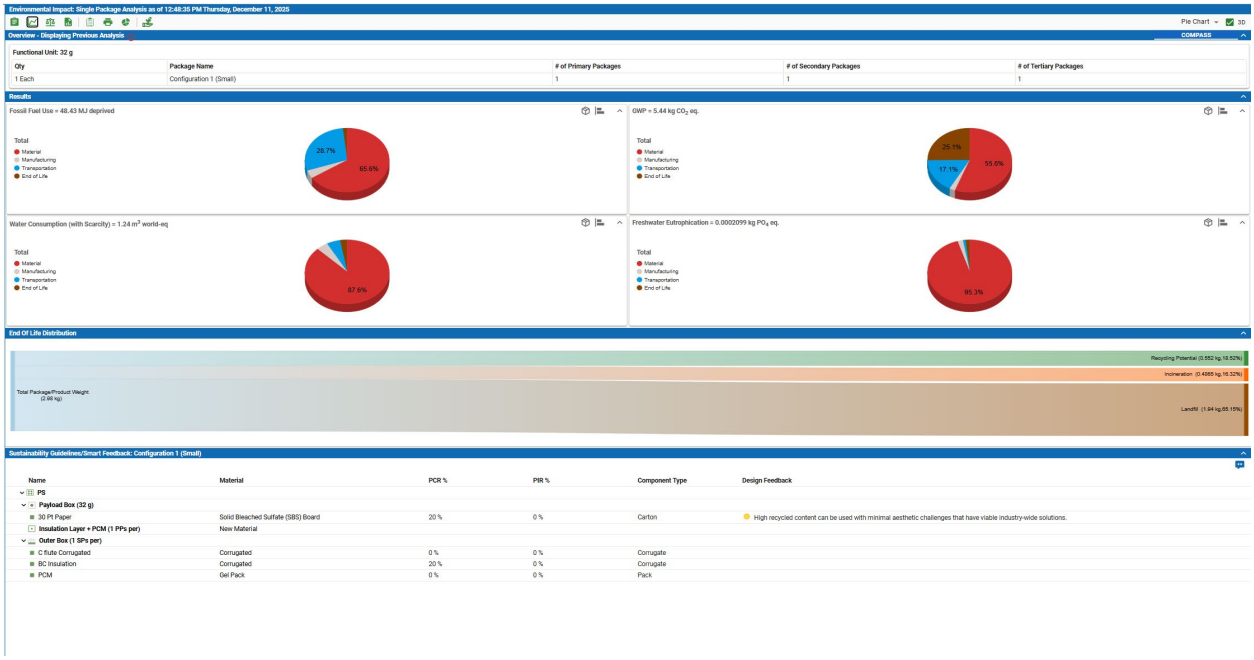

Figure 26: Environmental impact report for configuration 1 (small)

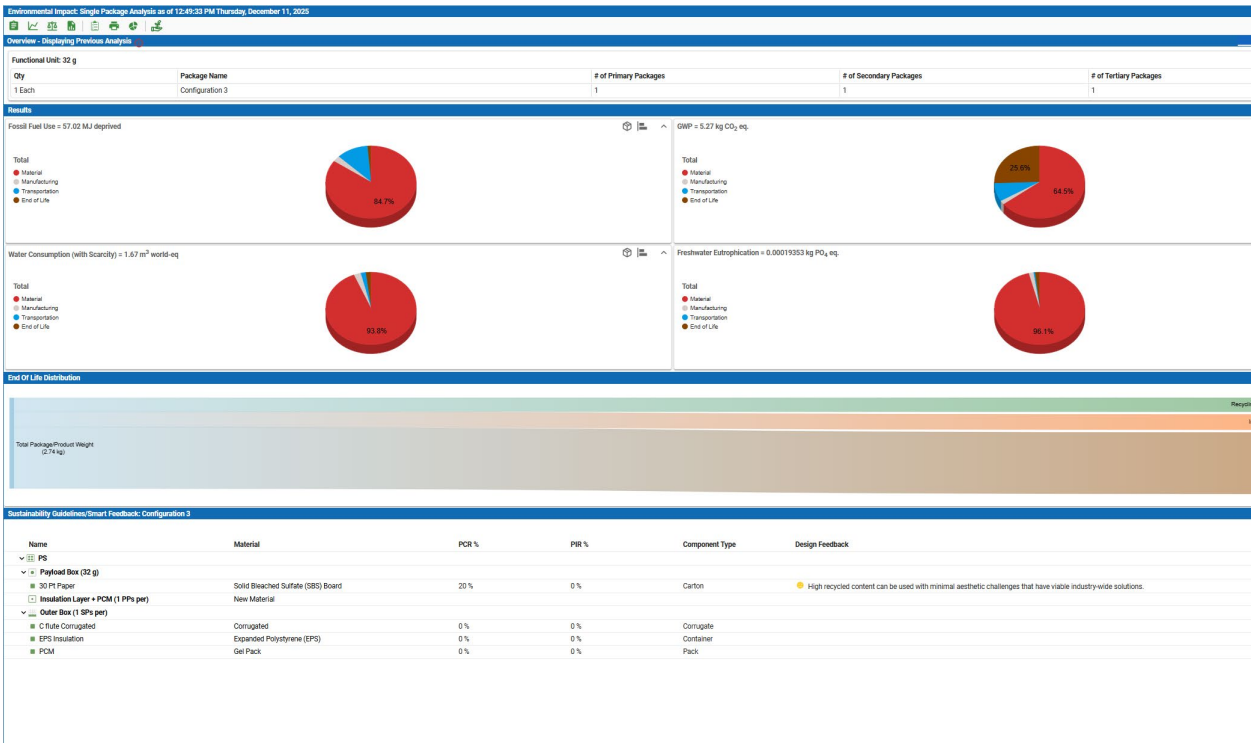

Figure 27: Environmental impact report for configuration 3

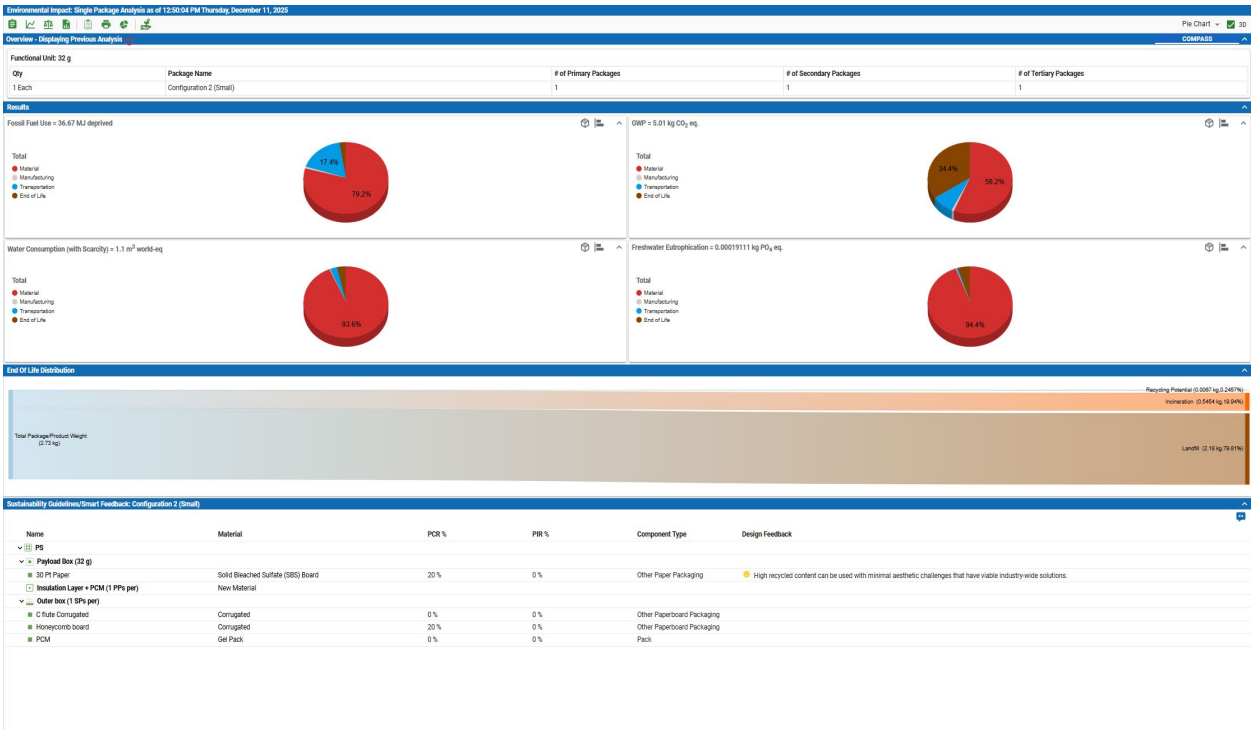

Figure 28: Environmental impact report for configuration 2 (small)

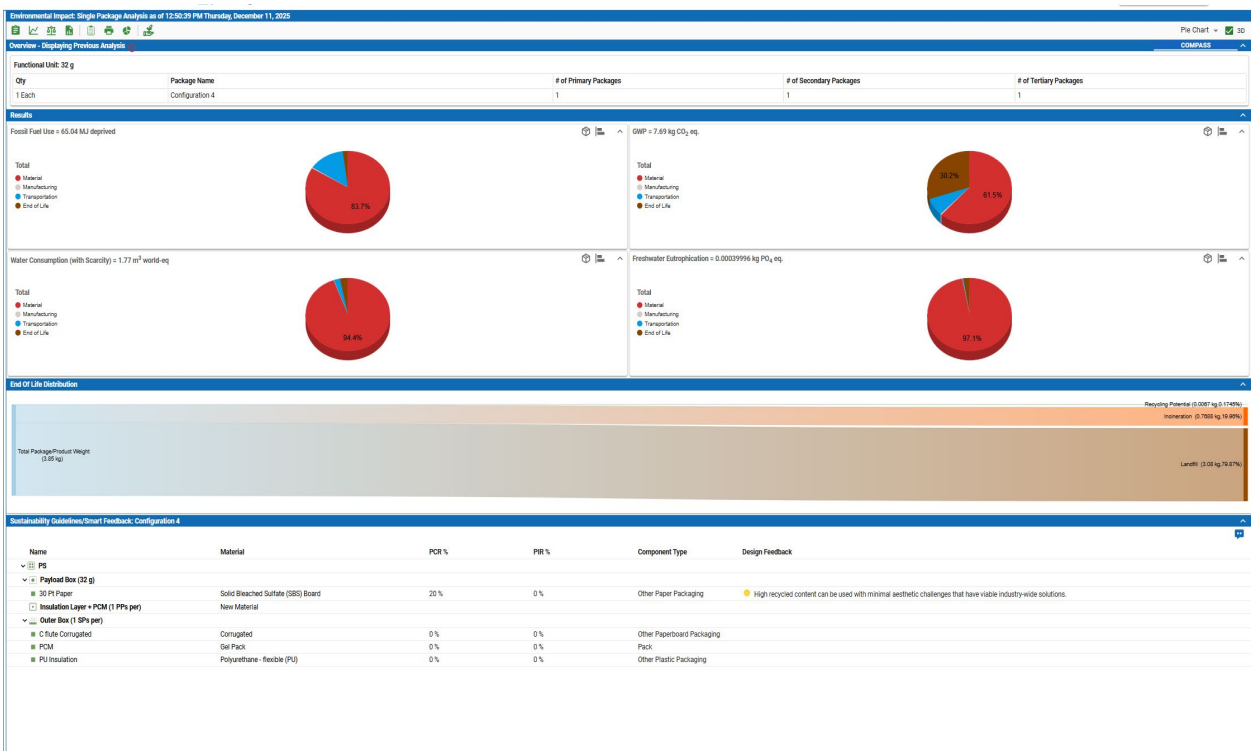

Figure 29: Environmental impact report for configuration 4

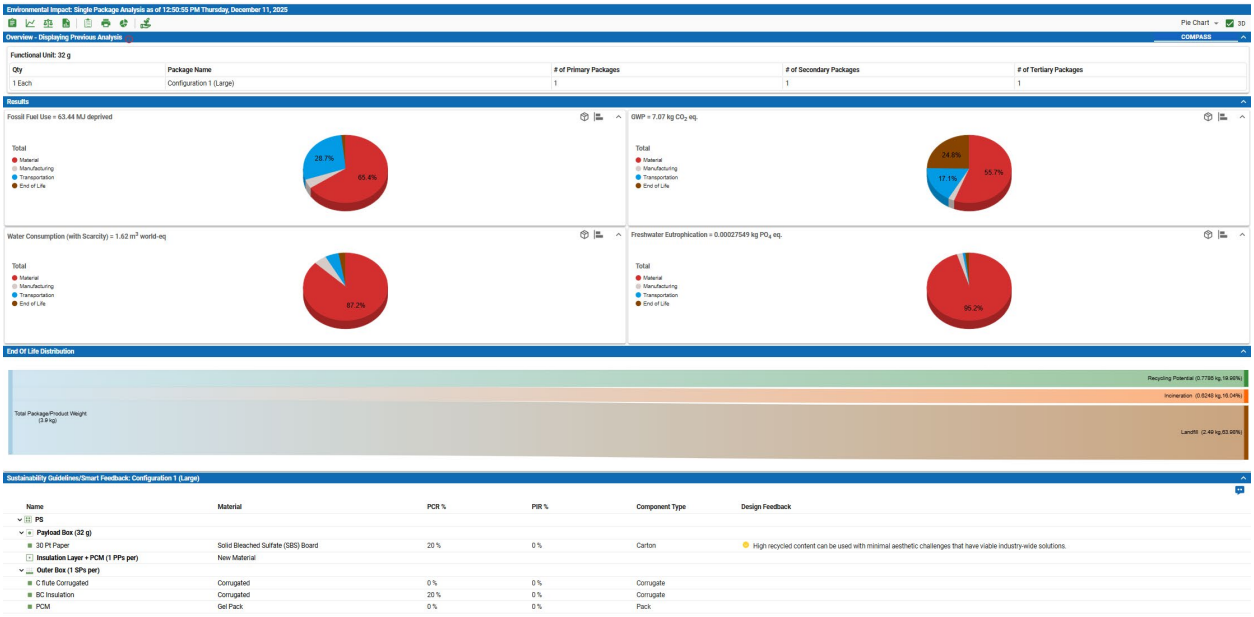

Figure 30: Environmental impact report for configuration 1 (large)

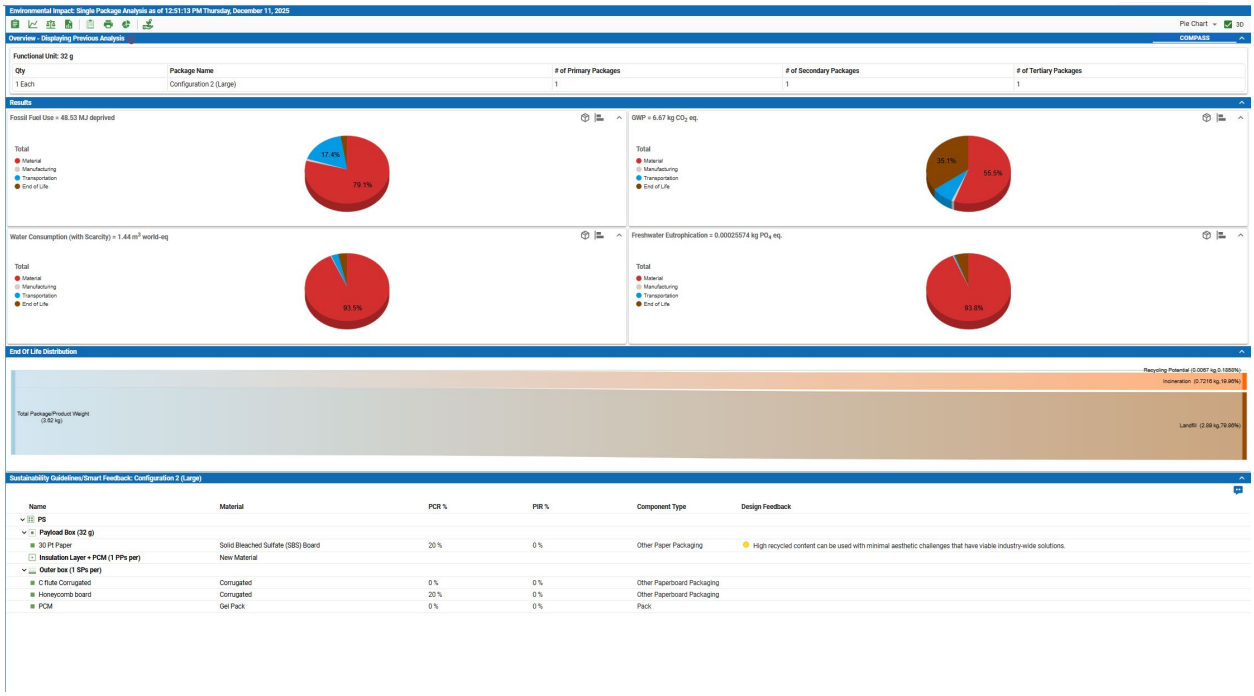

Figure 31: Environmental impact report for configuration 2 (large)